Characterization of Bases and Subbases for AASHTO ME Pavement Design

FINAL REPORT

Prepared by:

Serji Amirkhanian
Mary Corley
Tri-County Technical College

FHWA-SC-21-01

January 2021

Sponsoring Agencies:

South Carolina Department of Transportation
Office of Materials and Research
1406 Shop Road
Columbia, SC 29201

Federal Highway Administration
South Carolina Division
Strom Thurmond Federal Building
1835 Assembly Street, Suite 1270
Columbia, SC 29201

Technical Report Documentation Page

1. Report No FHWA-SC-21-01	2. Government Accession No.	3. Recipient's Catalog No.	
4. Title and Subtitle Characterization of Bases and Subbases for AASHTO ME Pavement Design		5. Report Date January 2021 6. Performing Organization Code	
7. Author/s Serji Amirkhanian, Ph.D. and Mary Corley		8. Performing Organization Report No. TCTC 21-01	
9. Performing Organization Name and Address Tri-County Technical College 7900 U.S. Hwy. 76 Pendleton, SC 29670		10. Work Unit No. (TRAIS) 11. Contract or Grant No. SPR No. 736	
12. Sponsoring Organization Name and Address South Carolina Department of Transportation Office of Materials and Research 1406 Shop Road Columbia, SC 29201		13. Type of Report and Period Covered Final Report 14. Sponsoring Agency Code	
15. Supplementary Notes			

16. Abstract

The characteristics of base and subbase layers play a very important role in pavement performance under the complex conditions of traffic loading and environment. Unreasonable and inaccurate base design parameters can result in poor pavement performance as well as higher construction and maintenance costs. This study was conducted to develop material input databases for several common types of base and subbase layers in South Carolina including Graded Aggregate Base (GAB), Cement Stabilized Aggregate Base (CSAB), Cement Modified Recycled Base (CMRB), and Soil-Cement (S-C). Seven South Carolina aggregate sources were used to evaluate GAB. Five of these sources were used to evaluate CSAB. Two subgrade sources (clay soil and sandy soil) and one RAP source were utilized to evaluate CMRB. The same two subgrade sources were also used to evaluate S-C. One GAB source was also utilized in a laboratory test pit to simulate field conditions and correlate with other testing. Compressive strength, elastic modulus, dry shrinkage, resilient modulus, and other properties were characterized through laboratory testing. Optimum mathematical resilient modulus models and material coefficients were recommended for the different kinds of base layers. A database was compiled, which considers the effect of moisture content, cement content, material type, curing period, and so on.

17. Key Words	18. Distribution Statement		
Base, Subbase, MEPDG, Resilient Modulus	No restrictions. This document is available to the public through the National Technical Information Service, Springfield, VA 22161.		
19. Security Classification (of this report) Unclassified	20. Security Classification (of this page) Unclassified	21. No. Of Pages 132	22. Price

Form DOT F 1700.7 (8-72) Reproduction of form and completed page is authorized

DISCLAIMER

The contents of this report reflect the views of the author who is responsible for the facts and the accuracy of the data presented herein. The contents do not necessarily reflect the official views or policies of the South Carolina Department of Transportation or the Federal Highway Administration. This report does not constitute a standard, specification, or regulation.

The State of South Carolina and the United States Government do not endorse products or manufacturers. Trade or manufacturer's names appear herein solely because they are considered essential to the object of this report.

ACKNOWLEDGEMENTS

The authors wish to extend their appreciation to the South Carolina Department of Transportation (SCDOT) and the Federal Highway Administration (FHWA) for sponsoring this research project. The assistance of Messrs. Carroll, Gibson, Harrington, Lockman, Swygert, Thompson, and Zwanka of SCDOT, Mses. Kim and Kline of SCDOT, and Ms. Fisher of FHWA was instrumental in the completion of this project.

EXECUTIVE SUMMARY

Base and subbase layers as the main bearing structure layer of highway engineering play a very important role in the mechanical and physical deformation process of pavements under the complex conditions of traffic loading and environment. The behaviors under traffic loading conditions can be characterized by some widely used parameters in research and engineering construction such as compressive strength, resilient modulus, dry shrinkage, etc. A major problem is that those parameters have not been well summarized for many common base and subbase layer types, including Graded Aggregate Base (GAB), Cement Stabilized Aggregate Base (CSAB), Cement Modified Recycled Base (CMRB), and Soil-Cement (S-C), which brings huge challenges to engineering design.

In order to solve this problem, multiple material sources were utilized to evaluate various bound and unbound base types in this research study. Seven typical South Carolina aggregate sources (Hanson Jefferson, Vulcan Gray Court, Martin Marietta Cayce, Martin Marietta Berkeley, Wake Stone North Myrtle Beach, Martin Marietta Rock Hill and Vulcan Pacolet) were used to evaluate unbound GAB materials. Five of these seven aggregate sources were also evaluated as CSAB materials. Two subgrade soil sources (clay soil and sandy soil), one RAP source, and three RAP contents were utilized to evaluate CMRB materials. The same two subgrade soil sources were also used to evaluate S-C. In addition, one GAB aggregate source (Martin Marietta Cayce) was utilized in a laboratory test pit to simulate field conditions and correlate with other laboratory testing for GAB. Compressive strength, elastic modulus, dry shrinkage, resilient modulus, and other properties were characterized through laboratory tests for typical base course materials. Optimum mathematical resilient modulus models and material coefficients were recommended for the different kinds of base layers.

A complete database of three different types of base and subbase layers was compiled, which considers the effect of moisture content, cement content, material type, curing period, and so on. Based on the test results, the main conclusions were drawn:

- Compressive strength and elastic modulus of CSAB both increased with increasing cement content; however, it could be a convex curve or concave curve depending upon the aggregate source.
- Increased curing duration increased both the compressive strength and elastic modulus of CSAB regardless of cement content and aggregate source.
- Dry shrinkage values of CSAB increased with increasing cement content with the data following a concave-curve trend due to the impacts of water loss and hydration behavior.
- Stress-strain curves for CSAB exhibited a noticeable increase with the increase of stress regardless of cement content. This implies that the resilient modulus was generally stress-dependent.

- OMC and MDD of clayey soil-based and sandy soil-based CMRB showed an opposite change tendency with the increase of RAP content: OMC values went down while MDD values increased.
- Compressive strength and elastic modulus of CMRB and S-C both increased with increasing cement content; however, compressive strength exhibited different increasing trends over time. After 7 days curing, the strength curve exhibited a concave trend, while after 28 days-curing, it showed a convex trend.
- Increased curing duration significantly increased both the compressive strength and elastic modulus of CMRB and S-C regardless of cement content, RAP content, and soil type.
- Compressive strength and elastic modulus values of sandy soil-based CMRB and S-C were higher than clayey soil-based samples, regardless of cement content, RAP content, and curing duration. Additionally, this difference increased as cement content increased.
- Elastic modulus values of S-C specimens were remarkably lower than the values from the CMRB specimens containing RAP, regardless of soil type, cement content, and curing duration.
- The resilient and elastic modulus values for CMRB materials generally increased with increasing RAP content. This may not be representative of all CMRB materials as the gradation of the RAP would have an affect and only one source of RAP was tested in this study.
- Stress-strain curves for CMRB and S-C exhibited a noticeable increase with the increase of stress regardless of cement content. This implies that the resilient modulus was generally stress-dependent.
- The soil test pit results indicated that the resilient modulus measured using the AASHTO T-307 method of a GAB material (MC) matched the "real-life" loading behavior of a 12" thick GAB layer.

The results of this study will directly support the SCDOT's current efforts to initiate a statewide Mechanistic-Empirical Pavement Design Guide (MEPDG) program to improve the overall experience of the design system. The characterization of various base and subbase materials through the testing programs and materials described in the experimental design section will provide necessary inputs for the MEPDG for SCDOT. It is estimated that the use of the proposed system will improve the efficiency of South Carolina's pavement designs in the near future. In addition, it is believed that the findings of this research project will produce more accurate predictions of base and subbase materials. This has the potential to produce a major cost savings for the Department over the life of the pavements. This can also enable SCDOT engineers and designers to establish proper and timely maintenance procedures optimizing the maintenance strategies around the state. It is predicted that cost savings will be a major outcome of this proposed project after the implementation process has been completed. The findings of this research project will enable the SCDOT engineers to design pavements resisting specific distress throughout the life of the structure. In addition, SCDOT staff could use the information to evaluate different alternative designs, based on developed models, and analyze the cost benefit of

each methodology. The quality of the field construction and the utilization of new materials in mixtures could also be affected.

This research could not have been completed without the help from the Chairman of the Steering and Implementation Committee, Eric Carroll of SCDOT, and the Steering and Implementation Committee members: Luke Gibson, Kevin Harrington, Mike Lockman, Dahae Kim, and Laura Kline of SCDOT and Carolyn Fisher of FHWA. Specifically, Eric Carroll and Jay Thompson provided detailed support and guidance throughout the project and their leadership is much appreciated.

TABLE OF CONTENTS

LIST OF FIGURES

LIST OF TABLES

CHAPTER 1: INTRODUCTION

1.1 Problem Statement

The Mechanistic-Empirical Pavement Design Guide (MEPDG) adopted by AASHTO represents a fundamental change and sophistication compared to the previous 50-year-old empirical pavement design procedure, which was developed from the AASHTO Road Test many years ago. The MEPDG system is predicted to provide more cost-effective and better-performing pavement designs. This new system considers many variables, including but not limited to, traffic volumes, vehicle characteristics, pavement materials, and construction/rehabilitation techniques as well as current and future performance demands. In general, the MEPDG design procedures will be implemented in the AASHTOWare PavementME software.

For any pavement analysis, system material characterization is vital. For many years, this issue has received much attention since it forms a critical component in recent improvements to many state DOT's pavement design programs. The properties of construction materials affect all aspects of pavement engineering including analysis, design, construction, quality control/quality assurance (QC/QA), pavement management, and rehabilitation. At any of these steps during the life of the project, several fundamental engineering material properties have a major impact on the long-term performance of pavements. Since there is currently a greater emphasis on optimizing pavement performance, there is a need for more information about material properties so that they can be characterized accurately for predicting pavement performance. In addition, this can help verify material quality during the construction phase.

Since it takes many resources (e.g., time and money) to perform laboratory and field tests to determine material properties, there is a need for secondary means to obtain the construction material property values. One method that many agencies use is correlations or predictive models based on data from routine or less expensive tests. AASHTOWare PavementME offers users the option of using inputs obtained through correlations.

The design software considers traffic, structural features, materials, construction, and climate by using a hierarchical approach to determine the design inputs. Three levels of input are provided depending on the desired level of accuracy of input parameters, from Level 1 (highest level of accuracy) to Level 3 (lowest level of accuracy). Depending on the available resources and the importance of the project, the designer could choose any input levels or a combination of levels. In general, the material parameters required for unbound granular materials could be classified into one of three major groups:

1. Pavement response model material inputs,
2. Enhanced Integrated Climatic Model (EICM) material inputs, and
3. Other material inputs.

The input requirements for the pavement response model are resilient modulus (M_R) and Poisson's ratio (μ) used for quantifying the stress-dependent stiffness of unbound materials under

moving wheel loads. EICM inputs (Atterberg limits, gradation, and saturated hydraulic conductivity) are associated with those parameters used by the models to predict the temperature and moisture conditions within a pavement system. In addition, the "other" category of materials properties includes special properties required for the design such as the coefficient of lateral pressure (K). The M_R has a significant effect on computed pavement responses and the dynamic modulus of subgrade reaction (k-value) computed internally by the PavementME system. The three different levels of inputs shown below are available for M_R of unbound materials in the Design Guide. It is recommended to use Levels 1 and 2 testing for M_R.

- LEVEL 1 – laboratory testing using standard test methods (e.g., NCHRP 1-28A (NCHRP, 2004b) and AASHTO T307 (1999),
- LEVEL 2 – correlations with other material properties (e.g., CBR, R-value, AASHTO layer coefficient, DCP, etc.), and
- LEVEL 3 – typical values based on calibration.

A detailed and comprehensive research work plan is needed to establish a library of PavementME input values for typical unbound materials used in South Carolina in order to successfully implement the PavementME system. The materials inputs required are those of unbound granular and subgrade materials defined using the standards of AASHTO M145 (1991) and ASTM D 2487, 2006. Unbound materials are categorized in many ways including grain size distribution, liquid limit, and plasticity index value. The required pavement response model material inputs include resilient modulus (M_R) and Poisson's ratio (μ) parameters used for quantifying the stress-dependent stiffness of unbound materials under moving loads.

1.2 Background

The MEPDG outputs of pavement distresses include rutting, top-down longitudinal cracking, bottom-up fatigue cracking (alligator cracking), thermal cracking (transverse cracking), and international roughness index (IRI) [1]. The primary focus of these distresses varies for pavements containing different types of bases. For instance, the pavement performance of flexible pavement is highly dependent upon the strength of the unbound granular base layer [2], while fatigue cracking of the base layer is a critical factor for chemical stabilized base [3]. The detailed information is introduced in the literature review section of this report.

Currently, common base courses include unbound granular base, asphalt treated base, cement treated base, permeable base, and recycled pavement base. In fact, some base categories include the combination of several common bases. For instance, permeable base includes asphalt treated permeable base, cement treated permeable base, and so on. However, the influences of various input variables on the pavement performance of base courses are different.

For unbound material (soils and aggregates), the resilient modulus and Poisson's ratio are very important [4], especially the resilient modulus, which can characterize the relationship between stress and strain [5]. Therefore, the effects of stress state, temperature, moisture content, and aggregate gradation on resilient modulus have been summarized in the literature review.

Furthermore, the influence of Poisson's ratio on pavement performance and the rutting prediction model are also integrated.

For pavements containing asphalt treated base [6], the influences of binder type and content have been analyzed first. The types of binder mainly include hot mix asphalt, foamed asphalt, and emulsified asphalt. When the base remained unchanged, various binder grades and temperature changes affected the pavement performance.

Chemical stabilized base includes rigid base and semi-rigid base. Lean concrete is representative of a rigid base [7]. Cement, lime, fly ash, slag and calcium carbide residue (CCR) are regarded as common stabilizers of semi-rigid bases. The strength of a chemical stabilized base is relatively higher than a non-stabilized base; thus, it is not as sensitive to the traffic volume. However, change of temperature still plays a significant role in the pavement performance of chemical stabilized bases.

Permeable base is often used in urban roads and public areas such as parking lots to improve the drainage [8]. The common types of permeable base include unbound aggregate base, asphalt treated permeable base, and cement treated permeable base. The influences of traffic volume, climate condition, binder content, and binder type on pavement performance have been summarized in the literature review.

Recently, the recycled materials used in base layers have gained much interest [9]. Common recycled materials include reclaimed asphalt pavement, reclaimed cement pavement, and crushed brick. The type and content of recycled materials play significant roles in pavement performance.

1.3 Significance of Work

When implemented, the findings of this research project will help the designers and SCDOT engineers to have a more effective methodology for designing pavements in the future. The data provided by the research will enable the State to save both time and financial resources by selecting the most cost-effective alternatives. The people of South Carolina (SC) can benefit by having more reliable, durable, and cost-effective pavement system that they can use for many years to come. The engineers using the data from this research can have a systematic way of designing pavements in which most factors have been considered before making the final decision. A thorough understanding of the properties and laboratory performance of existing pavement materials is necessary in order to implement the findings and thus provide more optimized pavement designs in SC. Although limited research has been conducted in this area, this research project can answer many of the remaining unknowns about the properties of materials used specifically to construct SC's pavements. As a result, it is necessary to develop technical guidance and potentially modify the existing methodology used to determine inputs for pavement design. This could ultimately optimize the use of the limited funds that are available each year to the State for various pavement systems around South Carolina.

CHAPTER 2: LITERATURE REVIEW

2.1 Influences of Unbound Aggregate Base and Subbase on Pavement Performance

2.1.1 Introduction of Unbound Granular Base

Unbound granular base (UGB) is the most fundamental type of base course, and its influence on pavement performance has been studied thoroughly. The most frequently used unbound materials include crushed stone, crushed slag, crushed gravel, natural gravel, and crushed reclaimed concrete or asphalt material. UGB consists of one layer or two layers. For the former, the base layer is directly on top of the subgrade. For the latter, a subbase layer is between the base layer and the subgrade [10].

For UGB, the resilient modulus and Poisson's ratio are two important parameters. Enhanced Integrated Climate Model (EICM) is used in MEPDG to predict the variations of temperature and moisture content and calculate the adjusted coefficients of resilient modulus, pore water pressure, water content, and freezing and thawing depths for the base layer. In other words, these factors have influence on the resilient modulus [2]. Therefore, the models predicting resilient modulus have been summarized in Section 2.1.4, and the influence factors of resilient modulus are analyzed in Section 2.1.2. Furthermore, the influences of Poisson's ratio on pavement performance have been summarized.

The portions of pavement performance considered include fatigue cracking (includes alligator cracking and longitudinal cracking), thermal cracking, rutting, and International Roughness Index (IRI). However, for UGB, rutting and fatigue cracking are common distresses that have been thoroughly studied; therefore, many rutting prediction models and fatigue models have been summarized in Section 2.1.4.

2.1.2 Influence Factors of Resilient Modulus

2.1.2.1 Effect of Stress

Previous studies show that confining pressure and principal stress had the most significant impact on the resilient properties of granular materials [11]. Principal stress minus confining pressure is the deviator stress, which has a slight effect on resilient modulus. Monismith reported an increase of 500% in resilient modulus as the confining pressure increased from 20 to 200 kPa [12]. Smith and Nair found that resilient modulus increased by 50% when the sum of principal stresses changed from 70 to 140 kPa [13]. The results from testing Mexican limestone conducted by the Louisiana Department of Transportation (LDOT) indicated that the resilient modulus increased with the increase of confining pressure [14]. Due to the stress-dependence of unbound materials, resilient modulus decreased with the increase of depth as the confining stress decreased [11].

As for deviator stress, it is less influential on the resilient modulus of unbound granular materials (UGM) than confining pressure. Morgan reported that resilient modulus decreased slightly with the increase of deviator stress [15]. And Hicks found that the material exhibited slight softening at low deviator stress levels and slight hardening at higher stress levels [16]. Furthermore, the LDOT found that resilient modulus increased with increasing deviator stress [14].

2.1.2.2 Effect of Traffic Load

Since 1960, many research efforts have been devoted to characterizing the resilient behaviors of granular materials. The deformation of unbound base layers under repeated traffic-type loading consists of recoverable deformation and a residual deformation [11]. However, the deformation mechanism of aggregates in the deformation process includes three stages: consolidation, distortion, and attrition [17]. Unbound granular base does not show pure elastic characterization; instead, it shows a time-dependent elastoplastic and nonlinear characterization when subjected to the traffic load.

Research efforts indicated that load duration and frequency had slight effects on the resilient properties of UGB [12, 15, 16, 18, 19]. A study indicated that the resilient modulus of sands slightly increased from 160 to 190 MPa as the action time of load decreased from 20 mins to 0.3 s [12]. In addition, when the lasting time of load was changed to 0.1, 0.15, and 0.25 s, the change in the resilient modulus and Poisson's ratio was very slight [16]. The resilient modulus may have decreased with an increased loading frequency when the water content was close to saturation state due to the decrease of effective stress resulting from the development of transient pore pressures [11]. In general, the test sequences where the load was applied to a specimen had no influence on the resilient response of UGB [16, 20].

2.1.2.3 Effect of Underlying Layer

The pavement performance is a function of strength or modulus, while the resilient modulus of the base layer is a function of the layer thickness and the modulus of the next underlying layer. If the subbase layer exists, the modulus of subbase is related to the modulus of subgrade [21].

Subbase is an underlying layer beneath the base layer that plays an important role in bearing traffic load and protecting the subgrade. When the subgrade is of high quality, the subbase layer is generally omitted. In fact the subbase strength, gradation, and plasticity were not emphasized in the specification [11]. Rounded rock, sand and soil mixtures are generally used in the subbase. The strength and stiffness of the subbase can be characterized by the resilient modulus, California Bearing Ratio (CBR), or R-value. Of course, resilient modulus is widely used.

Meanwhile, it is widely believed that the modulus ratio of the upper layer to the next underlying layer is equally important in M-E pavement design. In general, the modulus of base layers ranged from 137,895.14 to 335,602.30 kPa [11]. The Design Manual of Colorado Department of Transportation indicated resilient modulus values of base courses changed with the change of

resilient modulus of the underlying layer and the thickness of the base layer. It also limited the maximum value of 100,000 MPa.

2.1.2.4 Effect of Moisture Content

In MEPDG, the soil-water characteristic curve (SWCC) is used to characterize the relationship between moisture content fluctuation and resilient modulus. At the same time, it is given that moisture content can affect the permanent deformation of unbound materials [22].

The moisture content of unbound granular materials plays an important role in determining the resilient modulus. It was widely believed that the resilient response of UGM in a dry state was similar to that of the saturated granular material, but the resilient response could change significantly when the moisture content approached the optimum water content (OWC) [13, 23]. The resilient modulus of UGM decreased by 50% when the degree of saturation increased from 70% to 97% [24]. The resilient modulus decreased significantly when the moisture content increased above its optimum value [16].

It is well known that the effective stress determines the strength and deformation properties of the material [25-28]. Therefore, the assumption that the decrease of resilient modulus is not caused by degree of saturation but decrease of effective stress resulting from the increase of pore-water pressure had aroused many research studies. When the analysis was based on the total stresses, resilient modulus decreased with the change of saturation [16, 29, 30]. Similarly, if effective stress remained unchanged, the resilient modulus also remained unchanged regardless of the total stress. In the latter research results, it was found that there was a relative slip among aggregates due to the effect of water lubrication, and it could lead to the reduction of resilient modulus even without generation of any pore-water pressure [18]. A study demonstrated that, below optimum moisture content, resilient modulus increased as water content increased due to the development of suction. Beyond the optimum moisture content, the resilient modulus started to decrease fairly rapidly because the excess pore water pressure increased [31].

The LDOT tested the resilient modulus of Mexican limestone samples and Recycled PCC (RP) samples at optimum moisture content (OMC), 2% above OMC (OMC+2%), and 2% below OMC (OMC-2%), which were shown in Figure 2-1(a) and (b) [32]. Figure 2-1(a) showed that the resilient modulus of Mexican limestone sample at OMC+2% was smaller than that at OMC, while the resilient modulus at OMC-2% was larger than that at OMC. Additionally, Figure 2-1(b) showed that the resilient modulus of RP sample at OMC+2% was smaller than that at OMC while the resilient modulus at OMC-2% was slightly larger than that at OMC.

For all materials, design values of resilient modulus have been recommended at optimum moisture content [4]. The specification also defined that the density of base layer was not less than 95 percent of the maximum density conducted [33]. Menqi illustrated the change of resilient modulus of unbound granular materials with the RAP with the help of Kw model and demonstrated that the resilient modulus decreased with the increase of moisture content. The test

results were shown in Figure 2-1(c) [22]. Makhaly et al also reported that the resilient modulus at OMC-2% was the highest, followed by that of Basalt sample at OMC and OMC+2% [34].

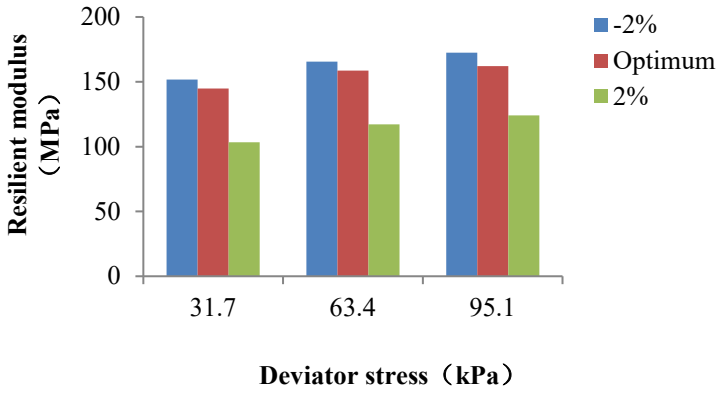

(a)Mexican limestone sample

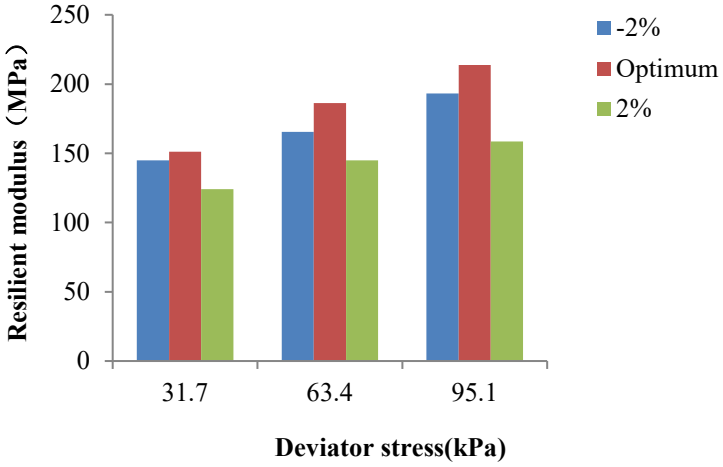

(b) Recycled PCC sample

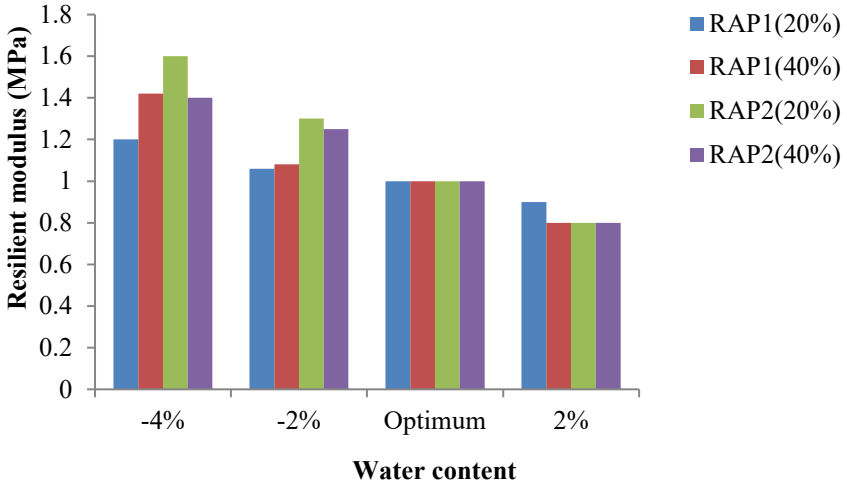

(c) RAP1 and RAP2

Figure 2-1: Test Results of Resilient Modulus: (a) Mexican Limestone Sample (b) Recycled PCC sample (C) RAP1 and RAP2

2.1.2.5 Effect of Grain-Size Distribution

In order to ensure that the unbound granular layer has the enough load bearing capacity, many criteria associated with the gradation of aggregate have been used. For example, the gradation design of unbound granular base materials must meet the requirement of the grading envelope specified in BNQ 2560-114 [35] in which it specifies the maximum particle size of 31.5mm, an average diameter ranging from 2.9 to 9 mm, and the percentage of fine particles ranging from 2% to 7%. As for the grading envelope described in BNQ 2560-114, grain-size distribution of a given aggregate was shown to have a 30% effect on the resilient modulus [3, 10].

The performance of crushed limestone at different gradations was studied by Thom and Brown, reporting that the uniformly-graded aggregates were stiffer than well-graded aggregates [18]. However, Plaistiow concluded that the aggregate gradation had a significant influence on resilient modulus when the water existed in the pores of the aggregate [36]. By comparing the effect of gradation on resilient modulus from gravel, limestone, and slag, Heydinger reported that resilient modulus of limestone decreased but the resilient modulus of slag reduced with a denser gradation [37]. After that, the research about the resilient modulus of sands, crushed masonry, and crushed concrete was conducted by Van Niekerk [38], who reported that the well-graded aggregates showed higher resilient modulus than the uniformly graded aggregates. However, the result was opposite than the above-mentioned project with Nierketk reporting that a large deviator stress caused higher resilient modulus values for a well-graded material with a larger number of contact areas at equal confining pressure.

It is believed that the grading envelope cannot exceed the maximum density line (MDL) [39]. In the corresponding equation, n is a coefficient value influencing the shape of the gradation. When n is equal to 0.45, aggregate has the maximum dry density [38]. Of course, n has been adjusted by Fuller and Thompson according to the original work based on the empirical determination of Federal Highway Administration (FHWA) [39, 40].

2.1.2.6 Effect of RAP Content

Wu [41] conducted multiple tests on two kinds of RAPs at different contents and reported that resilient modulus increased with the increase of both RAP1 and RAP2 contents at a high or low cyclic stress. Resilient modulus values of samples did not change as the percentage of RAP increased from 0% to 20%; however, this value increased by around 30% when the RAP content increased to 60%. Therefore, the resilient modulus increased with the increase of RAP content. Contrasting with conventional aggregate base, RAP showed opposite effect to permanent performance with higher resistance to rutting and higher resilient modulus in MEPDG due to the involvement of aged binder [42, 43].

2.1.3 Influence of Poisson's Ratio on Pavement Performance

Poisson's ratio (u) and resilient modulus are two parameters used to calculate the resilient response in the elastic layer program. Compared with resilient modulus, Poisson's ratio has a

smaller effect on the resilient response. Fortunately, Ali and Thomas have done multiple studies for this subject [44].

The MEPDG software [45] was used to analyze the influence of Poisson's ratio of unbound aggregate base on the pavement performance. PG 64-22 and PG 76-22 as the asphalt binder of the surface course were used commonly in New Jersey. The sensitivity results of alligator cracking and longitudinal cracking were shown in Figure 2-2.

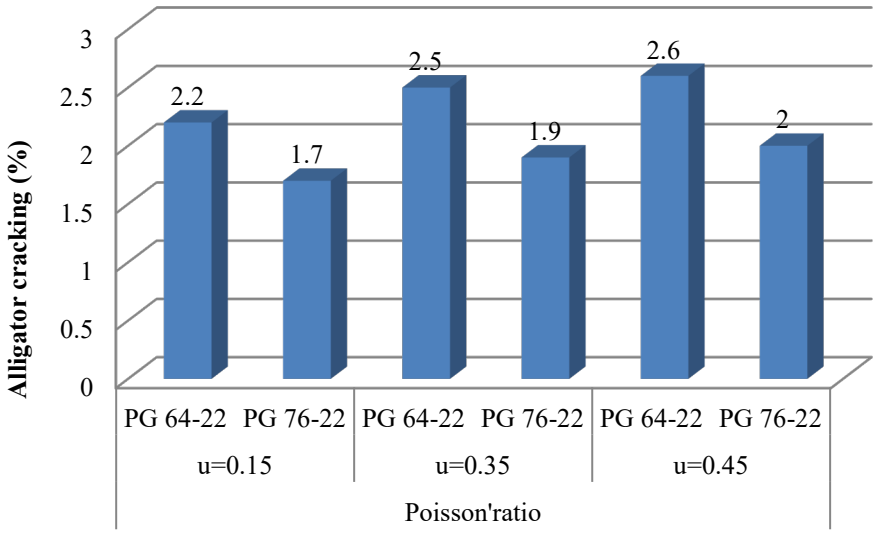

(a) Alligator Cracking

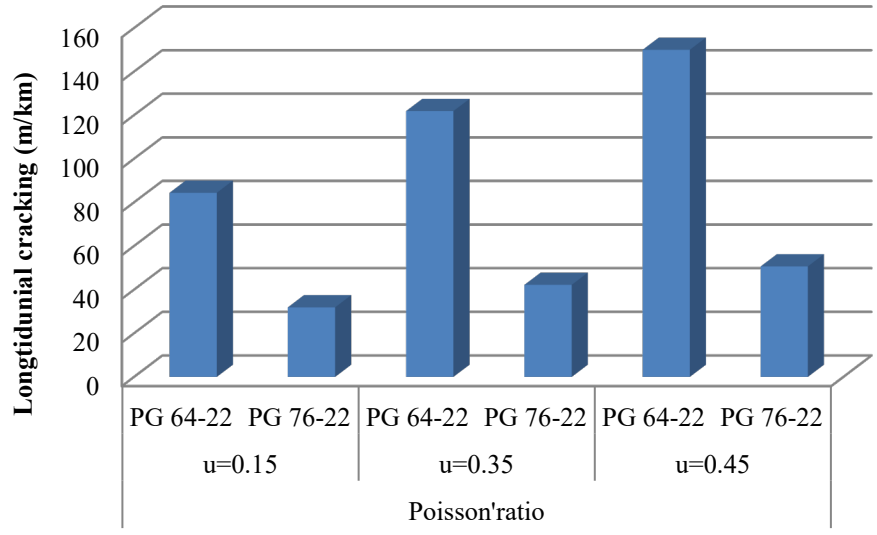

(b) Longitudinal Cracking

Figure 2-2: Crack Widths of Pavements with PG 64-22 and PG 76-22 after 15 Years of Service, (a) Alligator Cracking (b) Longitudinal Cracking

The study indicated that the change of Poisson's ratio in unbound aggregate base had a slight influence on rut depths generated in asphalt surface, base and subgrade. Fatigue cracking (top-down) was affected significantly by the Poisson's ratio. The crack width of the pavement containing PG 64-22 increased by 65.6 m/km when u increased from 0.15 to 0.45, and for PG 76-22, the crack width increased by 18.8 m/km. The magnitude of longitudinal fatigue cracking of the PG 64-22 pavement was significantly larger than that of the PG 76-22 pavement at the same Poisson's ratio. Therefore, the fatigue cracking (alligator cracking) was not sensitive to the change of Poisson's ratio, and the percent of alligator cracking decreased with the decreased Poisson's ratio. The percent of fatigue cracking of PG 64-22 pavement section was slightly lower than that of PG 76-22.

2.1.4 Model Development of Rutting Prediction

For flexible pavement with unbound granular base, rutting is the major distress. Under cyclic loading, the strain can be divided into resilient strain and the permanent strain [46]. The resilient strain is recoverable, which is characterized by the resilient modulus and Poisson's ratio [47], while permanent strain is used to calculate the permanent deformation [48]. Stress level and the number of load repetitions play significant roles on the permanent strain [49, 50]. Additionally, in the base course of flexible pavements, the stress-distribution is not uniform. Therefore, it is critical to quantify the influence of stress level on permanent performance of unbound granular material for predicting the rut depth of the unbound base layer.

Many models have been developed to predict the rut depth of unbound granular base. First, these models are mechanics-based, complicated, and time-consuming in predicting the rutting resistance, so they are hard to apply in pavement design. Second, the mechanistic-empirical models, which were developed based on the relationship between load repeated times and permanent performance, are widely used in M-E pavement designs [51]. According to stress level, mechanistic-empirical models can be divided into single-stage models and multi-stage models. If the repeated load triaxial test (RLT) is conducted at one stress level in a test, it belongs to single-stage [52], while multi-stage corresponds with the multiple stress levels [1, 53]. The development of the single-stage model has been listed in Table 2-1.

Table 2-1: Development of Rutting Prediction Models of Unbound Granular Materials

Model	Tseng-Lytton model[5]	MEPDG model[54]	Korkiala-Tanttu (K-T) model[55]	UIUC model[56]	MER model[51]
Year of Development	1989	2003	2009	2014	2016
Advantages	It is efficient for predicting the accumulated PD at one stress level.	It considers the effect of stress on permanent deformation.	It uses a deviatoric stress ratio to capture the nonlinear effect of stress state.	It can predict the plastic deformation of the UGM with very high R^2 values.	It considers different stress states.
Disadvantages	It is not accurate to represent the stress dependent Permanent behavior.	Underestimates the permanent behavior of the tested materials for most of the stress states.	It cannot capture the trend of permanent deformation behavior when stress states vary.	It needs to be validated for the stress states at different confining pressures.	It needs to be checked by all field work.

2.2 Influences of Chemical Stabilized Base and Subbase on Pavement Performance

2.2.1 Introduction of Chemical Stabilized Base

Chemical stabilized base (CTB) materials consist of soil, gravel material, and manufactured aggregate and binder. Generally, binders include cement, lime, fly ash, cement-lime-fly ash, lime fly ash and so on. It is widely used due to the balance of high quality and low cost. Compared with non-stabilized base, CTB is stiffer and provides the function of frost-resistance under Portland cement concrete (PCC) surfaces and asphalt surfaces.

In MEPDG, the material properties such as the type and content of stabilizers, traffic grade and change of temperature can affect the pavement performance, especially for fatigue performance of CTB. In this view, the type and content of stabilizers are the internal causes to influence the performance of base layer, while the traffic condition and environment are considered as the external causes.

2.2.2 Influence Factors of Pavement Performance

2.2.2.1 Effect of Material Type

The fatigue performance of semi-rigid materials is the important foundation of pavement structure [82]. Type of material plays a significant role in affecting fatigue life of semi-rigid base. SH-A et al conducted a series of tests on fatigue performance of different stabilizations including cement stabilized sand, cement stabilized crushed stone, cement stabilized soil, and lime-fly ash stabilized crushed stone [83]. The test results indicated that the fatigue performance of lime-fly ash stabilized crushed stone was the best, followed by cement stabilized crushed stone, cement stabilized sand and cement stabilized soil. In addition, the lower voids in lime-fly ash soil delays the development of cracking [84].

Drying shrinkage and temperature shrinkage of semi-rigid base materials resulted in reflection cracking on the surface of pavement [85]. The study indicated that at the same curing time, the coefficient of dry shrinkage of lime-fly ash stabilized crushed stone was 15.2% less than that of cement stabilized crushed stone and that the resilient modulus of cement-fly ash or lime-fly ash stabilized crushed stone was lower than that of cement stabilized crushed stone [84].

2.2.2.2 Effect of Stabilizers Content

Cement content in cement treated materials was studied to meet the strength requirement, improve the durability and reduce moisture susceptibility [86]. Miller et al conducted compaction tests and tube suction tests (TST) on the several materials with various cement contents and tested the corresponding relationship between water content and cement content [87].

The results of unconfined compressive strength are shown in Figure 2-3. The results indicated that the value of unconfined compressive strength (UCS) increased with the increasing cement content. Generally, the value of unconfined compressive strength was recommended from 2068.4 kPa to 2757.9 kPa [86, 88]. At 2% -3% of cement content, the UCS values of material A and M1 were in the mentioned scope. CTB shrinkage cracking could occur at relatively high contents (6%-8%) of cement [89, 90]. For material A, the water content decreased with the increase of cement content at a low cement content, and increased with the increasing cement content at a high cement content. However, the water content of material M1 decreased with the increase of cement content.

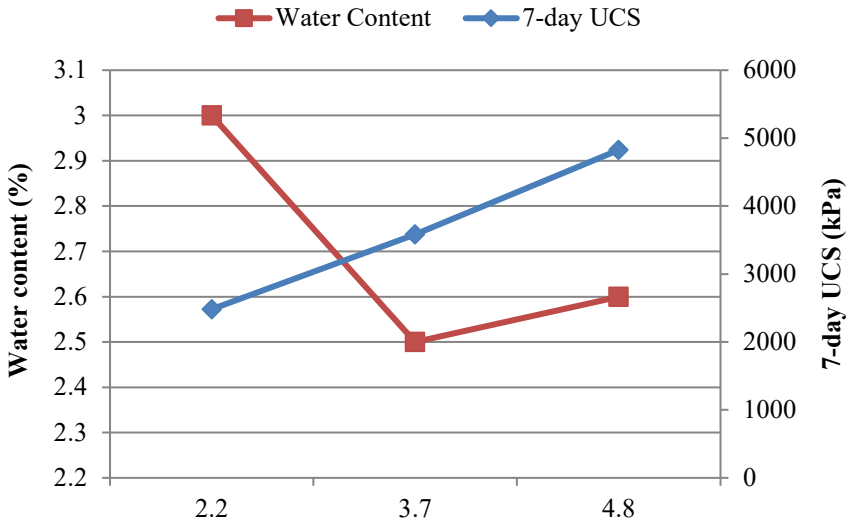

(a) Material A

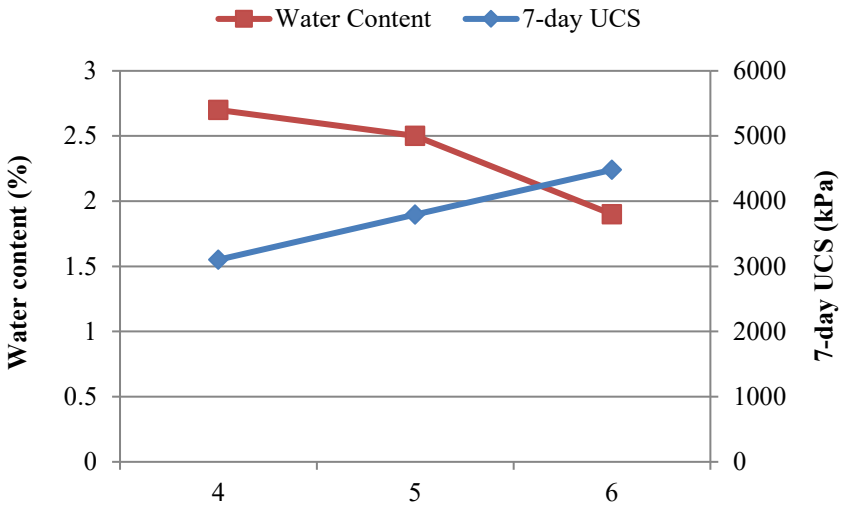

(b) Material M1

Figure 2-3: Test Results of Water Content and 7-day UCS: (a) Material A; (b) Material M1

2.2.2.3 Effect of Temperature

Transverse and longitudinal cracks can be frequently observed on the pavement surface with cement treated bases, which are sensitive to the change of temperature [91]. There are two major reasons for transverse cracking: one is due to the shrinkage of pavement at low temperatures, and the other is reflective cracking. Temperature cycling in one day is the major reason for the generation of reflective cracks, which slowly grow and reflect to the asphalt surface after one or two years [92]. Compared to transverse cracking, an extra reason for longitudinal cracking is poorly constructed joints. These cracks generally are not associated with traffic loads [93].

2.2.2.4 Effect of Traffic Load

Generally, pavement performance weakens as a result of continued traffic loads. Under heavy traffic loading, the cement treated base with a high cement content showed brittle behavior [94]. Additionally, the initial strength of cement treated base was adversely affected by the early traffic load. Test results from falling weight deflectometer (FWD) testing indicated that the stiffness value was not sensitive to the early traffic load [95]. However, the stiffness of cement treated base decreased by 26% after one day of curing and by 11% after two days. Therefore, early traffic may cause the reduction of stiffness of cement-treated base, especially under heavily-loaded construction traffic [96].

Transverse cracks generate because of the thermal and drying shrinkages. However, the traffic load may lead to the extension of cracks in the longitudinal direction as shown in Figure 2-4. First, the transverse crack generates with the thermal and dry shrinkages. The tensile strain increases significantly when the wheel load acts at the transverse crack, which results in the development of longitudinal cracking. Molenaar reported that cracking induced by load did not generate in CTB when strain level was below 41μm/m [97]. The strain level was 50μm/m when the load could transfer well across the transverse crack, which was suggested as the endurance limits for the pavement materials [97].

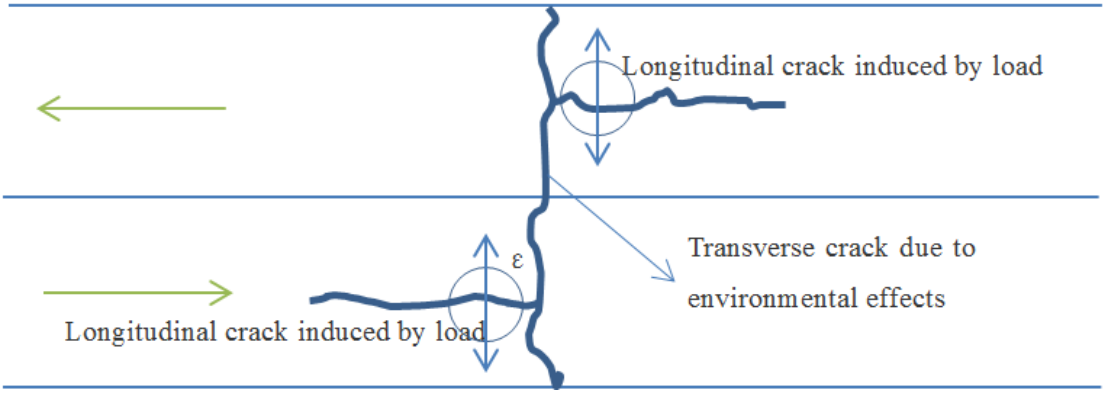

Figure 2-4: Formation Mechanism of Longitudinal and Transvers Cracks (Internal Causes or External Causes)

2.3 Influences of Reclaimed Pavement Base on Pavement Performance

2.3.1 Introduction of Reclaimed Pavement Base

Recycled construction and demolition materials (C&D) such as crushed brick (CB), recycled crushed aggregate (RCA), and reclaimed asphalt pavement (RAP) have been widely used in base course [123, 124], which not only replaces more expensive virgin aggregates but also reduces environmental pollution and landfilling. C&D materials without virgin aggregates and stabilizers are generally recommended as base materials due to their inferior gradation and bonding characteristics [125, 126]. Stabilizers generally include asphalt, cement, fly ash and slag and so

on. Arul, Alireza and Itthikorn analyzed the influence of calcium carbide residue (CCR), an economical and low-carbon geopolymer binder, on the strength and modulus of the C&D aggregates [125].

Recycled asphalt pavement (RAP) and recycled concrete aggregate (RCA) are the most widely used C&D materials [127, 128]. RAP is obtained from reclaimed asphalt pavements while RCA is produced by dismantling concrete structures such as buildings and highways. In contrast with virgin aggregate, RAP shows a higher resilient modulus but a lower resistance to the plastic deformation. This is contradictory with the relationship between permanent deformation and resilient modulus provided by MEPDG [129]. When RAP is mixed with aggregate, the distress prediction model in MEPDG is not suitable to use. Thus it is necessary to make clear what affects the performance of the base layer and pavement distress. Du et al studied the application of cement-treatment of waste materials in pavement engineering. In addition, fly ash–stabilized RAP aggregate was studied by Li et al. and Cetin et al [130].

2.3.2 Influence Factors of Pavement Performance

2.3.2.1 Effect of Material Type

Resilient modulus as an important parameter in MEPDG reflects the potential to resist permanent performance. For typical unbound aggregates, the resilient modulus ranged from 125MPa and 300MPa [131]. Many C& D materials such as recycled concrete aggregates (RCA) and crushed brick (CB) were thrown into waste streams in developing countries [132, 133]. Thus, Arulrajah et al studied the influence of various C&D materials and stabilizers on resilient modulus and strength [134]. The analyzed results are displayed in Figure 2-5.

It can be observed that C&D stabilized with 10% CCR and 10% slag (S) exhibited the same resilient modulus. UCS results showed that fly ash had a lower flexural strength due to inactivated fly ash particles in the mixture [134]. The slag played a significant role in improving the resilient modulus of C&D aggregate. However, it reduced the ductility of the materials. Thus for the slag stabilized base, resilient modulus had an opposite effect on resisting permanent deformation. However, the fly ash and CCR had significant effects on pavement performance. Fly ash slightly reduced the UCS value and resilient modulus of C&D material due to the lack of an alkaline environment [135]. Fly ash also reduced the optimum moisture content, resulting in improvement of the workability of the mixture [134]. Arul et al suggested that part of the slag could be replaced with CCR or fly ash to reduce the overall construction cost. The resilient modulus of geopolymer stabilized CB was larger than that of geopolymer stabilized RCA. At same time, Arul pointed out that the three-parameter model was more accurate than the bulk stress model although AASHTO recommended that the bulk stress model was more suitable to predict resilient modulus of unbound granular materials [135].

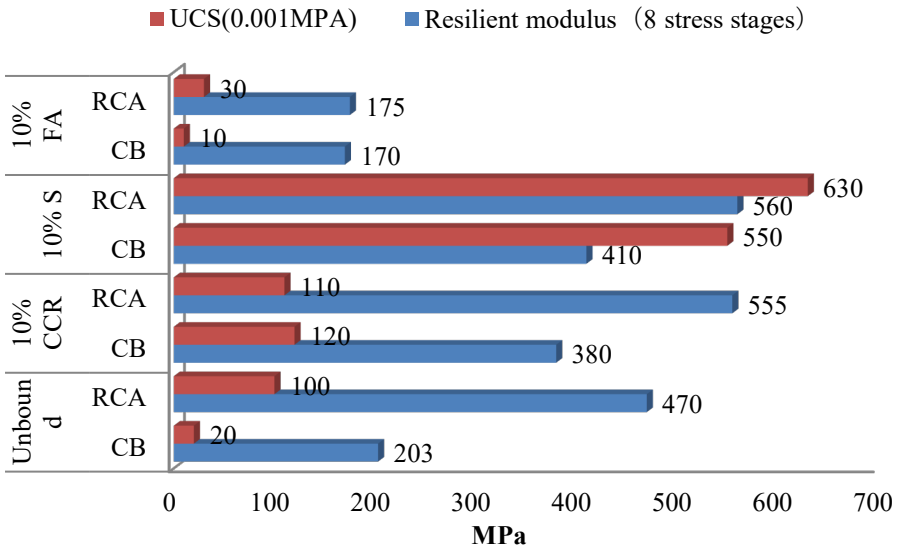

Figure 2-5: Resilient Modulus and UCS Values of Base Layers with Various Stabilizations

2.3.2.2 Effect of RAP Content

Although Tseng and Lytton had developed the most reliable equations for granular materials, these equations were not suitable for the base layers containing RAP. According to the previous studies [136, 137], RAP percentage had a significant effect on the rut depth for RAP base. Thus it is necessary to consider the influence of RAP content to the three parameters (εo/εr, b, and q). Wen et al developed the improved model, which accounted for the influence of RAP content on permanent performance. Of course, future study needs to consider the influence of binder content, CB, and so on.

Approximately 97% of RCA was comprised of concrete cement and rock aggregate. CB contained approximate 70% brick. Major components of RAP were the asphalt and aggregate with a small fraction of other materials such as glass, brick, and wood [134].

The maximum RAP content recommended to use in pavement layers was about 30% by weight of virgin aggregates [138, 139]. This RAP percentage value can prevent the pavement from premature failures in the base layer, but a high percentage of RAP may bring too much aged asphalt and reduce the bonding strength between asphalt and aggregate. MacGregor et al. found no correlation between RAP content and optimum water content (OWC) [140]. Ayan reported that the CBR values decreased as the RAP content increased due to the sliding of the asphalt-coated aggregates under the repeated loads [141].

2.3.2.3 Effect of Traffic Loading

Under the same wheel load, a thicker base course exhibited a lower resilient modulus and plastic strain [130]. The permanent strain is the accumulation of strains from each cycle, which is called

the rutting model [139]. Figure 2-6 demonstrated that the plastic strain of recycled pavement material (RPM), reclaimed road surface gravel (RSG), and UGM containing 60% RAP increased with an increasing number of cycles [130]. The rutting resistance of RSG was the worst, followed by RPM and RAP [110].

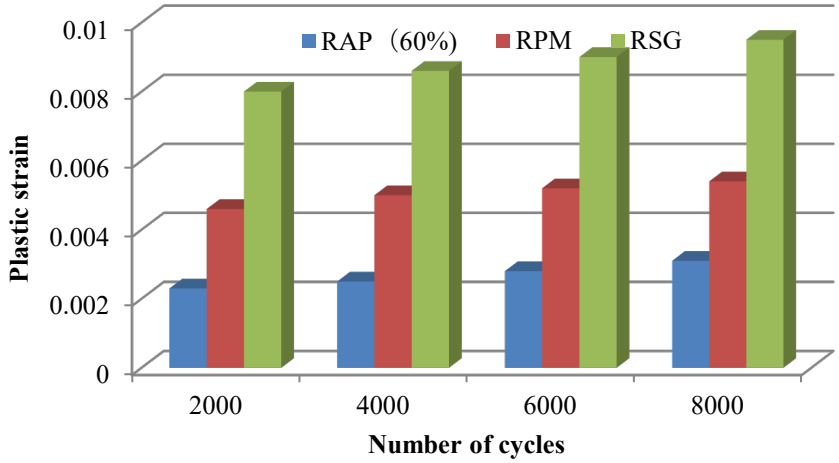

Figure 2-6: Plastic Strain of PAP, RPM and RSG at Various Cycles

2.3.2.4 Effect of Temperature

Resilient modulus of UGB was significantly affected by the temperature and moisture content [142]. The influence of low temperature on the performance of RAP was studied by Sargious et al who reported that the resilient modulus decreased as the temperature decreased from -20°C to -40°C [143]. Furthermore, MEPDG did not consider the influence of high temperature on resilient modulus [144]. For frozen coarse-grained material, the value of resilient modulus was specified from 10.34 MPa to 34.47 MPa by MEPDG [145]. The KT model and SigmoidalT model were recommended to be concluded in the MEPDG software by Wen, and the two models were effective for the base course containing RAP [144].

2.4 Influences of Subbase Course on Pavement Performance

The subbase course is generally located on the bottom of base course and laid on the top of subgrade, which plays a role of spreading the load over the subgrade [146]. However the subbase course is usually not used unless heavy traffic is involved or the subgrade is weak [146, 147]. In fact, subbase courses are typically studied together with the base course; therefore, the influence of subbase course on pavement performance is correspondingly slight compared to the base course, especially for the inherent mechanism. Kim et al studied the influence of thickness and resilient modulus of subbase course on the cracking, rutting and IRI with the help of MEPDG software [148]. The results indicated that the longitudinal cracking increased slightly with the increased thickness. In addition, the transverse cracking, alligator cracking, surface rutting, base rutting, and subbase rutting, and subgrade rutting were not sensitive to the thickness or value of

resilient modulus. The relevant design for subbase layers in MEPDG needs to be studied in the future.

2.5 Literature Review Conclusions

In MEPDG, the influences of inputs on the pavement performance are complex. Therefore, this review summarizes the influence of various factors on pavement performance with five kinds of base materials. The following conclusions can be drawn:

2.5.1 Unbound Granular Base

- The resilient modulus increased with increased confining stress.
- The increase of loading time resulted in no obvious increases of resilient modulus, while the loading sequences were not related with resilient modulus.
- The resilient modulus value corresponding with the optimum water content was typically selected. The resilient modulus of unbound granular base increased with an increased water content below the optimum water content, but was the opposite if water content was above the optimum water content.
- The resilient modulus of uniformly graded aggregate was higher than other graded aggregates. In addition, the increase of fine aggregate might cause the decrease of resilient modulus.
- The fatigue cracking (alligator cracking) was not sensitive to the change of Poisson's ratio, and the percent of alligator cracking decreased with the decrease of Poisson's ratio.

2.5.2 Cement Treated Base

- The early traffic might cause stiffness reduction of cement-treated base, especially under heavily-loaded traffic.
- Temperature cycling per day was the major reason for reflective cracks, which extended and reflected to the asphalt surface after one or two years.
- The value of UCS increased with an increased cement content for cement treated base while the optimum moisture content decreased with the increase of cement content.

2.5.3 Recycled Pavement Base

- Compared with virgin aggregates, RAP showed a higher resilient modulus but a lower resistance to plastic deformation.
- The three-parameter model was more accurate than the bulk stress model.
- The resilient modulus of CB stabilized with geopolymer was larger than that of RCA.
- The maximum RAP content recommended to use in pavement layers was about 30% by weight of virgin aggregate. CBR values decreased as the RAP content increased. The

source material, whether soil or aggregate, can significantly influence the effective percentage of RAP that can be utilized in recycled bases.

- Resilient modulus of RAP base materials was more sensitive to water content than that of UGB materials. MEPDG did not consider the influence of high temperature on resilient modulus, thus the KT and SigmoidalT models were used in MEPDG software.
- Under same wheel load, a thicker base course had a lower resilient modulus and strain. The permanent strains showed positive correlation with the number of load cycles.

2.5.4 Subbase Course

- According to the MEPDG software, the thickness and resilient modulus of subbase course had no influence on the pavement performance except that the longitudinal cracking increased slightly with an increased thickness of subbase course.

CHAPTER 3: METHODOLOGY

3.1 Materials and Experimental Design

For this research project, materials were selected from various sites around the state. Three areas of the state were selected, including three geographical/geological sections, as shown in Figure 3-1, including: 1) Upstate, 2) Midlands, and 3) Coastal. From each geographical area (e.g., Midlands), several material types were selected for each of the following categories for a limited testing program:

- Graded Aggregate Base (GAB),
- Cement Modified Recycled Base (CMRB),
- Cement Stabilized Aggregate Base (CSAB), and
- Soil-Cement (S-C).

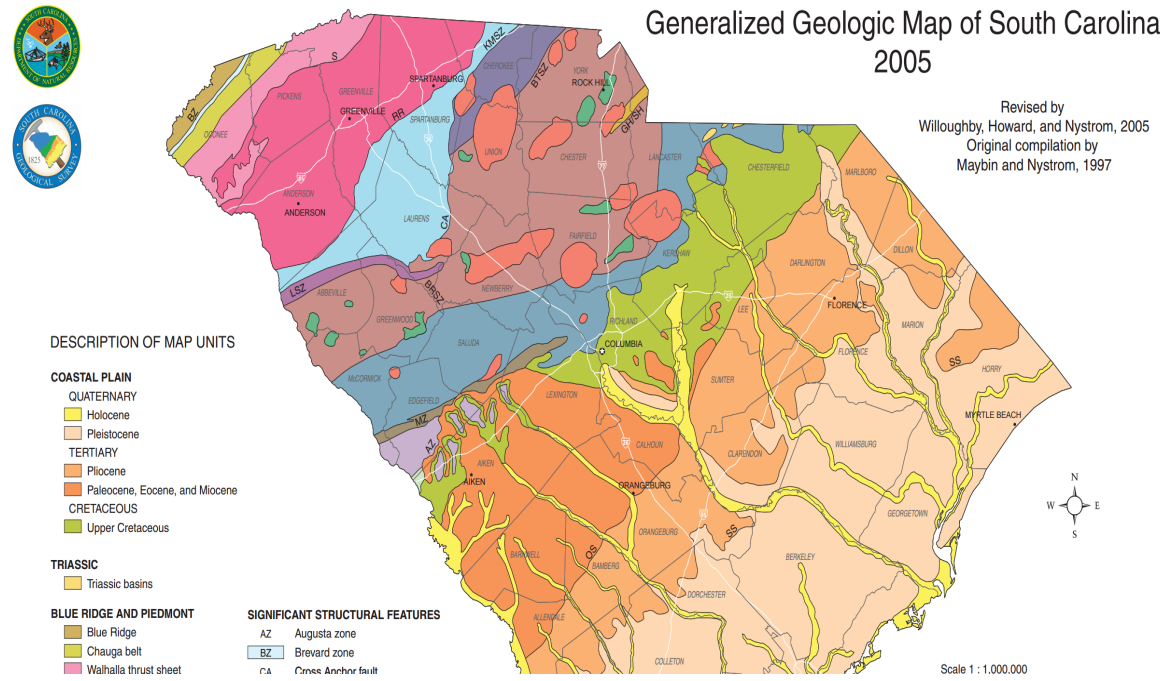

Figure 3-1: South Carolina Map Divided into Geological Sections

In this study, seven sources of GAB were selected as shown in Table 3-1 and Figure 3-2. Five of these same sources were mixed with Type I cement to produce CSAB samples as shown in Table 3-1 and Figure 3-3. One clayey soil (CS) source and one sandy soil (SS) source, one reclaimed asphalt pavement (RAP) source, and Type I cement were utilized with different mix ratios to investigate the effects of RAP content and cement content on CMRB and S-C as shown in Table 3-1and Figure 3-4In the test pit facility, a test section consisting of a Tuscaloosa local red clay

subgrade and a GAB layer made from source MC was constructed and tested as shown in Table 3-1 and Figure 3-5. All test methods and test results of are presented in the following sections.

Table 3-1: Materials Used for Samples of Various Base Layer Types

Type of Base Layer	Material Used for Samples
GAB	• Vulcan Gray Court (VG) • Martin Marietta Cayce (MC) • Martin Marietta Berkeley (MB) • Wake Stone North Myrtle Beach (WN) • Hanson Jefferson (HJ) • Vulcan Pacolet (VP) • Martin Marietta Rock Hill (MR)
CSAB	• Vulcan Gray Court (VG) • Martin Marietta Cayce (MC) • Martin Marietta Berkeley (MB) • Wake Stone North Myrtle Beach (WN) • Hanson Jefferson (HJ) • Type I cement
CMRB	• Non-fractionated RAP source (F&R Easley) • 1 soil source from upper state (Clayey soil) • 1 soil source from lower state (Sandy soil) • Type I cement
S-C	• 1 soil source from upper state (Clayey soil) • 1 soil source from lower state (Sandy soil) • Type I cement
Test pit	• Subgrade Layer: Red clay • Base Layer: Martin Marietta Cayce (MC)

Notes: GAB ~ Graded aggregate base; CSAB ~ Cement stabilized aggregate base; CMRB ~ cement modified recycled base

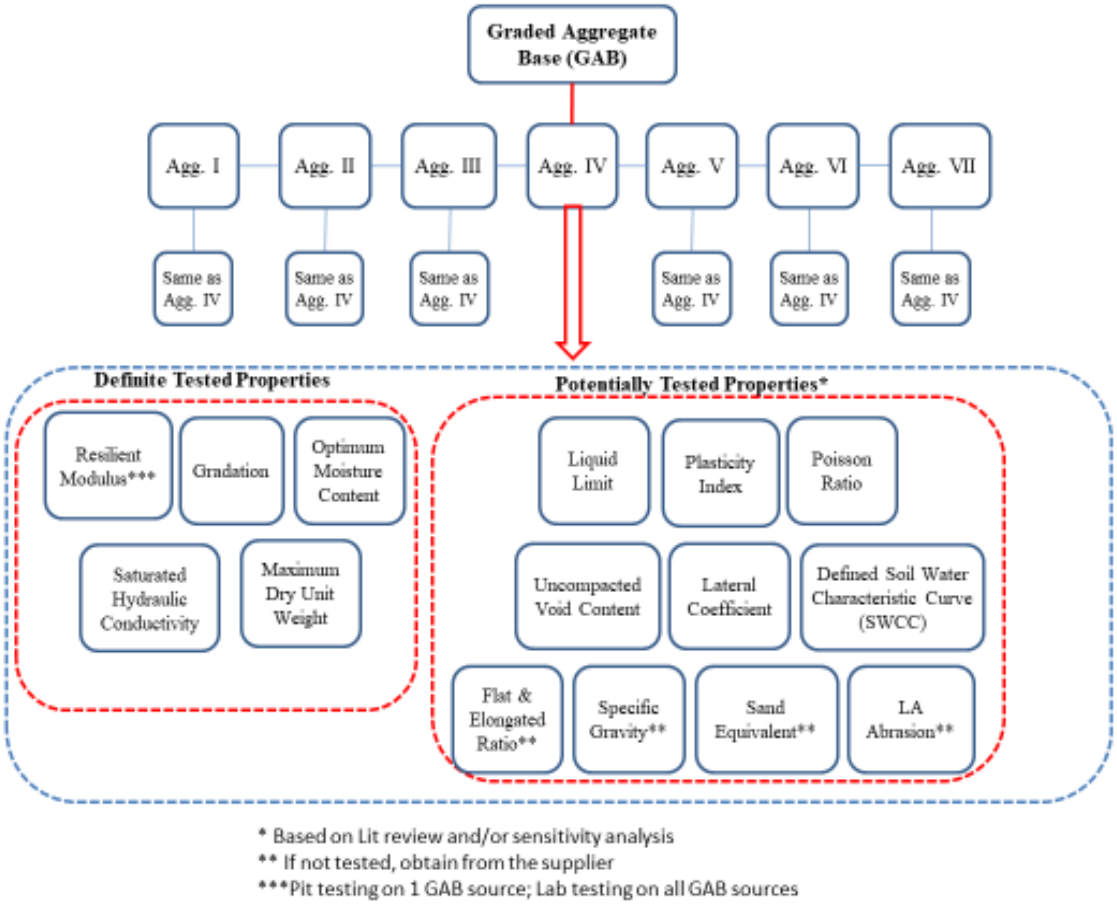

Figure 3-2: Flow Chart of Data Collection in Terms of Graded Aggregate Base

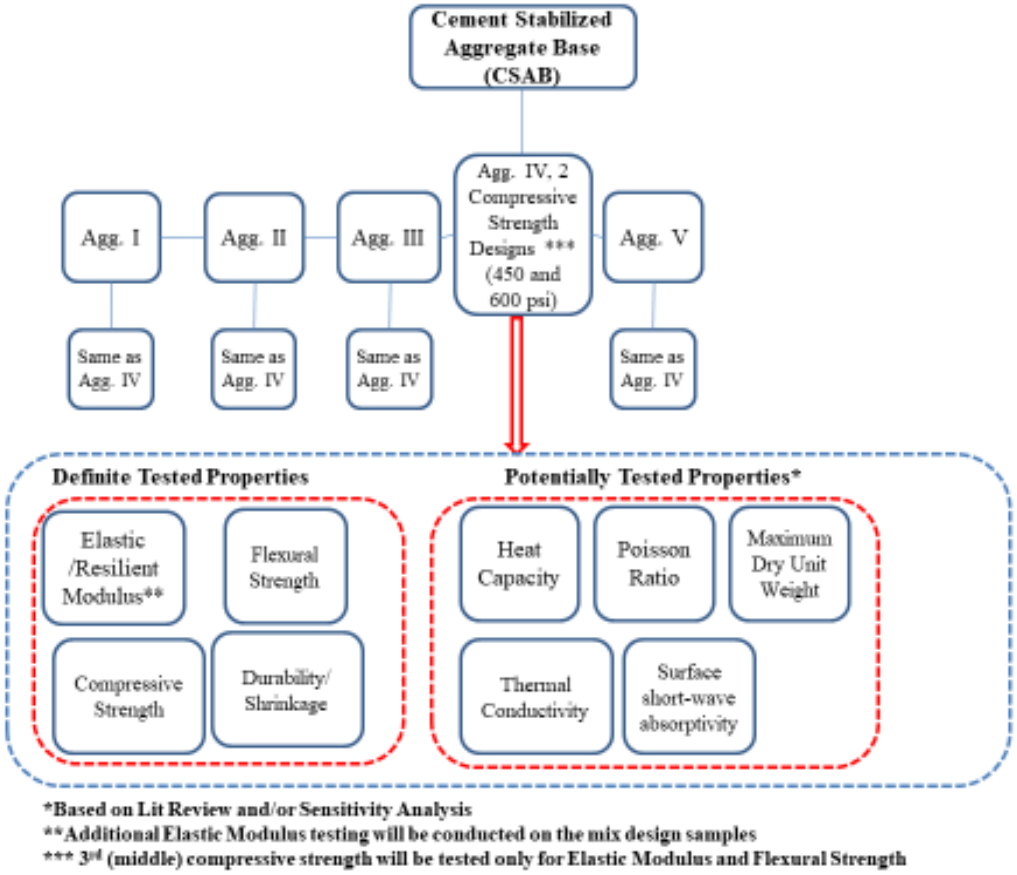

Figure 3-3: Flow Chart of Data Collection in Terms of Cement Stabilized Aggregate Base

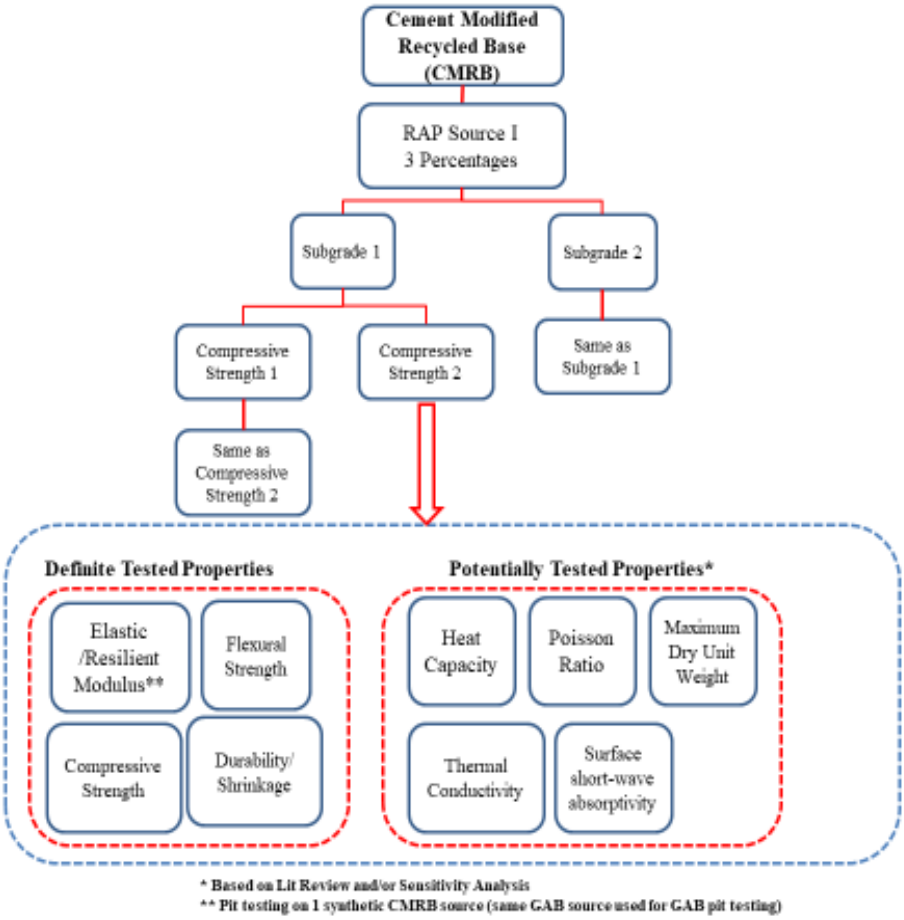

Figure 3-4: Flow Chart of Data Collection in Terms of Cement Modified Recycled Base

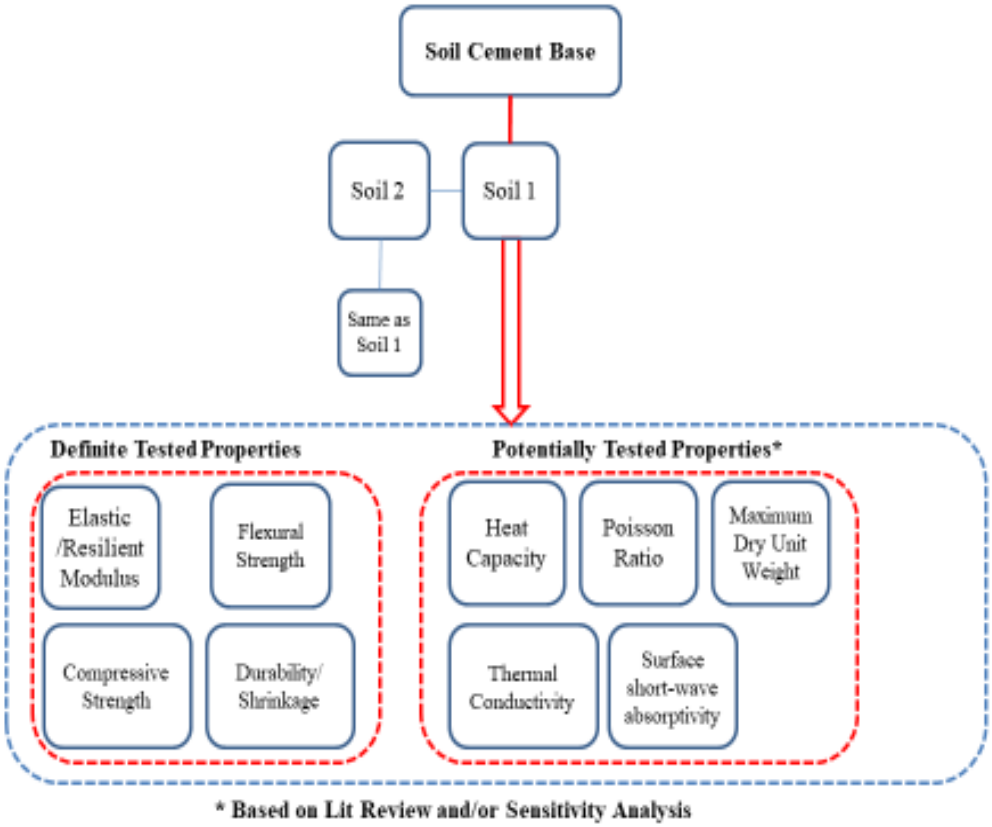

Figure 3-5: Flow Chart of Data Collection in Terms of Soil-Cement

3.2 Sample Fabrication and Test Method

Figure 3-6 shows the steps of this research study, including sample fabrication, curing, testing, and data processing. The three assembled molds shown were used for different materials and tests. As shown in Table 3-2, the 6-inch diameter fabricated samples were used in all tests for GAB and CSAB mixtures, while the 4-inch diameter samples were utilized in compressive strength tests for CMRB. The 2-inch diameter sample size was used to test the S-C specimens. According to SCDOT's requirement, compressive strength values at 7 days were obtained as a basic index to evaluate the cement treated materials. After 28 days curing duration, the cement was fully hydrated, and the resilient modulus tests were also completed. Data processing ensured the reliability and repeatability of test results in this study.

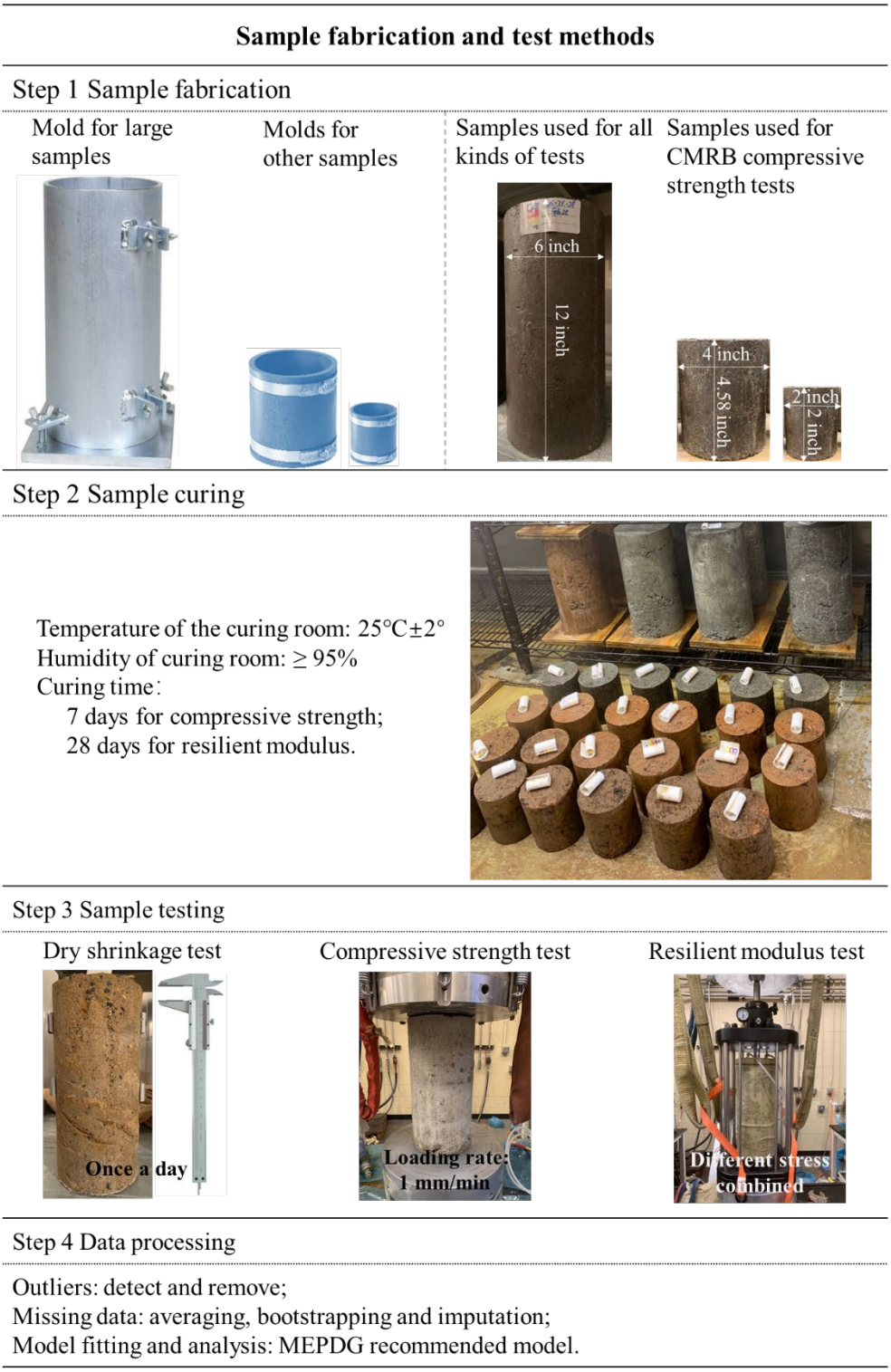

Figure 3-6: Flow Chart of Implementation Process of Sample Fabrication and Tests

3.2.1 Sample Fabrication

For GAB and CSAB, samples that were 6 inches in diameter and 12 inches in height were used to test compressive strength, dry shrinkage, elastic modulus, and resilient modulus. The GAB samples were compacted by hand hammer, but a vibratory hammer was employed when making CSAB samples shown in Table 3-2, as required by SC-T-142. In addition, two other sample sizes for CMRB specified by SCDOT (SC-T-26 and SC-T-38 test procedures) were utilized in this study.

The test pit consisted of a layer of geofoam, protective plywood, a fat clay, and various thicknesses of GAB material from source MC. The fat clay was compacted using a portable tamping compactor (i.e. jumping jack) until a compaction of at least 95% was achieved as measured by a sand cone test. The GAB layer, consisting of MC aggregate, was also compacted using a portable tamping compactor (i.e. jumping jack) until a compaction of at least 95% was achieved as measured by a sand cone test. It is noted that SC-T-140 requires 100% compaction of GAB materials but due to the use of a jumping jack in a relatively confined space, this was lowered to a minimum of 95% for constructability purposes.

Table 3-2: Mold Size and Corresponding Compacting Tools for Different Samples

Type of Base Layer	Mold Size	Sample Compacting Tool
GAB	• 6 in. diameter x 12 in. height	• Hand Hammer
CSAB	• 6 in. diameter x 12 in. height	• Vibratory Hammer
CMRB	• 6 in. diameter x 12 in. height • 4 in. diameter x 4.58 in. height	• Vibratory Hammer • Hand Hammer
S-C	• 2 in. diameter x 2 in. height	• Hand Hammer
Test Pit	• 3 ft. length x 3 ft. width	• Portable Tamper

Notes: GAB ~ Graded aggregate base; CSAB ~ Cement stabilized aggregate base; CMRB ~ cement modified recycled base

3.2.2 Raw Materials Test Methods

Prior to making samples of the various types of base layers, the raw materials were tested. According to ASTM specification, particle distributions and Atterberg limits need to be obtained prior to determining the aggregate classification. Due to the limits of physical sieving with respect to fine particles, the Hydrometer test was employed to obtain the particle distribution range below 0.075 mm for material containing more than 5% fine particles. The liquid limit and plastic index were also performed for the above-specified materials. For the macadam materials,

the flakiness content and crushing value were tested. The list of all test methods, devices, and specifications utilized in this study are shown in Table 3-3.

Table 3-3: Test Methods of Raw Materials

Material	Test Content	Test Method or Main Test Device	Specification
Aggregates	• Grain size • Crushing value • Flakiness content • Atterberg limits • Moisture-density relation	• Physical sieving • LA Abrasion • N/A • Casagrande cup • Compaction test	• ASTM E 112 • ASTM C 131 • ASTM D 3398 • ASTM D 4318 • ASTM D 558
Clayey and Sandy Soil	• Grain size • Hydrometer test • Atterberg limits • Moisture-density relation	• Physical sieving • Hydrometer • Casagrande cup • Compaction test	• ASTM E 112 • ASTM D 7928 • ASTM D 4318 • ASTM D 558
Red Clay	• Gradation • Hydrometer test • Atterberg limits	• Physical sieving • Hydrometer • Casagrande cup	• ASTM E 112 • ASTM D 7928 • ASTM D 4318

3.2.3 Fabricated Sample Test Methods

Once the raw materials had been analyzed, samples of the various types of base layers were fabricated and tested. In this study, compressive strength, elastic modulus, dry shrinkage and resilient modulus were evaluated according to standard test methods from ASTM or AASHTO as shown in

Table 3-4. The primary equipment used in the testing regime consisted of several closed-loop servo-hydraulic actuator systems with data acquisition capabilities.

According to Annex B of AASHTO T307, particles must be scalped if they are larger than 25% of the diameter of the specimen. Thus, for a 6” diameter specimen, all particles greater than 1.5” must be scalped. Of the aggregate sources used in this study, only MR, MB, and VG had any particles larger than 1.5”. For these sources, the larger particles (comprising less than 3% of the total gradation) were scalped prior to making the samples for resilient modulus testing. The remaining sources met the specification for particle size without scalping.

Table 3-4: Standard Test Methods for Compressive Strength, Elastic Modulus, Dry Shrinkage and Resilient Modulus

Material	Test Content	Main Test Device	Specification
GAB	• Resilient modulus	• Servohydraulic	• ASTM T307
CSAB and CMRB	• Compressive strength • Elastic modulus • Dry shrinkage • Resilient modulus	• Servohydraulic • Servohydraulic • Demec Gauges • Servohydraulic	• ASTM C 39 • ASTM C 39 • ASTM C 596 • AASHTO T307
Test pit	• Resilient modulus	• Servohydraulic	• N/A

Notes: GAB ~ Graded aggregate base; CSAB ~ Cement stabilized aggregate base; CMRB ~ cement modified recycled base

3.2.4 Elastic Modulus Method

At this time, there is no standardized test method to measure the elastic modulus of cement stabilized granular/soil materials. Numerous researchers have proposed different methods to evaluate the elastic modulus. Physical methods, such as static compressive testing, and non-destructive methods, such as ultrasonic pulse velocity and seismic response, have all been used to determine the elastic behavior of stabilized soil materials. With the physical methods, researchers have proposed using different portions of the stress-strain curve to determine the linear elastic response. Given the inherent non-linear behavior of soils, even those that are stabilized, a decision was made to use the secant method.

The physical testing procedure follows ASTM C39 with the exception that the strain in the specimen is also measured. This was measured with both the displacement setup on the testing frame as well as a non-contact 3D spatial positioning setup, and the results from the two methods were found to be similar. To calculate the elastic modulus, the slope of a line drawn from the origin to the stress-strain curve that represents 25% of the ultimate stress.

3.2.5 Resilient Modulus Data Processing Method

All resilient modulus testing was completed according to AASHTO T 307. In this study, 16 combinations of various confining and axial (vertical) stresses were examined for GAB and CSAB. Axial loads were dynamic (cyclic) using a haversine-shaped load pulse with 0.1-sec

loading and a 0.9-sec rest period. Confining stress was applied using a triaxial pressure chamber in static mode. During the testing process, it was found that the deviator stress could increase the resilient modulus of CSAB. This is not unexpected as granular materials, especially those that are stabilized, can exhibit an increased M_R. For CMRB materials, given the extremely stiff material, the testing was modified to include a total of 23 cycles (including the "0" cycle) for CMRB as shown in Table 3-5.

The PavementME-recommended stress dependent constitutive model (see Equation 3-1) was utilized to fit measured resilient modulus values for all samples and three k-values were calculated through regression analysis [149, 150]. The coefficient of determination, R^2, was used to evaluate the fitting quality.

Equation 3-1 $$M_R = K_1 P_a \left(\frac{\theta}{P_a}\right)^{K_2} \left(\frac{\tau_{oct}}{P_a} + 1\right)^{K_3}$$

Where

M_R = resilient modulus value;

k_1, k_2, and k_3 = regression coefficients;

Pa = normalizing stress (atmospheric pressure, e.g., 14.7 psi);

θ = bulk stress = $(\sigma_1 + \sigma_2 + \sigma_3) = (3\sigma_3 + \sigma_d)$

Where

σ_1, σ_2, and σ_3 = principal stresses and

$\sigma_2 = \sigma_3$ and σ_d = deviator (cyclic) stress = $\sigma_1 - \sigma_3$; and

τ_{oct} = octahedral shear stress = $\sqrt{(\sigma_1 - \sigma_2)^2 + (\sigma_1 - \sigma_3)^2 + (\sigma_2 - \sigma_3)^2}/3$

Equation 3-2 $$R^2 = 1 - \frac{(n-k-1)}{(n-1)} \left(\frac{S_e}{S_y}\right)^2$$

Equation 3-3 $$S_e = \sqrt{\frac{\sum_1^n (\hat{y}_i - y_i)^2}{n-k-1}}$$

Equation 3-4 $$S_y = \sqrt{\frac{\sum_1^n (y_i - \bar{y})^2}{n-1}}$$

Where

R^2 = the coefficient of determination;

S_e =standard error of estimate;

S_y = standard error of deviation;

y_i = measured dynamic modulus;

n = number of sample; and

K = number of independent variables used in model

Table 3-5: Deviator and Confining Stress Settings for Different Base Layer Types

No. of cycle	0	1	2	3	4	5	6	7	8	9	10	11	12	13	14	15	16	17	18	19	20	21	22
Applied Cyclic Stress, psi	13.5	2.7	5.4	8.1	4.5	9	13.5	9	18	27	9	13.5	27	13.5	18	36	45	63	81	99	45	63	81
Applied Confining Stress, psi	15.0	3.0	3.0	3.0	5.0	5.0	5.0	10.0	10.0	10.0	15.0	15.0	15.0	20.0	20.0	20.0	20.0	20.0	20.0	20.0	25.0	25.0	15.0
Deviator Stress, psi	3	3	6	9	5	10	15	10	20	30	10	15	30	15	20	40	49	67	85	103	49	67	85
Bulk Stress, psi	48	12	15	18	20	25	30	40	50	60	55	60	75	75	80	100	109	127	145	163	124	142	130
	GAB, CSAB, CMRB																Additional cycles for CMRB						

3.2.6 Soil Pit Testing and Data Processing

The full-scale effects of a single graded aggregate base material were quantified in a soil test pit. The test pit is comprised of a reinforced concrete structure with a nominal volume of 1,000 ft^3. For this project, the general configuration of the setup was:

- Geofoam layer: 3 feet thick
- Fat clay layer: approximately 18 inches thick
- GAB (Cayce): thicknesses of 8, 12, and 14 inches

The load cycles were applied using a closed-loop servo-hydraulic system. The 30-kip hydraulic actuator used a circular steel plate assembly to apply loads to the various configurations (Figure 3-7). The load plates were designed in a similar fashion to the plate load test commonly used on subgrade materials to measure modulus of subgrade reaction. A series of linear variable displacement transducers (LVDTs) were used to capture deflections throughout the test (Figure 3-8). There were three LVDTs equidistant apart along the edge of the loading plate to measure the displacement of the plate during each load pulse. The data from these LVDTs was analyzed to ensure that the load plate was uniformly displacing downward and not rotating during each pulse. Four additional LVDTs were placed at increasing distances away from the load plate, in a similar manner that geophones are used for Falling Weight Deflectometer (FWD) testing. All LVDTs used were spring loaded to ensure they would accurately measure both positive and negative displacements.

Figure 3-7: Photo of Load Plate Assembly. A set of three plates are used to increase the stiffness of the assembly.

Figure 3-8: Photo of LVDT Located on GAB Layer

The load pulse was modeled after the pulse shape (i.e. haversine) that is used in the AASHTO T-307 test method. Since the load plate diameter was larger than that used in for the previous GAB testing which followed the AASHTO T-307 specification, the pulse duration was doubled (Figure 3-9).

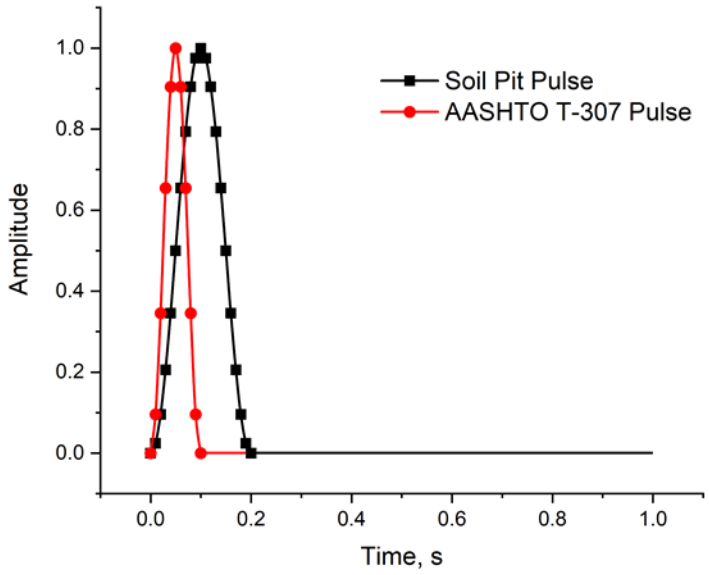

Figure 3-9: Comparison of AASHTO T-307 Load Pulse and Soil Test Pit Load Pulse. Both pulses are haversine pulses.

The testing regime consisted of a series of repeated load cycles at several loading levels (Table 3-6). To ensure uniform loading of the GAB material during each load cycle, a thin cement slurry was cast underneath the loading plate to ensure uniform contact. A seating load of 1,000 lbf was maintained on the test area once the testing process began (i.e. the load was never released between increases of load levels).

Table 3-6: Testing Plan for Soil Pit Materials

Load, lbf	*Stress at Top of GAB, psi*	*Number of Cycles*
3,000	13.2	1,000
5,000	22.0	1,000
7,000	30.8	1,000
9,000	39.7	1,000

Numerous studies have shown varying levels of correlation between the triaxial resilient modulus and the field back-calculated modulus from FWD testing. For this analysis, the FHWA-recommended ratio of 1.43 was used to convert laboratory-measured resilient modulus values to back-calculated field values.

To this end, the layered elastic back-calculation software BAKFAA, published by the Federal Aviation Administration (FAA), was used to verify the resilient modulus relationship. Unlike FWD testing in the field, the layer thicknesses were precisely known which likely increased the accuracy of the back-calculation process. Additionally, the load plate was precisely leveled and the GAB layer was uniformly loaded. This is not always the case with field-run FWD measurements as the typical bracketed load pad may not lie flat and level on a field constructed base.

CHAPTER 4: RESULTS AND DISCUSSION

4.1 Test Results of Raw Materials

4.1.1 Aggregate/Soil Classification

The gradations of the seven aggregate sources and both subgrade sources are shown in Figure 4-1 to Figure 4-10. It can be noted that Figure 4-1 (aggregate source MC) shows poorly graded stone with a high percentage of ¾" to #4 sized particles. Aggregate sources VG, MB, and VP are also poorly graded as shown in Figure 4-2, Figure 4-3, and Figure 4-6.

Atterberg limit testing was completed for the fine particles (≤ 200 mm) of these same materials listed above with the exception of VG, MR, VP, and the sandy subgrade source because these materials were mainly comprised of sand. For the remaining materials, the tested values were within the liquid limit range of 17-23. According to the liquid-plastic classification chart, it can be noted that these materials were low liquid soils. In addition, the results indicated that MB and the clayey subgrade source showed relatively higher liquid limits of 35 and 36, respectively.

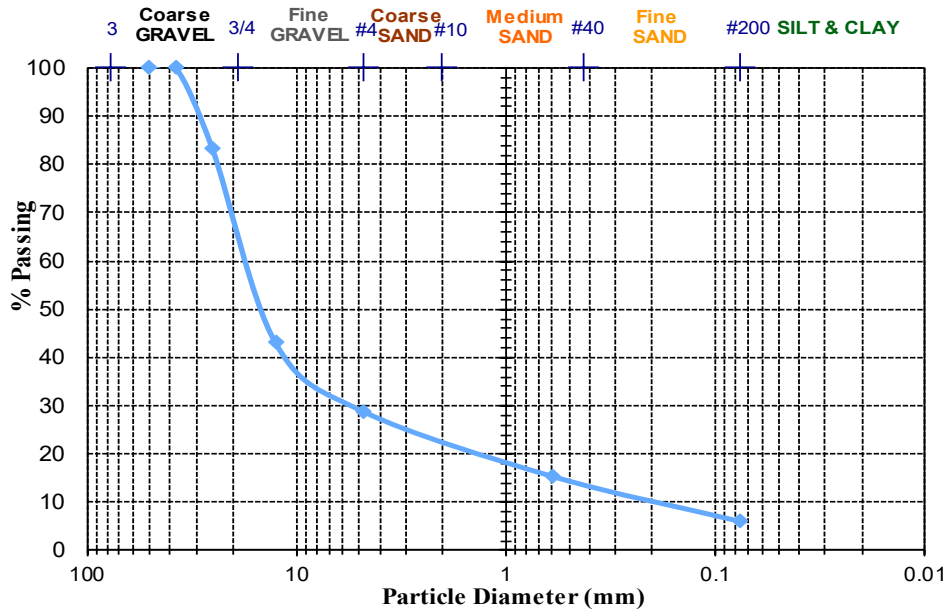

Figure 4-1: Gradation and Classification Results of Aggregate Source MC

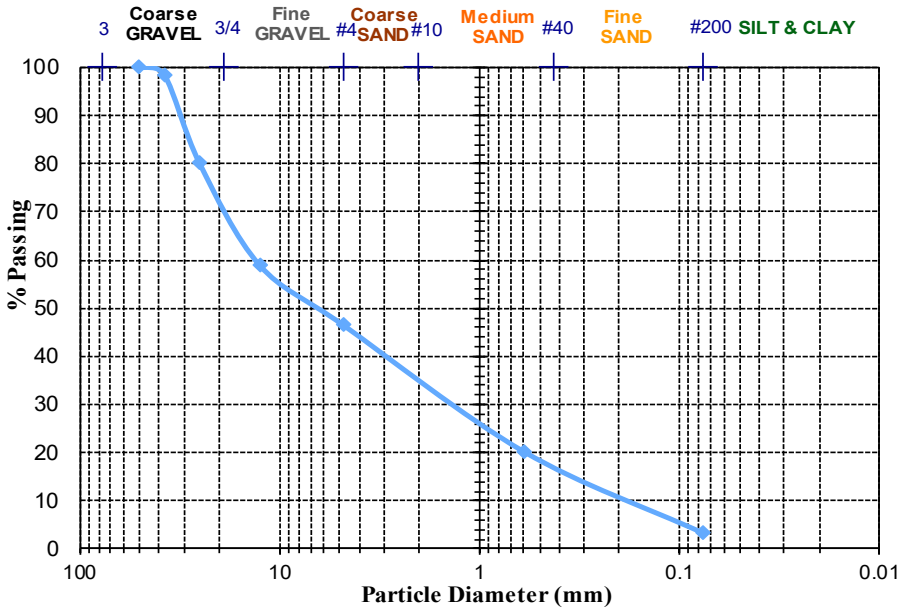

Grain Size Distribution Curve						Atterberg Limits:	
% Gravel:	53.67	D_{10}:	0.19	C_u:	73.68	LL:	NP
% Sand:	43.19	D_{30}:	1.50	C_c:	0.85	PL:	NP
% Fines:	3.14	D_{60}:	14.00			PI:	NP

Soil Classification: Poorly Graded Gravel with Sand (GP)

Figure 4-2: Gradation and Classification Results of Aggregate Source VG

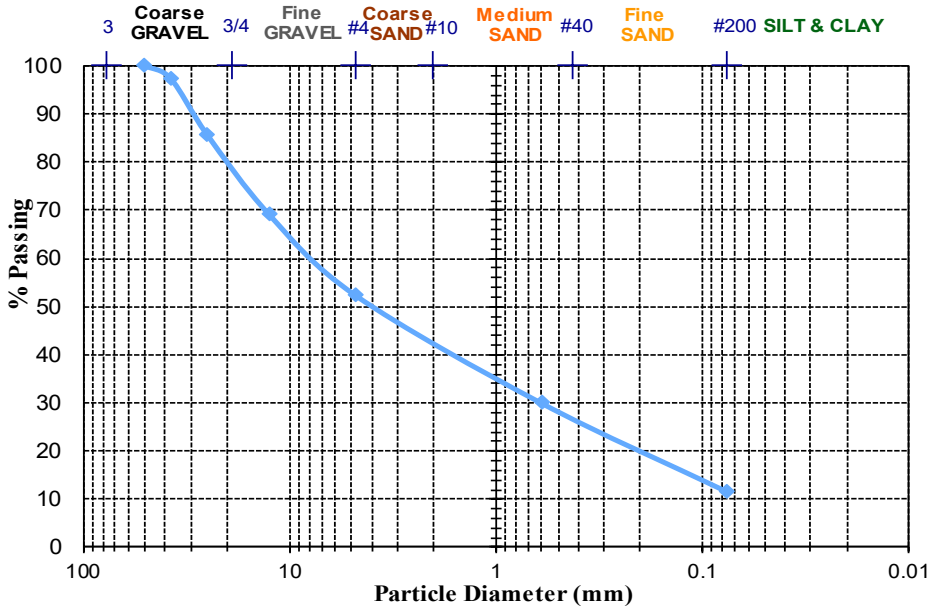

Grain Size Distribution Curve						Atterberg Limits:	
% Gravel:	47.69	D_{10}:	0.07	C_u:	119.40	LL:	35
% Sand:	40.77	D_{30}:	0.60	C_c:	0.67	PL:	25
% Fines:	11.54	D_{60}:	8.00			PI:	10

Soil Classification: Poorly Graded Gravel with Silt and Sand (GP-GM)

Figure 4-3: Gradation and Classification Results of Aggregate Source MB

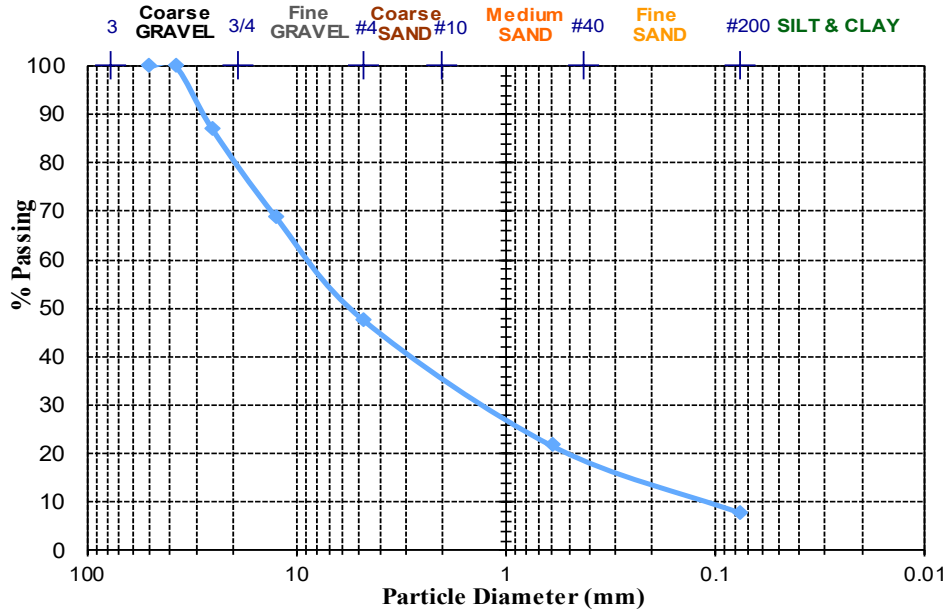

Grain Size Distribution Curve — **Atterberg Limits:**

% Gravel:	52.40	D_{10}:	0.12	C_u:	75.00	LL:	23
% Sand:	39.82	D_{30}:	1.40	C_c:	1.81	PL:	17
% Fines:	7.78	D_{60}:	9.00			PI:	6

Soil Classification: Well-Graded Gravel with Silty Clay and Sand (GW-GC)

Figure 4-4: Gradation and Classification Results of Aggregate Source WN

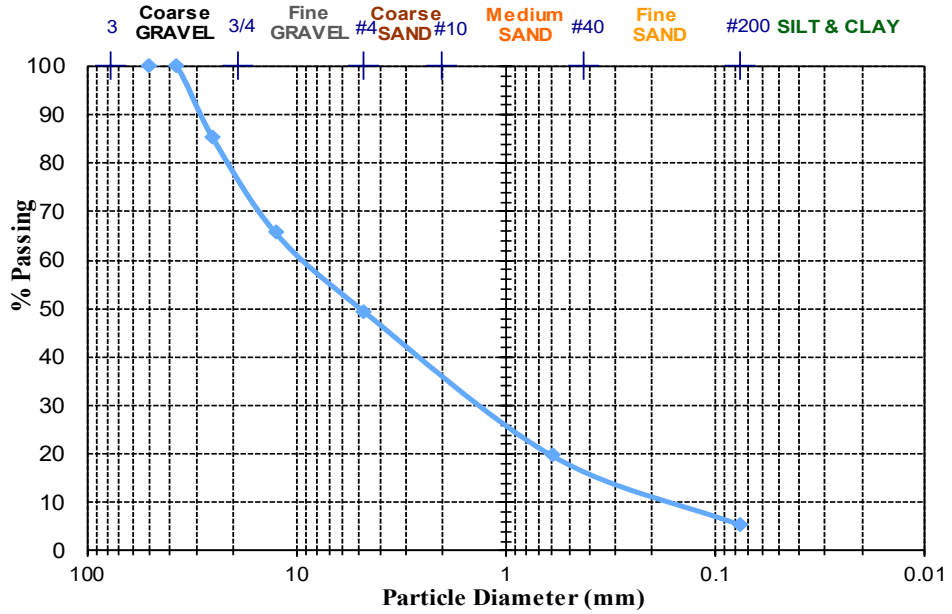

Grain Size Distribution Curve — **Atterberg Limits:**

% Gravel:	50.61	D_{10}:	0.17	C_u:	58.82	LL:	17
% Sand:	44.08	D_{30}:	1.50	C_c:	1.32	PL:	14
% Fines:	5.32	D_{60}:	10.00			PI:	3

Soil Classification: Well-Graded Gravel with Silt and Sand (GW-GM)

Figure 4-5: Gradation and Classification Results of Aggregate Source HJ

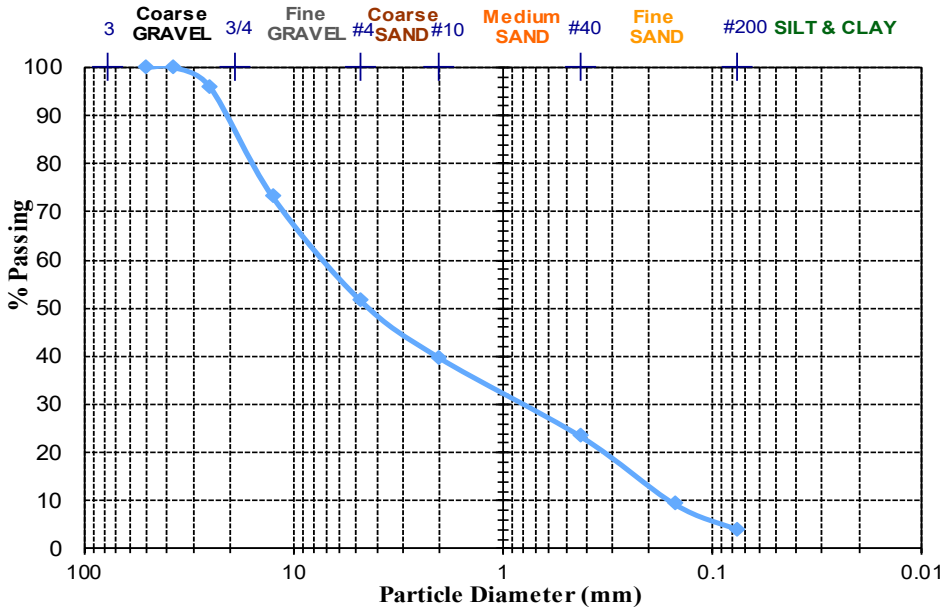

Grain Size Distribution Curve

% Gravel:	48.40	D_{10}:	0.17	C_u:	42.35	**Atterberg Limits:**	
% Sand:	47.53	D_{30}:	0.83	C_c:	0.56	LL:	NP
% Fines:	4.07	D_{60}:	7.20			PL:	NP
						PI:	NP

Soil Classification: Poorly Graded Gravel with Sand (GP)

Figure 4-6: Gradation and Classification Results of Aggregate Source VP

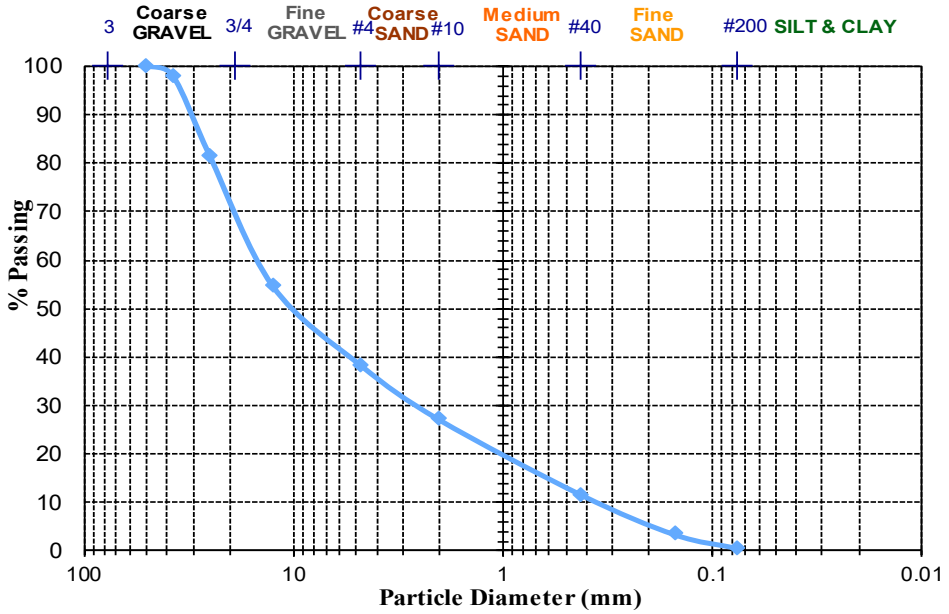

Grain Size Distribution Curve

% Gravel:	61.65	D_{10}:	0.36	C_u:	46.67	**Atterberg Limits:**	
% Sand:	37.70	D_{30}:	2.70	C_c:	1.21	LL:	NP
% Fines:	0.65	D_{60}:	16.80			PL:	NP
						PI:	NP

Soil Classification: Well-Graded Gravel with Sand (GW)

Figure 4-7: Gradation and Classification Results of Aggregate Source MR

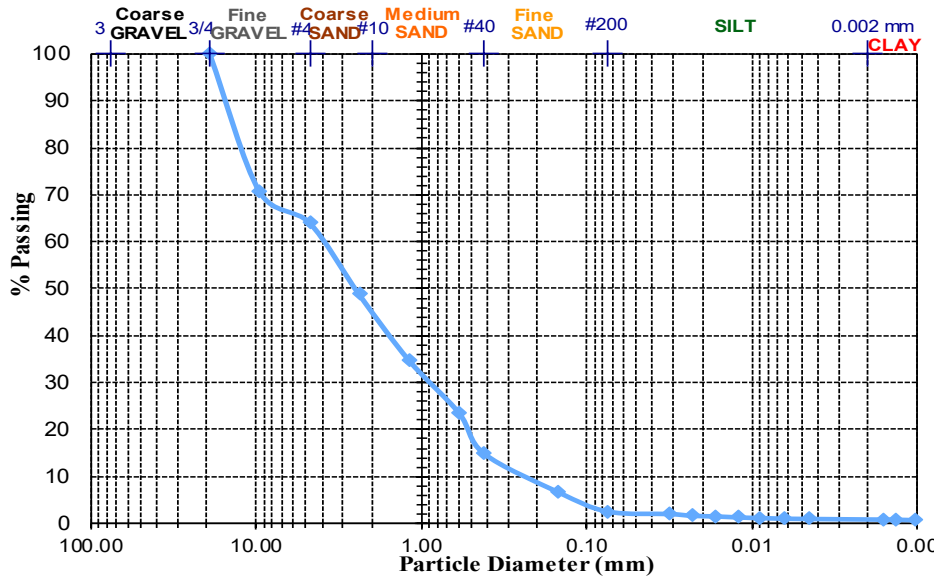

Grain Size Distribution Curve — **Atterberg Limits:**

% Gravel:	35.95	D_{10}:	0.23	C_u:	16.52	LL:	35.84
% Sand:	61.57	D_{30}:	0.94	C_c:	1.01	PL:	21.71
% Silt:	1.70	D_{60}:	3.80			PI:	14.13
% Clay:	0.78						

Soil Classification: Well-Graded Sand with Gravel (SW)

Figure 4-8: Gradation and Classification Results of Clayey Subgrade Source

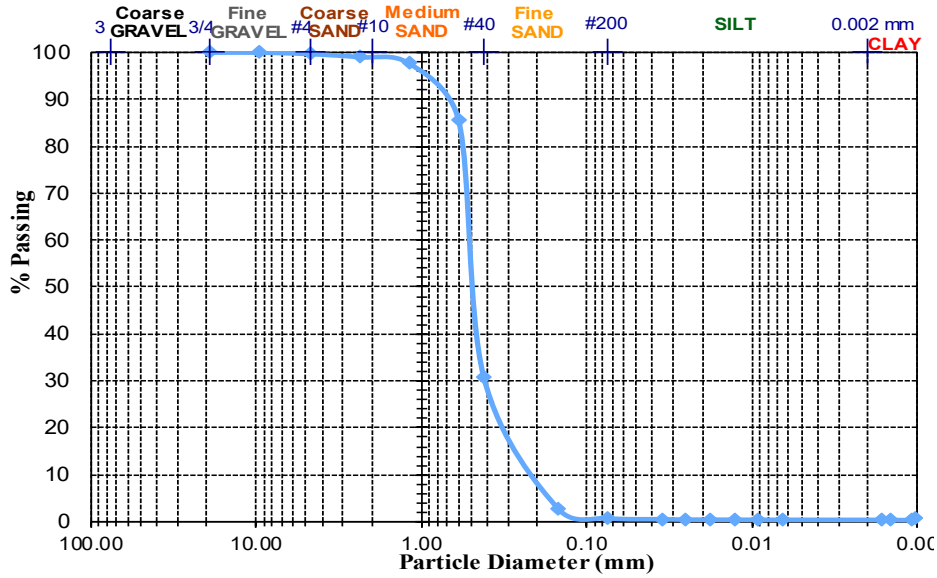

Grain Size Distribution Curve — **Atterberg Limits:**

% Gravel:	0.30	D_{10}:	0.23	C_u:	2.22	LL:	NP
% Sand:	99.04	D_{30}:	0.42	C_c:	1.50	PL:	NP
% Silt:	0.37	D_{60}:	0.51			PI:	NP
% Clay:	0.30						

Soil Classification: Poorly Graded Sand (SP)

Figure 4-9: Gradation and Classification Results of Sandy Subgrade Source

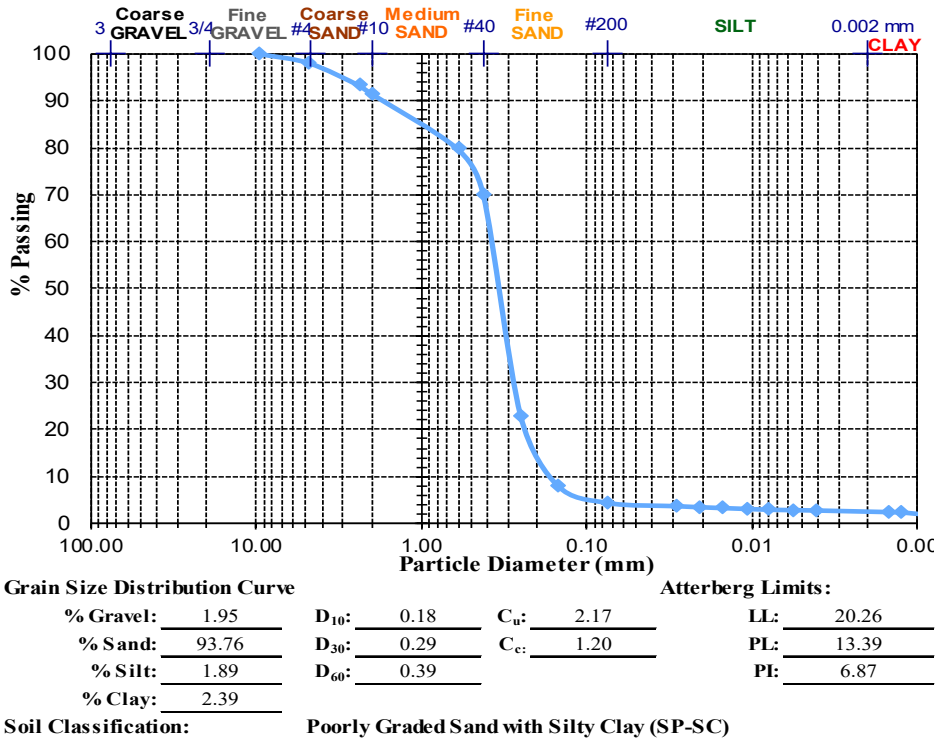

Figure 4-10: Gradation and Classification Results of Subgrade Clay for Soil Pit Testing

For the CMRB mixtures, the RAP gradation is shown in Figure 4-11. Most particles were within a diameter range of 0.6-12.5 mm, and it can be observed that the RAP was a uniformly distributed material that mainly provides a skeleton for the CMRB mixtures.

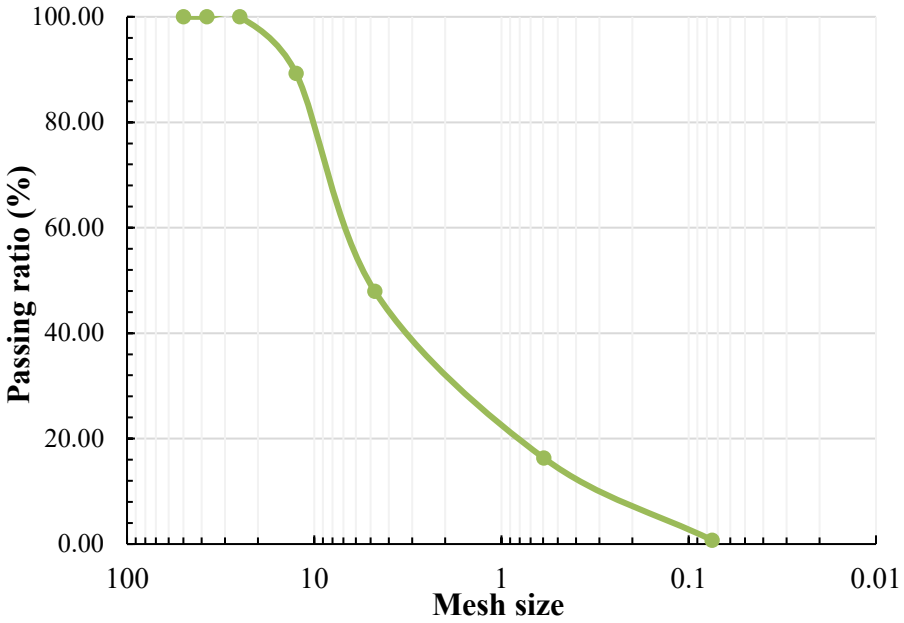

Figure 4-11: Gradation of RAP

4.1.2 Crushing Value

Crushing values of all aggregate sources are summarized in Table 4-1. It indicates that sources MB and WN show relatively higher crushing values when compared to the other five sources. A higher crushing value would cause a more significant change of aggregate gradation during compaction, which also makes these sources more sensitive to quality control processes before base construction.

Table 4-1: Crushing Values of Aggregate Sources

Aggregate Source	Crushing value (%)
MB	24.93
HJ	18.03
MC	13.58
WN	24.54
VG	17.86
MR	13.13
VP	15.56

Notes: VG ~ Vulcan Gray Court; MC ~ Martin Marietta Cayce; MB ~ Martin Marietta Berkeley; WN ~ Wake Stone North Myrtle Beach; HJ ~ Hanson Jefferson; VP ~ Vulcan Pacolet; MR ~ Martin Marietta Rock Hill

4.1.3 Flakiness Content

Flakiness contents of all aggregate sources are summarized in Table 4-2. Flakiness content of MR was the highest, followed by VP, MC, HJ, VG, MB, and WN. It can be noted that aggregates MR and VP have relatively higher contents compared with other aggregates in this study. It is also interesting to note that the two sources with the highest crushing values (MB and WN) exhibited the lowest flakiness contents. This reveals the different behaviors at work when various aggregate sources break down.

Table 4-2: Flakiness Content of Aggregate Sources

Aggregate Source	Flakiness content (%)
MB	6.24
HJ	11.87
MC	11.93
WN	4.78
VG	8.72
MR	40.99
VP	26.06

Notes: VG ~ Vulcan Gray Court; MC ~ Martin Marietta Cayce; MB ~ Martin Marietta Berkeley; WN ~ Wake Stone North Myrtle Beach; HJ ~ Hanson Jefferson; VP ~ Vulcan Pacolet; MR ~ Martin Marietta Rock Hill

4.1.4 Moisture-Density Value

In this study, a 6 (152.4-mm) diameter mold with a 10-lb (4.54-kg) rammer dropped from a height of 18" (457 mm) were used to compact the specimens in order to obtain moisture-density values of the various aggregate sources. Table 4-3 lists the optimum moisture content (OMC) and maximum dry density (MDD) values of all aggregate sources. Aggregate source MB exhibited a higher OMC value and lower MDD value than the other sources, indicating that this material has a higher specific surface area and lower density than the other sources.

Table 4-3: OMC and MDD of Aggregate Sources

Aggregate Source	OMC (%)	MDD (pcf)
MB	9.20	129.24
HJ	3.50	142.80
MC	4.35	139.33
WN	5.20	135.00
VG	4.93	140.98
MR	3.80	141.59
VP	6.30	131.94

Notes: OMC ~ optimum moisture content; MDD ~ maximum dry density; VG ~ Vulcan Gray Court; MC ~ Martin Marietta Cayce; MB ~ Martin Marietta Berkeley; WN ~ Wake Stone North Myrtle Beach; HJ ~ Hanson Jefferson; VP ~ Vulcan Pacolet; MR ~ Martin Marietta Rock Hill

The moisture-density curves, as determined from proctor testing (AASHTO T99), of the various CMRB mixtures are summarized in Figure 4-12 and Figure 4-13. The results show that an increased percentage of RAP resulted in a decrease in OMC and an increase in MDD of both clayey soil-based and sandy soil-based CMRB. In addition, CMRB mixtures made with clayey soil compared to sandy soil types generally exhibited different OMC and MDD values due to different clay properties.

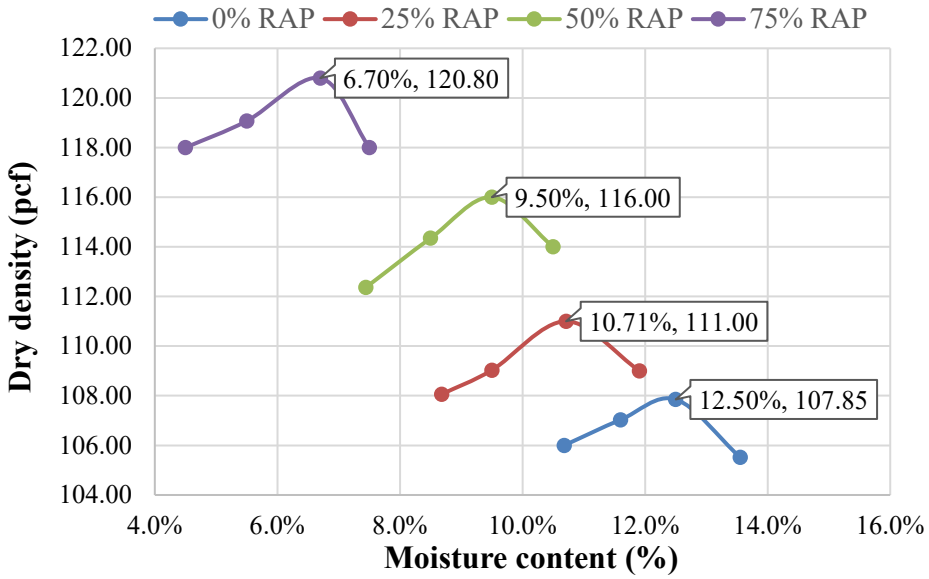

Figure 4-12: Relationship between Dry Density and Moisture Content of Clayey Soil with Various RAP Contents

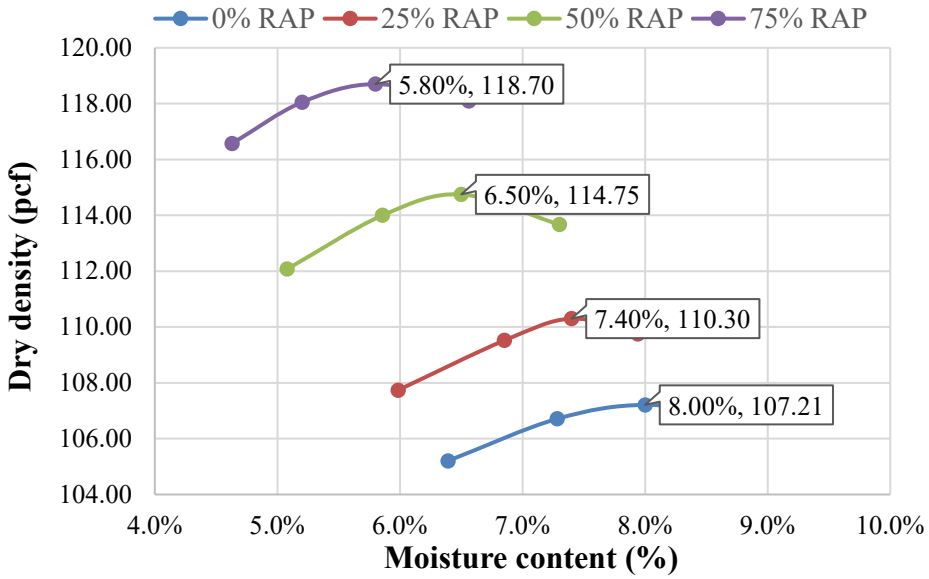

Figure 4-13: Relationship between Dry Density and Moisture Content of Sandy Soil with Various RAP Contents

4.2 Graded Aggregate Base (GAB) Test Results

4.2.2 Resilient Modulus

The resilient modulus of the GABs at different moisture contents (OMC-2%, OMC-1%, and OMC) were determined from testing following AASHTO T307. According to Annex B of AASHTO T307, particles must be scalped if they are larger than 25% of the diameter of the specimen. Thus, for a 6" diameter specimen, all particles greater than 1.5" must be scalped. Of the aggregate sources used in this study, only MR, MB, and VG had any particles larger than 1.5". For these sources, the larger particles (comprising less than 3% of the total gradation) were scalped prior to making the samples. The remaining sources met the specification for particle size without scalping. In Table 4-4, the generated coefficients of determination from tested results and predicted values were generally larger than 0.8, indicating that the models were appropriate.

The measured values were within the expected ranges. It is also known that moisture content can affect the resilient modulus behavior. There did not appear to be a consistent trend between the resilient modulus and moisture content (Figure 4-14). This is not necessarily unexpected, given the widely varying gradations, angularity, and other physical properties of the materials evaluated. Others have noted that trends can vary and "rules of thumb" may not be necessarily valid for larger, granular materials [151].

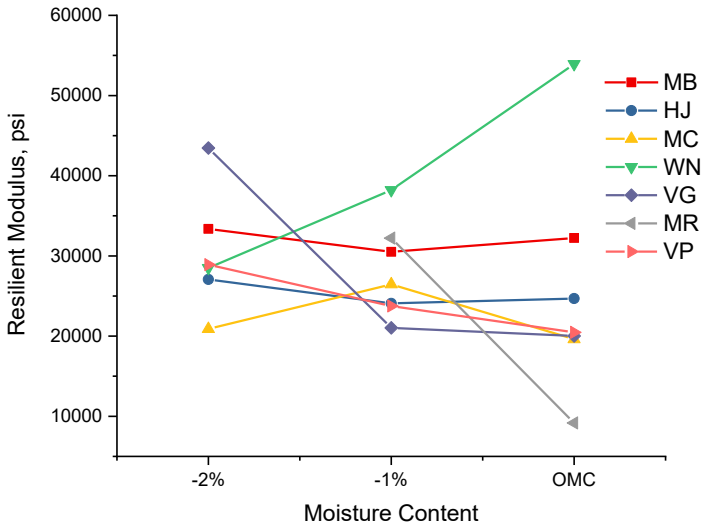

Figure 4-14: Relationship between Resilient Modulus and Moisture Content of GAB with Various Aggregate Sources

Table 4-4: Measured and Predicted Resilient Modulus Values of GAB at Different Moisture Contents

Aggregate Source	Moisture Content	K_1	K_2	K_3	Measured M_R, Seq. 6 (psi)	Predicted M_R (psi)	Coefficient of Determination (R^2)
MB	OMC-2%	778.92	0.44	0.29	19,391	17,066	0.81
	OMC-1%	538.02	0.34	0.87	13,710	13,217	0.89
	OMC	677.89	0.63	-0.09	15,861	14,520	0.81
HJ	OMC-2%	805.29	0.44	-0.05	15,810	15,486	0.73
	OMC-1%	396.69	0.35	0.82	8,981	9,041	0.89
	OMC	601.91	0.22	0.83	15,073	13,635	0.82
MC	OMC-2%	396.96	0.29	0.90	10,417	9,544	0.87
	OMC-1%	604.44	0.42	0.36	13,839	13,048	0.86
	OMC	466.66	0.25	0.74	10,899	10,034	0.84
WN	OMC-2%	3,153.76	0.08	-0.01	17,345	14,208	0.40
	OMC-1%	1,103.363	0.352	0.217	23,698	22,347	0.82
	OMC	556.93	0.25	0.99	50,452	48,831	0.86

Aggregate Source	Moisture Content	K_1	K_2	K_3	Measured M_R, Seq. 6 (psi)	Predicted M_R (psi)	Coefficient of Determination (R^2)
VG	OMC-2%	1,032.09	0.65	-0.26	21,035	21,247	0.92
	OMC-1%	515.39	0.34	0.44	11,149	10,404	0.80
	OMC	650.06	0.17	0.49	12,843	12,462	0.75
MR*	OMC-1%	690.49	0.29	0.76	18,840	16,317	0.84
	OMC	453.89	0.21	0.54	10,643	8,959	0.56
VP	OMC-2%	816.17	0.52	-0.12	16,298	15,818	0.81
	OMC-1%	583.95	0.30	0.56	12,600	11,999	0.87
	OMC	501.03	0.34	0.48	11,225	10,499	0.82

Notes: VG ~ Vulcan Gray Court; MC ~ Martin Marietta Cayce; MB ~ Martin Marietta Berkeley; WN ~ Wake Stone North Myrtle Beach; HJ ~ Hanson Jefferson; VP ~ Vulcan Pacolet; MR ~ Martin Marietta Rock Hill. Sequence 6 results are presented for comparison with outcomes listed in NCHRP Research Results Digest Number 285.

**The sample for -2% OMC could not be satisfactorily constructed due to low moisture content.*

4.3 Cement Stabilized Aggregate Base (CSAB) Test Results

4.3.1 Compressive Strength of CSAB

In this study, the effects of both cement content and curing time on compressive strength of CSAB were analyzed. Three cement contents (3%, 5%, and 7%) and two curing durations (7 days and 28 days) were used to fabricate the specimens. Five of the seven previously-used aggregate sources were selected for the CSAB portion of the study with two samples made at each condition. The mean value of compressive strength for each mixture from different sources are shown in Table 4-5.

Table 4-5: Compressive Strength of CSAB

Aggregate Source	Compressive Strength (psi)					
	3% Cement Content		5% Cement Content		7% Cement Content	
	7 days	28 days	7 days	28 days	7 days	28 days
WN	756.1	1,020.2	1,084.6	1,783.6	1,560.1	2,037.7
VG	697.9	1,005.6	1,399.0	2,203.7	1,894.0	2,518.2
HJ	985.1	1,091.0	1,764.0	2,682.7	2,272.0	2,828.7
MB	342.8	539.4	475.4	806.8	701.9	991.7
MC	532.9	661.7	803.1	1,370.5	1,418.9	2,034.1

Notes: VG ~ Vulcan Gray Court; MC ~ Martin Marietta Cayce; MB ~ Martin Marietta Berkeley; WN ~ Wake Stone North Myrtle Beach; HJ ~ Hanson Jefferson;

4.3.1.1 Compressive Strength of CSAB Fitted with S-Shape Curve

The compressive strength from the 7-day curing duration is one of the most important design factors for CSAB. Generally, a design value of 450 psi and 600 psi should be achieved for different conditions. In this study, the S-shape curve formula was utilized to show the

relationship between compressive strength and cement content as shown in Figure 4-15 to Figure 4-19. Typical cement contents generated compressive strengths that met the minimum requirements.

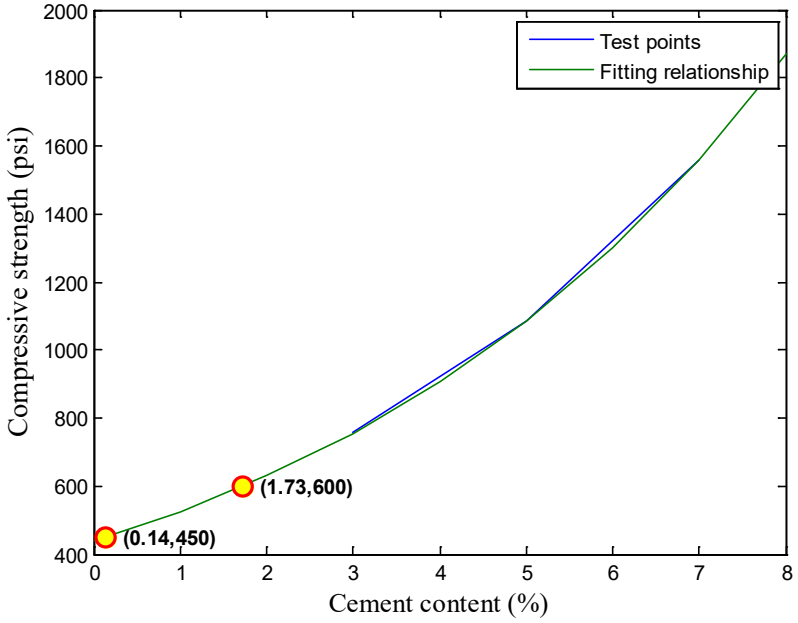

Figure 4-15: Fitting Results of WN Compressive Strength at 7 Days

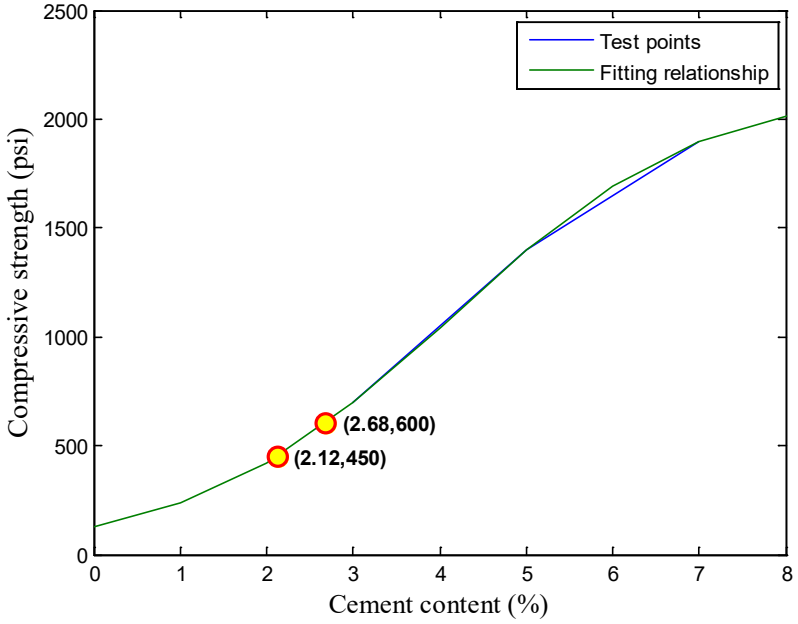

Figure 4-16: Fitting Results of VG Compressive Strength at 7 Days

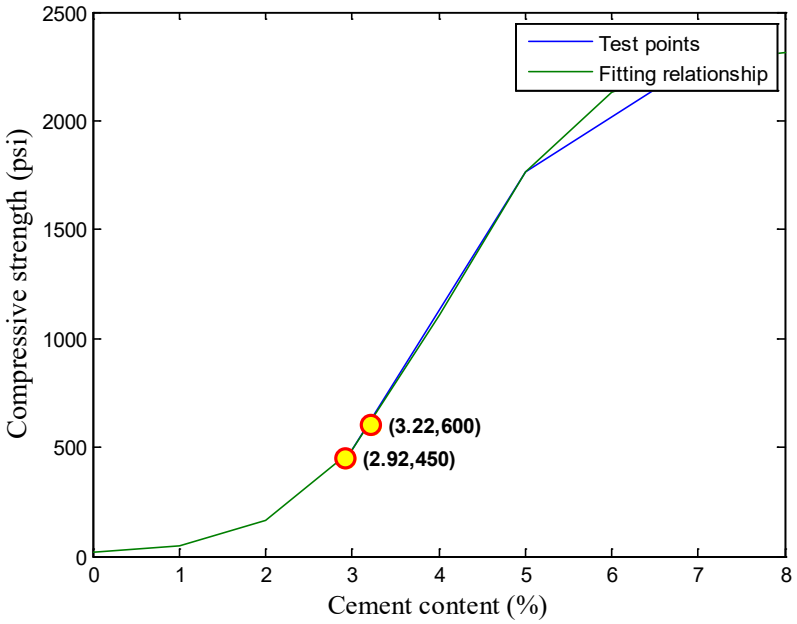

Figure 4-17: Fitting Results of HJ Compressive Strength at 7 Days

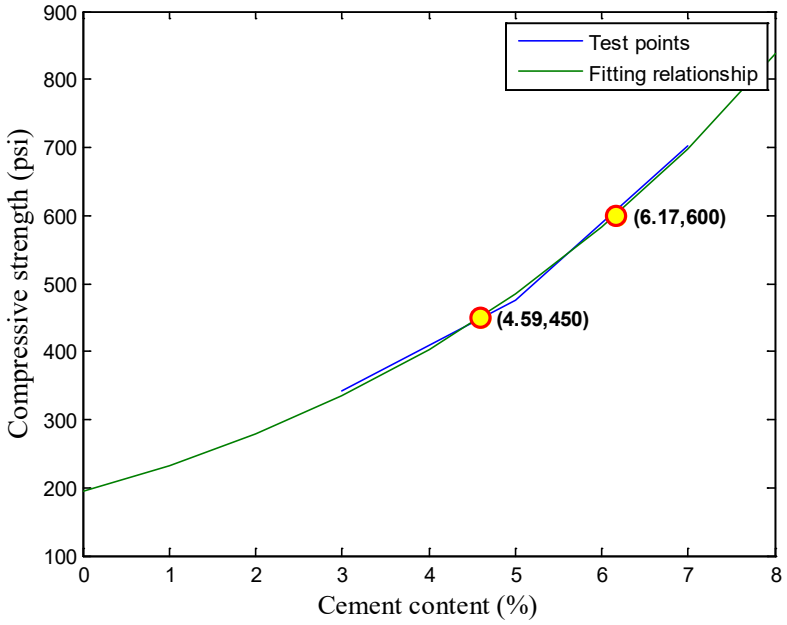

Figure 4-18: Fitting Results of MB Compressive Strength at 7 Days

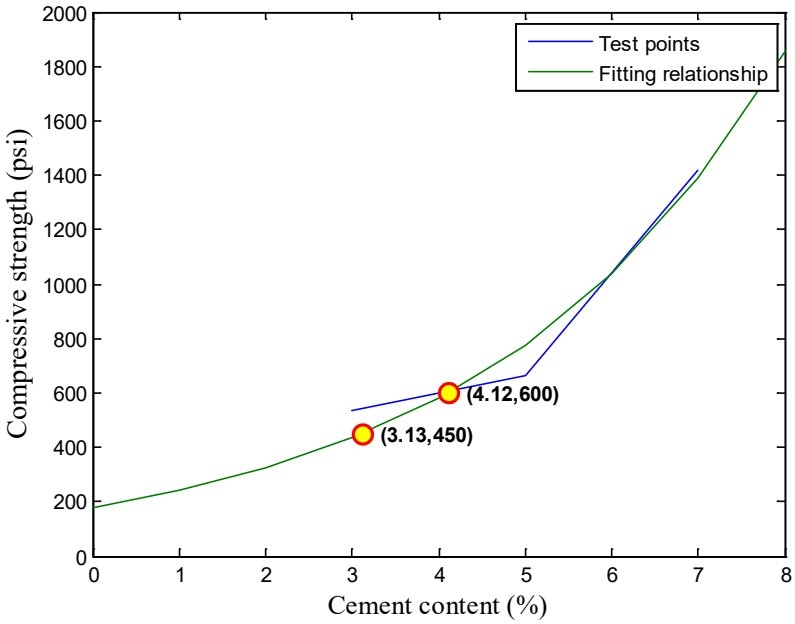

Figure 4-19: Fitting Results of MC Compressive Strength at 7 Days

4.3.1.2 Effect of Cement Content on Compressive Strength of CSAB

Figure 4-20 and Figure 4-21 show the compressive strength test results of mixtures from all five aggregate sources at various cement contents. These values obviously increased as the cement content increased regardless of aggregate source or curing duration. However, the results at 7 days curing showed that the value trends for increasing cement content were convex curves for from aggregates HJ and VG while value trends from aggregates WN, MB, and MC were concave curves. At 28 days curing, the value trends from HJ and VG were still convex while MB and MC were still concave, but the WN data exhibited a convex curve trend.

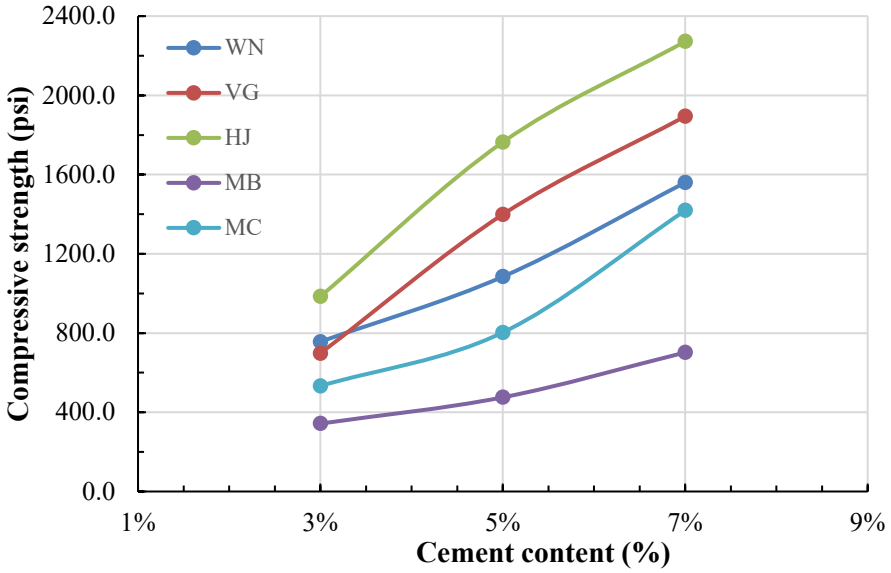

Figure 4-20: Influence of Cement Content on Compressive Strength of CSAB at 7 Days

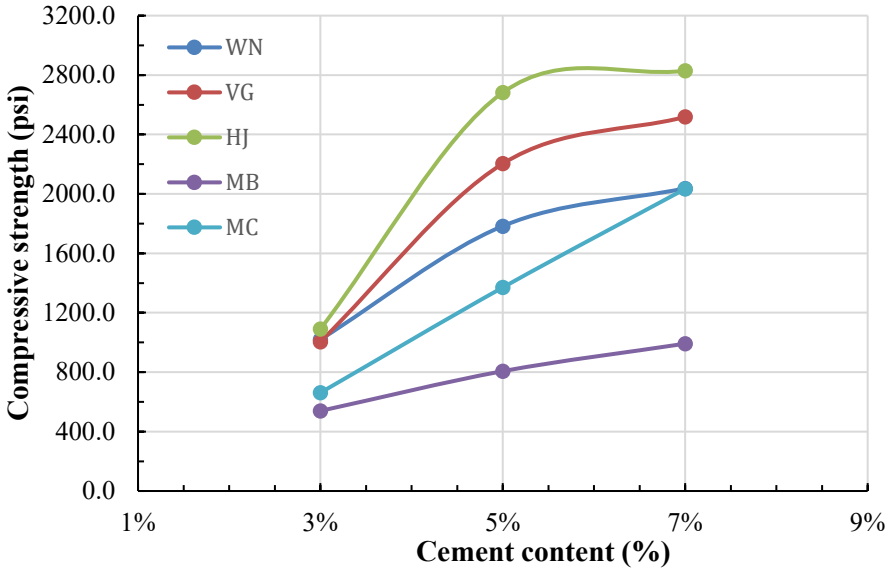

Figure 4-21: Influence of Cement Content on Compressive Strength of CSAB at 28 Days

4.3.1.3 Effect of Curing Duration on Compressive Strength of CSAB

Curing duration is another important factor affecting the compressive strength of a concrete material. Figure 4-22 shows that, as expected, the compressive strength values at 28 days were remarkably higher than the strengths of the respective mixtures at 7 days, regardless of aggregate source and cement content.

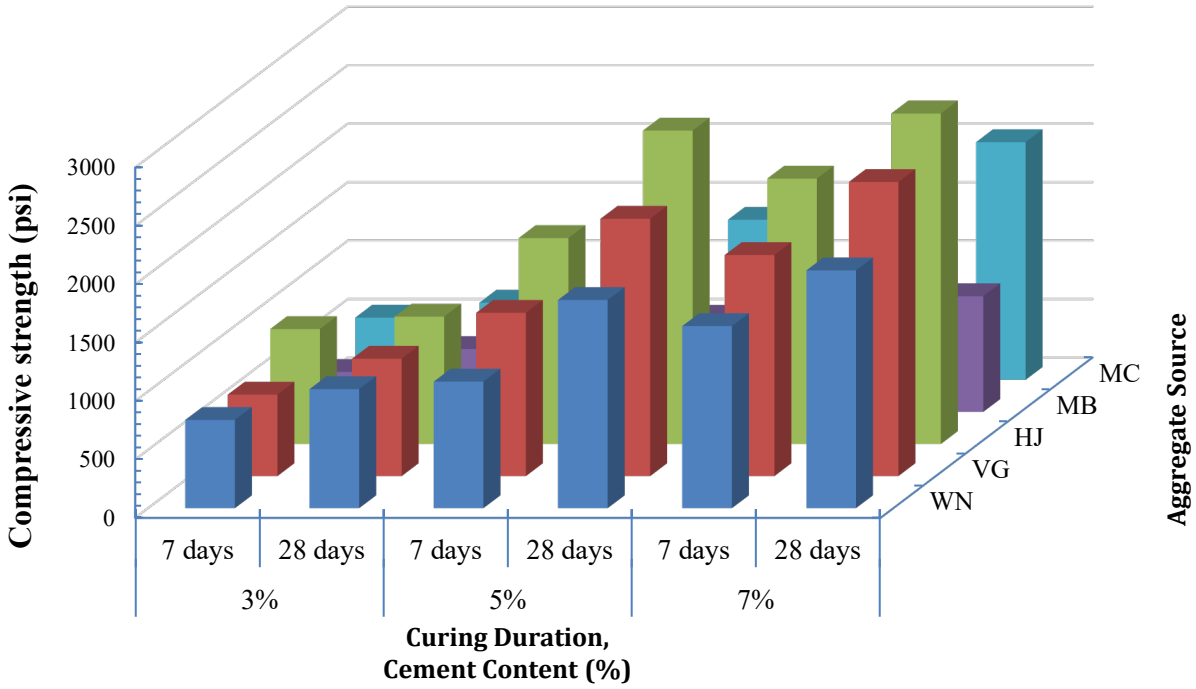

Figure 4-22: Influence of Curing Duration on Compressive Strength of CSAB at Various Cement Contents

4.3.1.4 Effect of Aggregate Source on Compressive Strength of CSAB

As shown in the graphs in the previous two sections (Figure 4-20 through Figure 4-22), regardless of cement content and curing duration, the compressive strengths from aggregate HJ were the highest, followed by aggregates VG, WN, MC, and MB. This indicates that aggregate source does affect compressive strength.

4.3.2 Elastic Modulus of CSAB

In this study, the effects of cement content and curing duration on elastic modulus were also analyzed. The same three cement contents (3%, 5%, and 7%) and two curing durations (7 days and 28 days) were utilized. As with the compressive strength testing, two samples were made at each condition for each of the five selected aggregate sources. Results are shown in Appendix F.

Elastic modulus values were affected by aggregate source, cement content, and curing duration. As expected, increased cement content resulted in an increase of elastic modulus regardless of

curing duration and aggregate source. In addition, the elastic modulus values at 28 days were remarkably higher than those values at 7 days regardless of cement content and aggregate source. However, the magnitude of the increase in elastic modulus value was dependent on both aggregate source and cement content.

The range of measured elastic modulus values in this study fell within the large range of values reported in the literature. Values as low as 100 ksi and as high as 1800 ksi have been reported by various researchers. Unfortunately, there does not exist a standardized procedure to measure the elastic modulus of a CSAB material. Nevertheless, the elastic modulus of a CSAB material is far less descriptive of the behavior than the resilient modulus, given the stresses applied to a CSAB material in the field. Therefore, it is recommended that the resilient modulus values, as indicated in the current version of AASHTO PavementME, should be used for CSAB analysis and design.

4.3.3 Dry Shrinkage of CSAB

Figure 4-23 presents the dry shrinkage values for the five selected aggregate sources with three cement contents (3%, 5%, and 7%) at 15 days. With the increase of cement content, dry shrinkage values increased regardless of aggregate source. The final dry shrinkage values of the mixtures from aggregate VG were the highest followed by aggregates HJ, MB, WN, and MC. Both cement content and aggregate source noticeably affected dry shrinkage values.

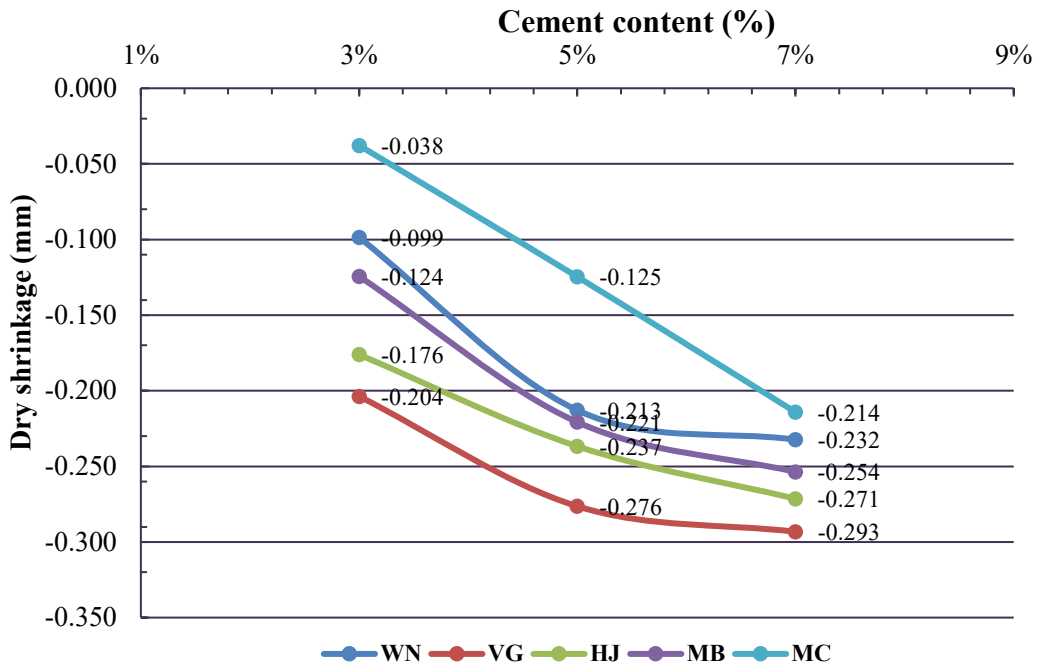

Figure 4-23: Final Dry Shrinkage Values of CSAB

4.3.4 Resilient Modulus of CSAB

The resilient modulus values at three different cement contents (3%, 5%, and 7%) and five aggregate sources were collected through the testing program described in Chapter 3 in accordance with AASHTO T 307. All samples were tested at OMC, and all measured values were corrected to account for frame stiffness of the testing equipment.

The developed models of these CSAB mixtures based on the previous equations all generally had coefficients of determination close to 0.90 as shown in Table 4-6. This indicates that the regression coefficients, or k-values, would be appropriate to calculate the resilient modulus at actual stress conditions in the pavement. Figure 4-24 shows the measured resilient modulus values vs. the predicted resilient modulus values for aggregate source WN. The remaining aggregate sources generally exhibited similar results as shown in Appendix A. Generally, the performance of the fitting is acceptable for engineering purposes as most fits had coefficients of determination above 0.90.

Table 4-6: Measured and Average Resilient Modulus Values of CSAB at Different Cement Contents

Aggregate Source	Cement Content	K_1	K_2	K_3	Measured M_R, Seq. 15 (psi)	Average M_R (psi)	Coefficient of determination (R^2)
WN	3%	1969.6	-0.15	2.90	245,039	91,929	0.93
	5%	1607.5	0.16	2.21	194,083	79,444	0.90
	7%	2147.9	-0.01	2.48	234,216	96,958	0.87
VG	3%	2254.5	-0.07	2.42	188,973	89,498	0.77
	5%	1766.0	-0.16	3.66	355,458	118,153	0.81
	7%	1444.5	0.14	2.93	332,563	103,945	0.94
HJ	3%	2074.9	-0.20	2.38	137,817	68,966	0.60
	5%	1968.9	0.22	1.47	150,173	73,393	0.91
	7%	1343.7	0.29	1.62	135,305	59,056	0.88
MB	3%	857.6	-0.39	5.79	755,222	158,386	0.92
	5%	2292.5	-0.06	3.24	N/A	117,399	0.78
	7%	438.7	-0.17	6.28	868,840	161,579	0.95
MC	3%	1663.7	-0.17	3.52	333,152	104,530	0.94

Aggregate Source	Cement Content	K_1	K_2	K_3	Measured M_R, Seq. 15 (psi)	Average M_R (psi)	Coefficient of determination (R^2)
	5%	1674.4	-0.14	3.63	411,360	118,619	0.89
	7%	1713.1	-0.06	2.78	221,382	83,463	0.92

Notes: Measured MR = resilient modulus at the last cycle; MR values corrected to account for frame stiffness.

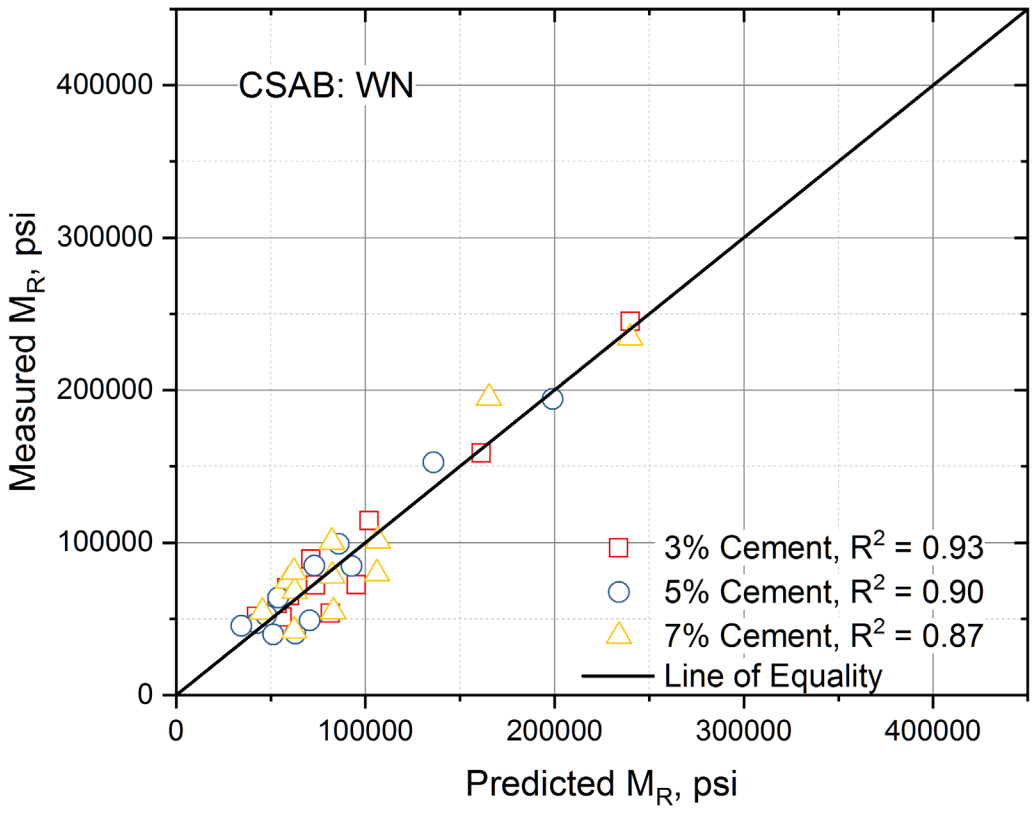

Figure 4-24: Measured vs. Predicted Resilient Modulus of WN at Various Cement Contents

4.3.4.1 Relationship between Stress and Strain during Repeated Loading Process for CSAB

A total of 15 cycles with different deviators and confining stresses (repeated 100 times) was applied to obtain strain and stress values. Figure 4-25 to Figure 4-27 show the stress and strain values at three cement contents for aggregate source WN. The stress-strain data for the remaining aggregate sources is shown in Appendix B. The stress-strain curves exhibited a noticeable increase with the increase of stress regardless of cement content. This implies that the resilient modulus of CSAB was generally stress-dependent.

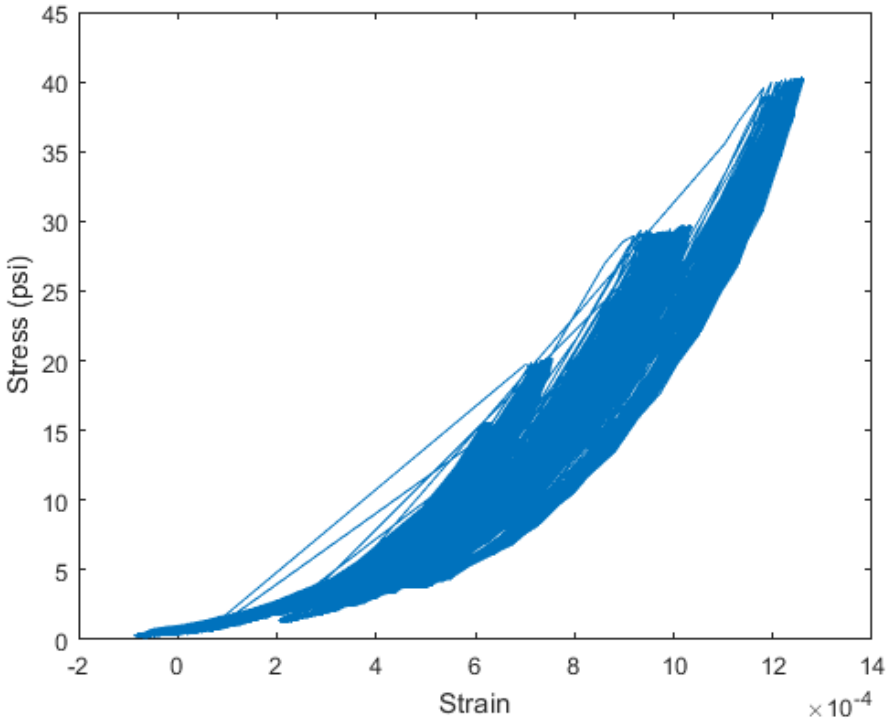

Figure 4-25: Stress and Strain Summation Curve of WN at 3% Cement Content

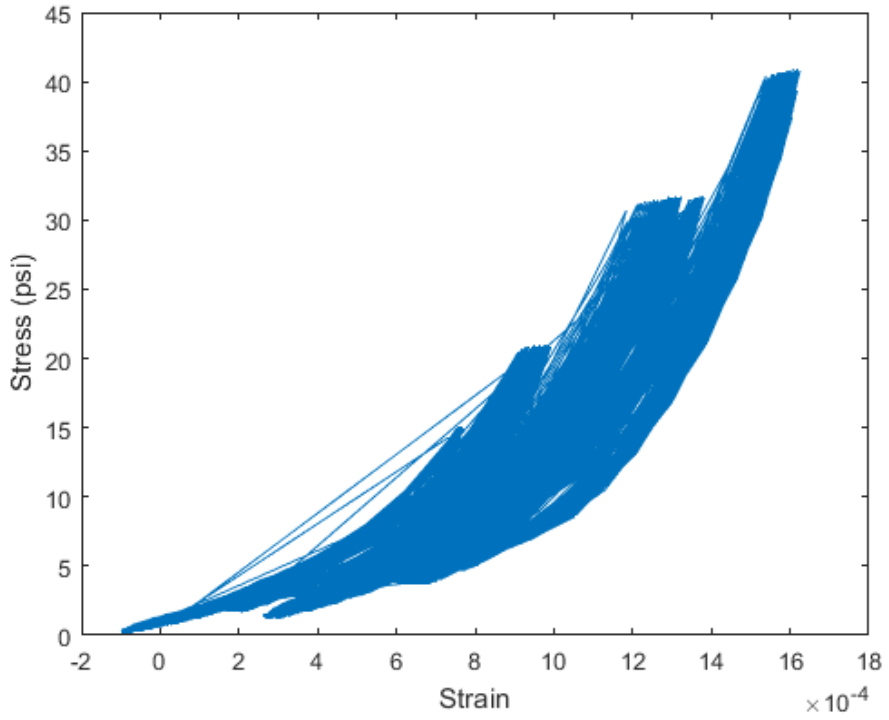

Figure 4-26: Stress and Strain Summation Curve of WN at 5% Cement Content

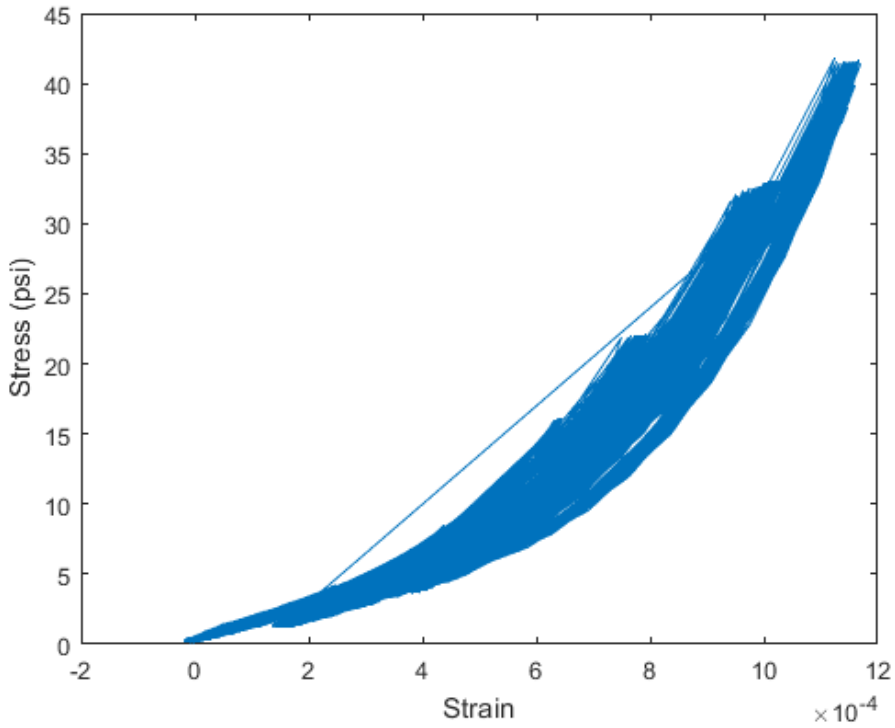

Figure 4-27: Stress and Strain Summation Curve of WN at 7% Cement Content

4.4 CMRB and S-C Test Results

4.4.1 Compressive Strength of CMRB and S-C

Two subgrade sources of different soil types (clayey soil and sandy soil) and four RAP contents (0%, 25%, 50%, and 75%) were used for this portion of the project. The 25%, 50%, and 75% RAP samples comprised the CMRB portion, while the 0% RAP samples comprised the S-C portion. For the S-C samples with 0% RAP content, cement contents of 6%, 9%, and 12% were utilized to improve the compressive strength of the soil materials. For the CMRB samples with 25%, 50% and 75% RAP contents, cement contents of 3%, 6%, and 9% were utilized. Table 4-7 summarizes the compressive strength results of all CMRB and S-C mixtures after 7-day and 28-day curing durations.

Table 4-7: Compressive Strength of CMRB and S-C

Soil Type and RAP Content (%)	Compressive Strength (psi)							
	3% Cement		6% Cement		9% Cement		12% Cement	
	7 days	28 days	7 days	28 days	7 days	28 days	7 days	28 days
CS-0%			132.02	179.19	185.00	292.03	290.30	494.44
CS-25%	73.2	84.73	128.0	208.62	257.7	294.43		
CS-50%	86.2	109.12	158.6	248.07	299.8	333.06		
CS-75%	139.2	176.96	213.7	288.25	322.4	365.55		
SS-0%			220.81	259.40	398.79	540.53	736.62	1,062.13
SS-25%	83.0	85.24	168.9	251.89	336.5	449.03		
SS-50%	92.6	116.26	234.0	317.01	439.8	536.46		
SS-75%	143.0	155.09	298.7	396.34	587.6	659.50		

Notes: CS ~ clayey soil; SS~ sandy soil

4.4.1.1 Compressive Strength of CMRB and S-C Fitted with S-Shape Curve

As with the CSAB samples in this study, in order to correlate compressive strength and cement content, the S-shape curve formula was utilized in lieu of repeating tests. The coefficients of determination shown in Table 4-8 indicate that this method was generally reliable. Figure 4-28 to Figure 4-31 show the fitting results of CMRB and S-C made with clayey soil. The fitting results of CMRB and S-C made with sandy soil are presented in Appendix C.

For clayey soil-based CMRB, a range of 10.94% to 11.58% cement was required to achieve a compressive strength of 450 psi, while a range of 12.31% to 13.96% cement was required to achieve 600 psi. For sandy soil-based CMRB, the cement contents were lower than those required with clayey soil. For clayey soil, the required cement contents for the S-C samples were

higher than all of the CMRB samples. However, this was not always this case with the sandy soil-based samples. In addition, the required cement contents for the sandy soil-based samples were generally lower than for the clayey soil-based samples. Therefore, soil type appears to affect the compressive strength and subsequently the required cement content.

In addition, for all cases tested, the compressive strength increased with increasing amounts of RAP. The amount of the increase varied but was consistently higher than the non-RAP soil. There is some caution warranted with this observation. Only two soil types were examined, and only one source of RAP was evaluated. It is unclear how a change in gradation of the RAP source might affect the compressive strength for comparable cement contents and soil types.

Table 4-8: Cement Contents for Various Compressive Strengths of CMRB and S-C

Soil Type and RAP Content (%)	Corresponding Cement Content and Compressive Strength Values (%, psi)		Coefficient of determination (R^2)
CS-0%	(15.27%, 450)	(17.38%, 600)	0.94
CS-25%	(11.56%, 450)	(12.87%, 600)	1.00
CS-50%	(10.94%, 450)	(12.31%, 600)	1.00
CS-75%	(11.58%, 450)	(13.96%, 600)	1.00
SS-0%	(9.57%, 450)	(10.99%, 600)	0.95
SS-25%	(10.31%, 450)	(11.66%, 600)	0.98
SS-50%	(9.15%, 450)	(11.95%, 600)	0.93
SS-75%	(7.77%, 450)	(9.16%, 600)	0.99

Notes: CS ~ clayey soil; SS~ sandy soil

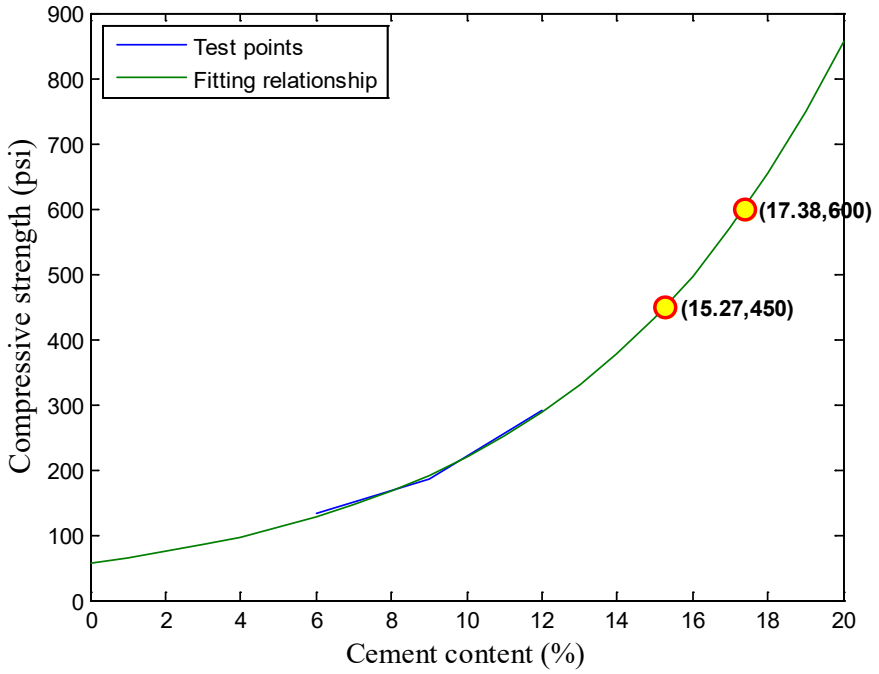

Figure 4-28: Fitting Results of CS-0% Compressive Strength at 7 Days

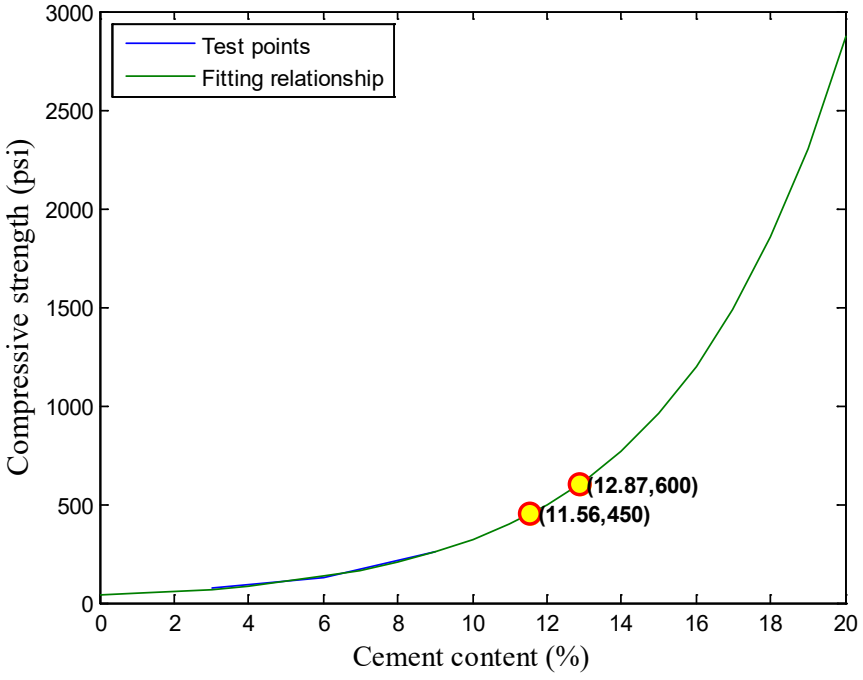

Figure 4-29: Fitting Results of CS-25% Compressive Strength at 7 Days

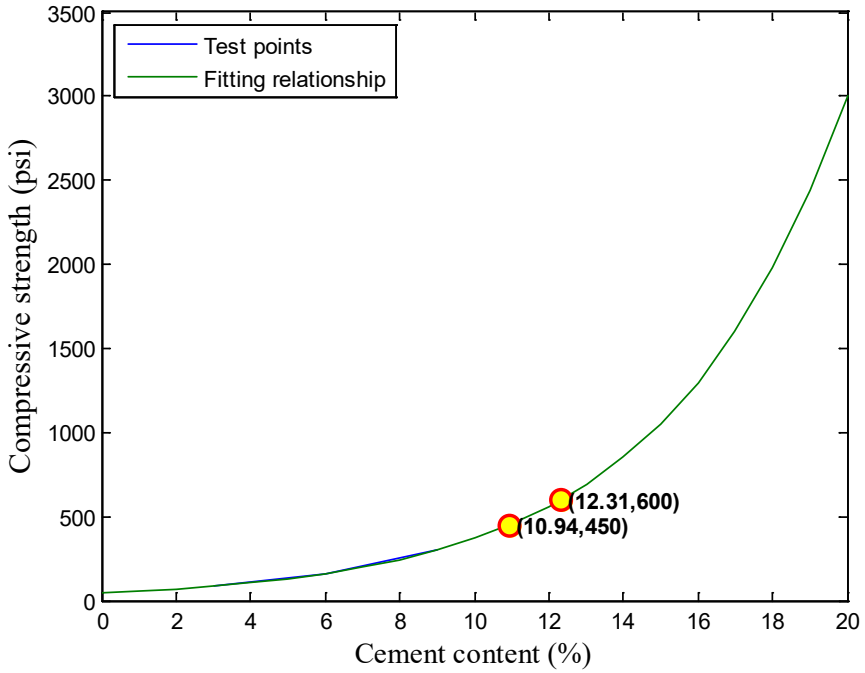

Figure 4-30: Fitting Results of CS-50% Compressive Strength at 7 Days

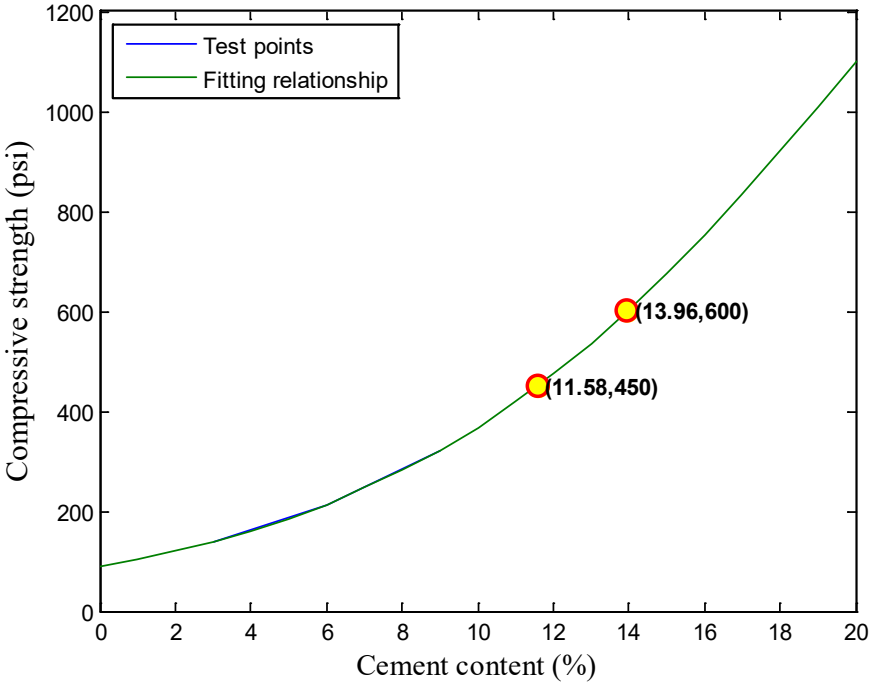

Figure 4-31: Fitting Results of CS-75% Compressive Strength at 7 Days

4.4.1.2 *Effect of Cement Content, Soil Type, and RAP on Compressive Strength of CMRB and S-C*

At 7 days curing duration, Figure 4-32 and Figure 4-33 show that the compressive strength of CMRB and S-C increased as the cement content increased, regardless of RAP content and soil type. Additionally, the sandy soil-based CMRB and S-C exhibited higher compressive strength values than clayey soil-based CMRB and S-C, regardless of cement content and RAP content. This difference was more pronounced as cement content increased. Furthermore, increasing RAP content generally resulted in an increase of the compressive strength regardless of soil type and cement content. However, the sandy soil-based S-C curve (0% RAP) was higher than that of the sandy soil-based CMRB with 25% RAP content. Similar findings were observed after a 28-day curing duration, as shown in Figure 4-34 and Figure 4-35.

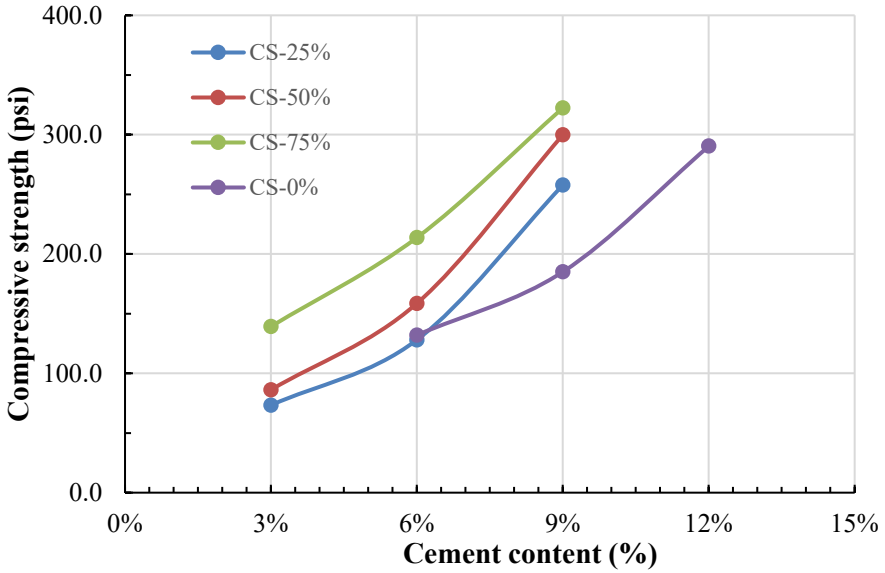

Figure 4-32: Influence of Cement Content on Compressive Strength of CMRB and S-C with Clayey Soil at 7 Days

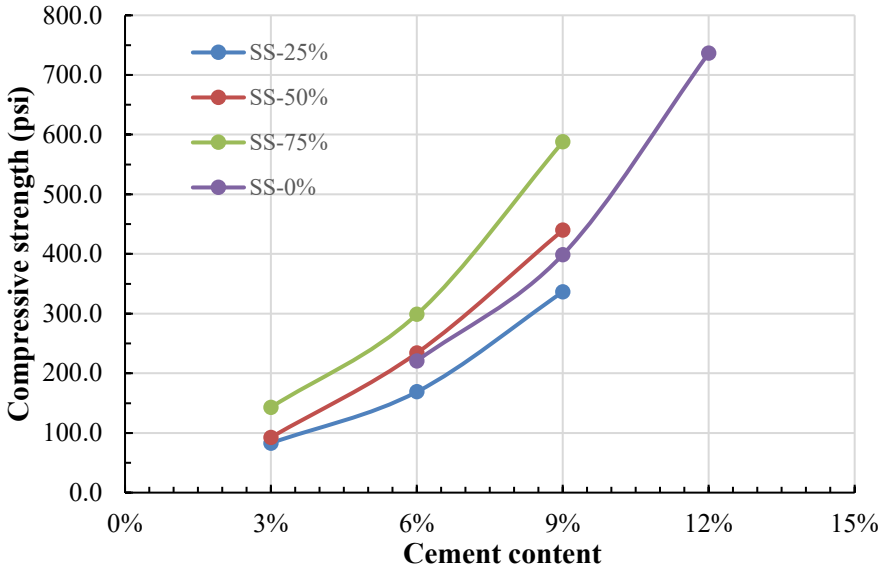

Figure 4-33: Influence of Cement Content on Compressive Strength of CMRB and S-C with Sandy Soil at 7 Days

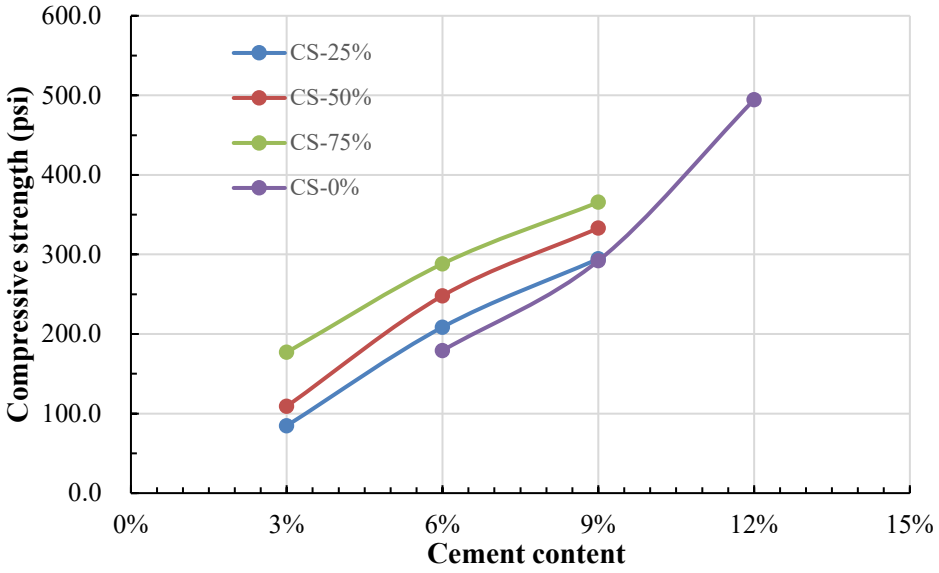

Figure 4-34: Influence of Cement Content on Compressive Strength of CMRB and S-C with Clayey Soil at 28 Days

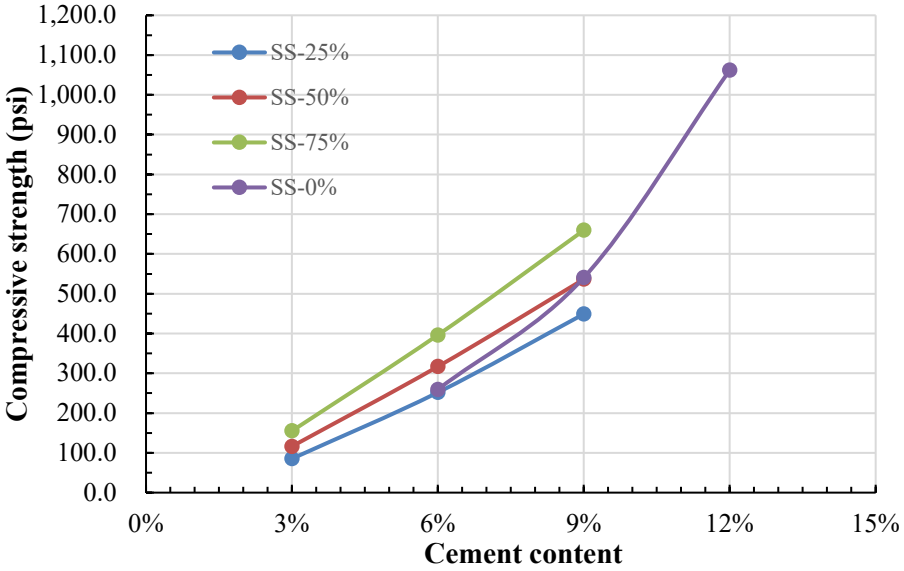

Figure 4-35: Influence of Cement Content on Compressive Strength of CMRB and S-C with Clayey Soil at 28 Days

4.4.1.3 Effect of Curing Duration on Compressive Strength of CMRB and S-C

In Figure 4-36, the compressive strengths of all CMRB and S-C combinations at 28 days curing duration are higher than the corresponding values at 7 days, regardless of cement content, soil type, and RAP content. Thus, it can be concluded that the cement hydration improves the compressive strength of CMRB and S-C materials.

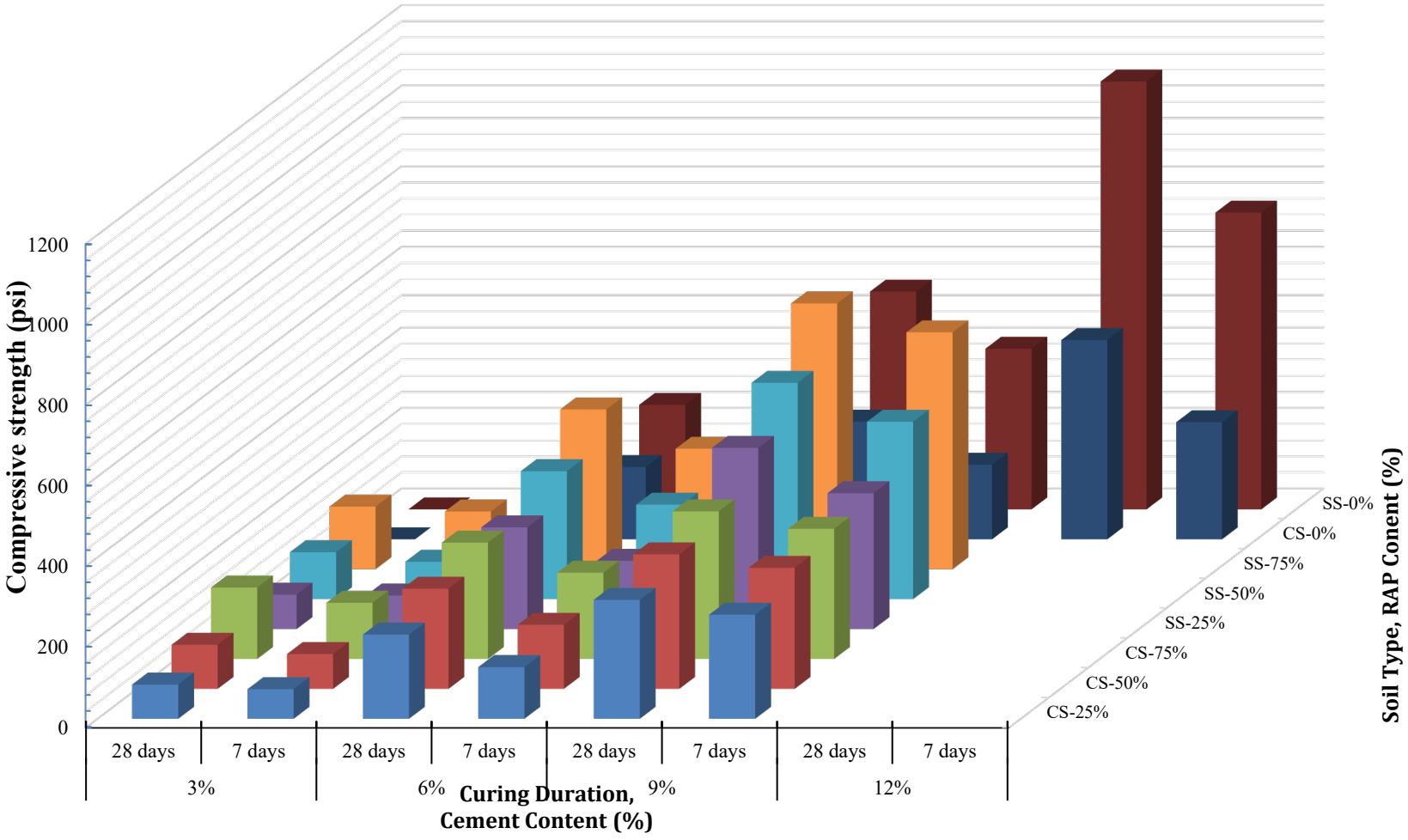

Figure 4-36: Influence of Curing Duration on Compressive Strengths of CMRB and S-C at Various Cement Contents

4.4.2 Elastic Modulus of CMRB and S-C

In this study, the effects of cement content and curing duration on elastic modulus were also analyzed. Four cement contents (3%, 6%, 9%, and 12%), two curing durations (7 days and 28 days), and two subgrade sources of different soil types (clayey and sandy) were used to produce the samples. Two specimens were tested for each combination. Results are shown in Appendix F.

Increasing cement content, increasing RAP content, and increasing curing duration all resulted in increased elastic modulus values of all CMRB and S-C combinations regardless of soil type. However, cement content did not exhibit the same influence on elastic modulus at different curing durations.

Sandy soil-based CMRB and S-C exhibited higher elastic modulus values than clayey soil-based CMRB and S-C, regardless of cement content, RAP content, and curing duration. Additionally, the elastic modulus values of the S-C specimens (0% RAP) were remarkably lower than the values from the CMRB specimens with RAP, regardless of soil type, cement content, and curing duration. Therefore, it can be concluded that RAP also plays an important role in elastic modulus value.

The measured elastic modulus values were relatively low, specifically when compared to the resilient modulus values. Similar to CSAB materials, the literature reports S-C mixtures to have elastic moduli values between 8 ksi and 800 ksi. This large range is due, in part, to the fact that there is no standardized procedure to measure the elastic modulus of a CMRB material. The AASHTO PavementME design procedure allows the user to input either an elastic modulus or resilient modulus for a soil cement mixture. It is recommended that the resilient modulus values be used for design as they were measured using standardized procedures and represent the loading condition and stress state actually observed in the field.

4.4.3 Dry Shrinkage of CMRB and S-C

Figure 4-37 presents the final dry shrinkage values of various mixtures at 15 days curing duration. As expected, it can be noted that increased cement content resulted in an increase of dry shrinkage values for CMRB and S-C. However, the data curve followed a concave trend with the shrinkage increasing more drastically between 3% and 6% cement than between 6% and 9% or 9% and 12%.

It can also be seen that an increase in RAP resulted in lower dry shrinkage values. This generally occurred regardless of cement content and soil type. This illustrates that RAP content could effectively decrease the dry shrinkage of CMRB.

Additionally, the CMRB and S-C samples made with sandy soil exhibited lower dry shrinkage values than the corresponding CMRB and S-C samples made with clayey soil, regardless of cement content and RAP content. Thus, it can be concluded that soil type also affects dry shrinkage.

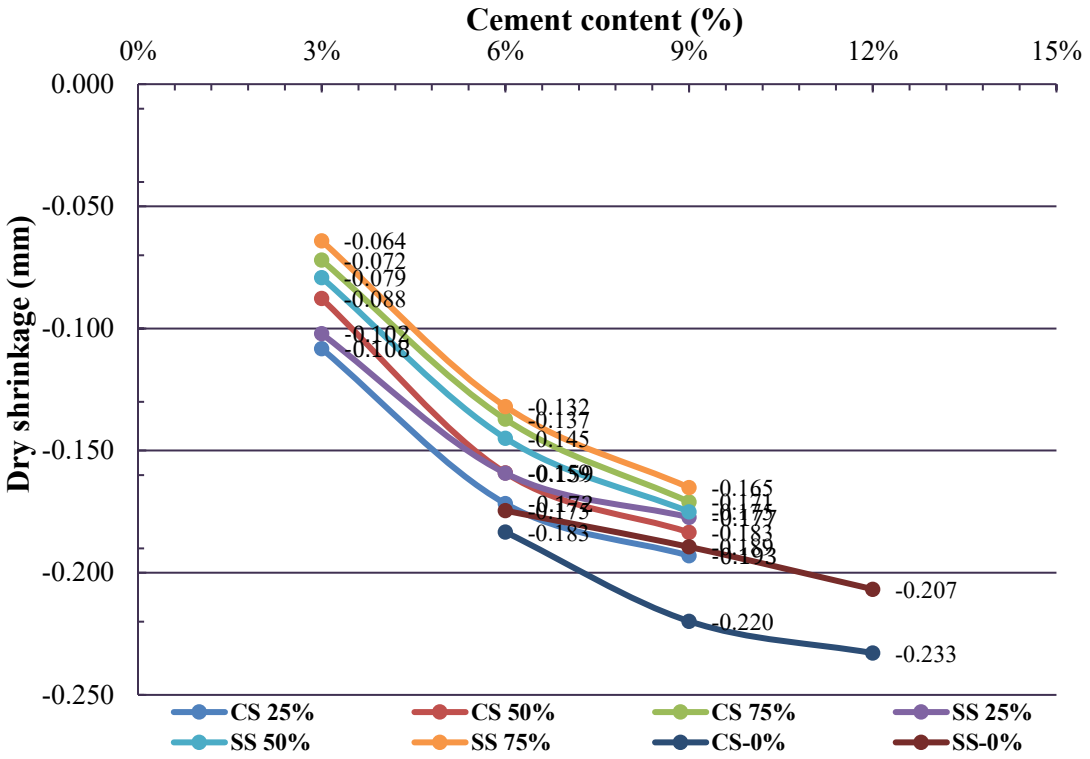

Figure 4-37: Final Dry Shrinkage Values of CMRB and S-C

4.4.4 Resilient Modulus of CMRB and S-C

For CMRB and S-C, the resilient modulus values at different cement contents (3%, 6%, 9%, and 12%) were collected through MTS in accordance with AASHTO T 307. All samples were tested at optimum moisture content.

The coefficients of determination for the models shown in Table 4-9 were generally higher than 0.8, which indicates that the fitting results are trustworthy. Thus, the conducted models (various K values) could be used to calculate the resilient modulus at actual stress conditions in the

pavement. Figure 4-38 shows the measured resilient modulus values vs. the predicted resilient modulus values for CMRB made with clayey soil and 25% RAP. The remaining material combinations for CMRB and S-C generally exhibited similar results as shown in Appendix D.

Table 4-9: Measured and Average Resilient Modulus Values of CMRB and S-C at Different Cement Contents

Soil Type and RAP Content (%)	Cement Content (%)	K_1	K_2	K_3	Measured MR, Seq. 15 (psi)	Average MR (psi)	Peak Measured MR (psi)	Coefficient of determination (R^2)
CS-0%	6%	21963	0.19	0.76	961,737	750,278	1,427,352	0.95
	9%	22093	0.33	0.61	1,118,417	849,952	1,652,699	0.94
	12%	17790	0.28	0.71	877,359	677,608	1,370,597	0.95
CS-25%	3%	31164	0.10	0.67	1,032,015	857,566	1,526,816	0.95
	6%	35776	0.18	0.51	1,182,808	995,377	1,740,268	0.94
	9%	26631	0.12	0.84	1,055,914	868,907	1,710,775	0.97
CS-50%	3%	19413	0.06	0.97	681,569	640,009	1,302,347	0.93
	6%	23873	0.23	0.61	985,115	776,215	1,395,515	0.93
	9%	25961	0.14	0.76	1,009,295	818,701	1,519,493	0.95
CS-75%	3%	15095	0.16	1.02	790,359	619,625	1,524,211	0.98
	6%	15708	0.46	0.56	968,604	718,629	1,432,983	0.91
	9%	24143	0.17	0.88	1,107,644	886,724	1,925,362	0.96
SS-0%	6%	13980	0.64	0.48	1,230,280	830,024	1,838,731	0.92

Soil Type and RAP Content (%)	Cement Content (%)	K_1	K_2	K_3	Measured MR, Seq. 15 (psi)	Average MR (psi)	Peak Measured MR (psi)	Coefficient of determination (R^2)
	9%	27188	0.34	0.55	1,204,503	1,008,617	1,964,774	0.93
	12%	26004	0.13	0.64	834,390	738,692	1,275,209	0.93
SS-25%	3%	12368	0.37	0.77	838,105	581,683	1,326,800	0.93
	6%	21461	0.30	0.68	1,101,990	833,463	1,679,267	0.96
	9%	22916	0.25	0.83	1,192,857	931,134	1,922,776	0.97
SS-50%	3%	16465	0.35	0.61	813,782	656,583	1,289,295	0.95
	6%	28172	0.29	0.53	1,226,711	945,120	1,742,858	0.93
	9%	7766.3	0.66	0.92	852,159	715,674	1,873,391	0.95
SS-75%	3%	31762	0.27	0.36	997,299	902,146	1,489,947	0.88
	6%	17375	0.44	0.66	1,175,926	844,518	1,904,833	0.95
	9%	16039	0.61	0.47	1,309,016	890,400	1,892,844	0.91

Notes: Measured MR = resilient modulus at the last cycle; MR values corrected to account for frame stiffness.

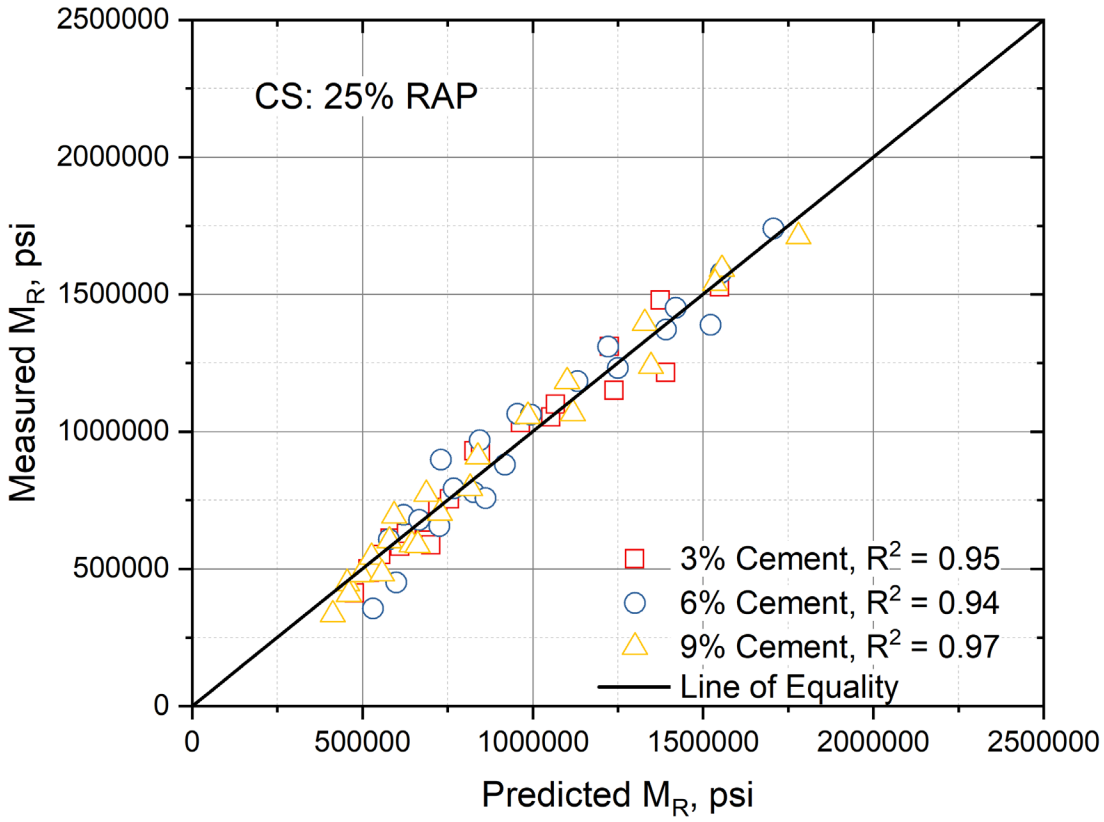

Figure 4-38: Measured vs. Predicted Resilient Modulus of CMRB with Clayey Soil and 25% RAP at Various Cement Contents

4.4.4.1 Relationship between Stress and Strain during Repeated Loading Process for CMRB and S-C

All the stress-strain data of each specimen during 23 cycles are summarized in Appendix E. Figure 4-39 shows the typical stress and strain summation curve of CS-0% at 6% cement content, which was similar to the results for all of the combinations. The stress-strain curves exhibited a remarkable increase with the increase of stress no matter how much cement was used. Therefore, it can be concluded that the resilient modulus of CMRB and S-C is stress-dependent.

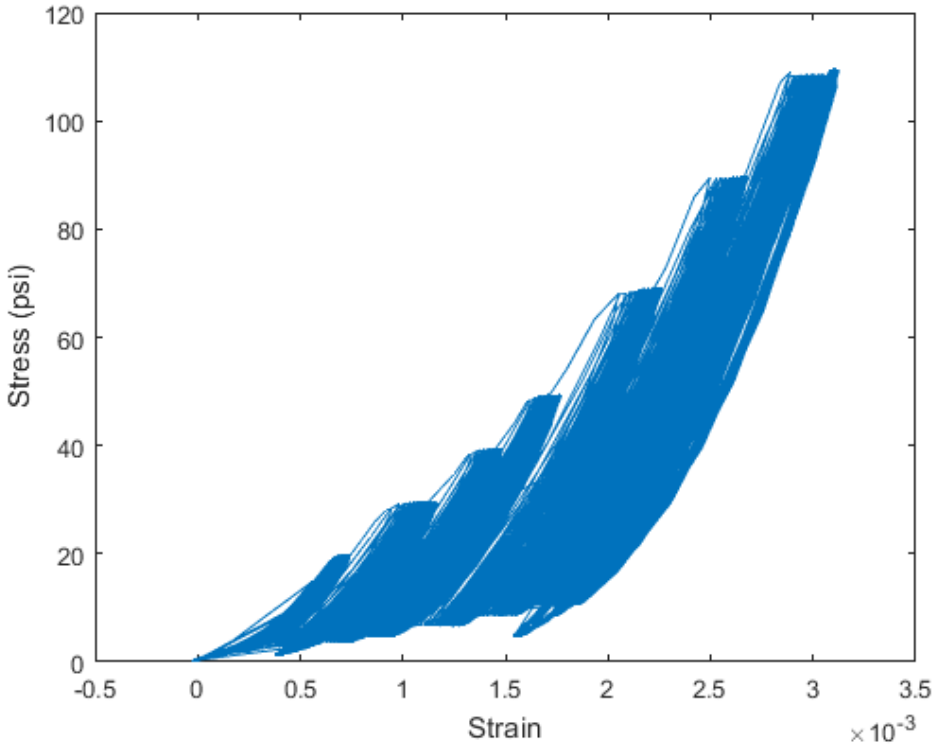

Figure 4-39: Stress and Strain Summation Curve of CS-0% at 6% Cement Content

4.5 Soil Test Pit Results

The critical deflection basins for each of the three loading scenarios were analyzed (Figure 4-40). Even though each load cycle experienced some level of permanent deformation, when normalized to itself, the deflection basin for any single cycle out of the 1,000 cycles run was statistically the same. Unlike FWD measurements conducted on pavement surfaces (i.e. asphalt or Portland cement concrete), the deflection basins for applied loads on granular base materials approaches zero rapidly.

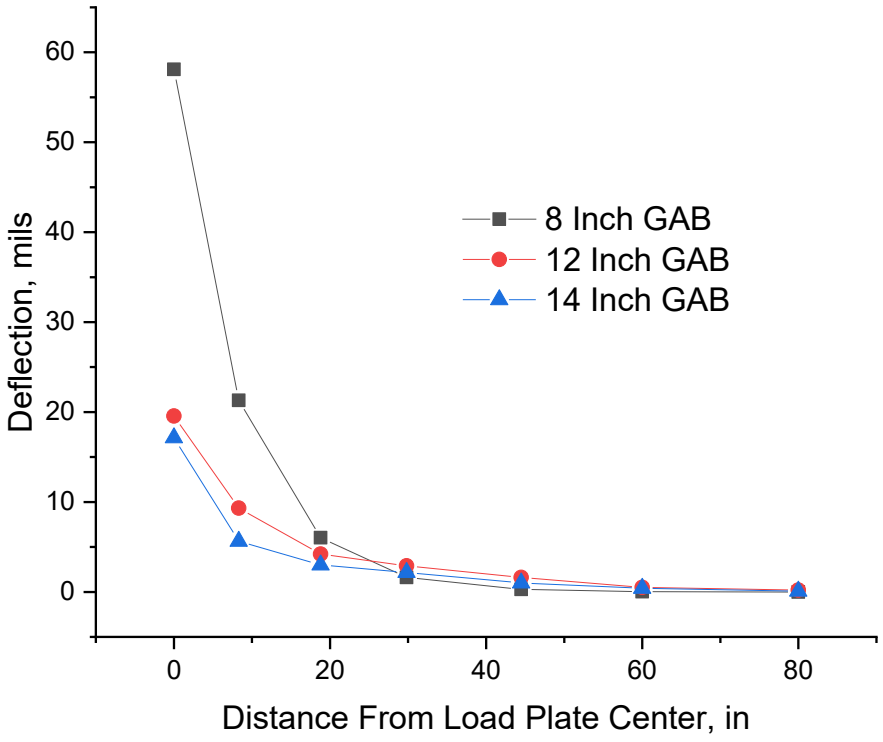

Figure 4-40: Deflection Basins for Soil Pit Tests at 9,000 lbf Loads

Any back-calculation procedure can be sensitive to the starting estimates for material properties. A consistent set of starting parameters was used for each analysis (Table 4-10). These seed parameters and the measured deflection basins (Figure 4-40) were used in BAKFAA to calculate the GAB resilient modulus value from the soil test pit at each thickness value.

Table 4-10: Seed Parameters for BAKFAA Backcalculation Analysis.

Layer	**Starting Modulus, psi**	**Poisson's Ratio**	**Thickness, in**
GAB	20,000	0.30	Varied
Clay Subgrade	20,000	0.40	18
Plywood	1,000,000	0.30	1
Geofoam	10,000	0.25	36
Concrete Floor	5,000,000	0.15	∞

In order to compare the results from the soil test pit and the laboratory triaxial resilient modulus testing, the previously described three parameter fitting models were used to calculate the resilient modulus at the applied load. However, unlike the triaxial test, the confining pressure for the soil test pit is unknown. For this analysis, a range of possible confining pressures from 1 psi to 20 psi was used to estimate the bounds of the possible resilient modulus value for a given load case (Figure 4-41).

The comparison is noteworthy in several aspects. First, it appears that there is a threshold base layer thickness before the material behaves as it does in the laboratory triaxial test. The laboratory test is conducted on a specimen that is 6 inches in diameter and 12 inches in tall. The 8 inch soil pit back-calculated resilient modulus was significantly lower than the laboratory measured value. However, the laboratory-measured resilient modulus using the AASHTO T-307 method of a GAB material (MC) matched the "real-life" loading behavior of a 12" thick GAB layer. This appears to validate the AASHTO T-307 results for GAB materials.

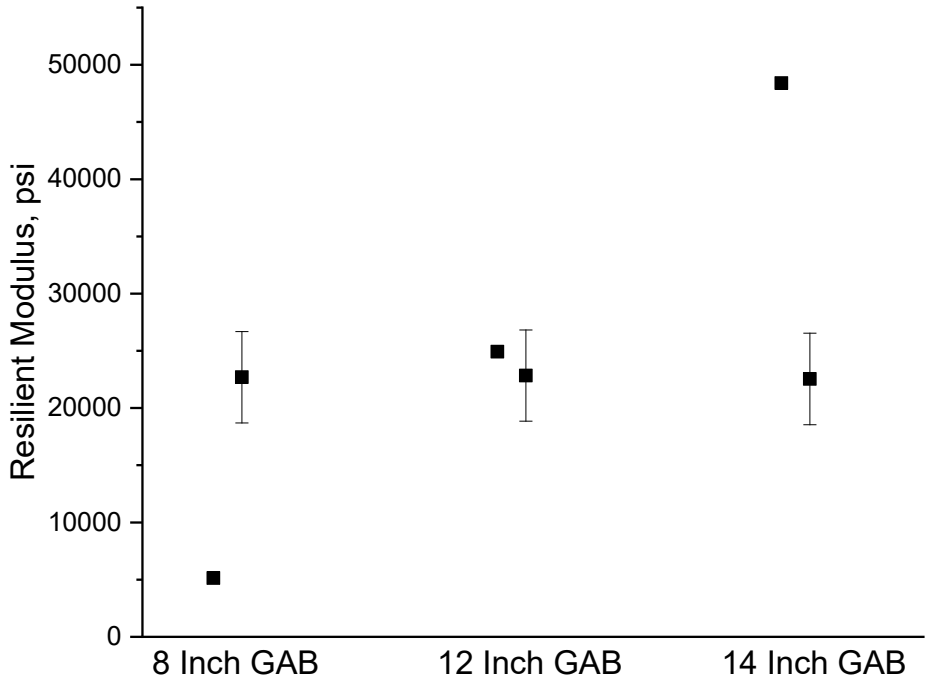

Figure 4-41:Comparison of Laboratory-Measured Resilient Modulus (data points with error bars) to Backcalculated Resilient Modulus from Soil Test Pit (single data points)

CHAPTER 5: CONCLUSIONS AND RECOMMENDATIONS

5.1 Lessons Learned

There is a difference in some of the results in this project report when compared to the literature. A variety of stabilized base materials have been studied over the decades using numerous test methods. Due to the different test methods employed, and even the difference in terminology related to the actual materials being evaluated, it can be extremely difficult to reconcile the widely-varying values reported in the literature.

Fortunately, the resilient modulus of most subbase and base materials can be quantified using AASHTO T307. While the test method has been used for a wide range of materials, both in this study and in the literature at large, it has not been standardized for use on stabilized subbase/base materials. While an elastic modulus measurement might be appropriate in some cases, it was seen that the behavior of the materials evaluated in this study was better evaluated using resilient modulus testing. However, this is an area that deserves significantly more research as there has been little work done to evaluate the connection between elastic modulus and resilient modulus in stabilized subbase and base materials, especially those materials that contain discrete particles, such as CMRB.

There is also a point of confusion at this time because the AASHTO PavementME software uses the term “Elastic/Resilient Modulus” for inputs in stabilized base layers. This can lead an engineer to look in the literature and find a wide range of values that seem acceptable for use in the design process. Furthermore, the official AASHTO PavementME documentation is not consistent in delineating between elastic modulus and resilient modulus.

Another lesson learned was with the samples themselves. When originally evaluating the static elastic modulus of the various materials, a 4-in by 4.58-in cylinder specimen size was used. The results from this testing were different than some elastic modulus values reported in the literature. However, it was difficult to ascertain if the values in the literature were the same material (i.e. stabilized, non-stabilized, type of source material, etc.) as those in this project. Additionally, when larger specimen sizes were evaluated in this project (i.e. 6-inch by 12-inch cylinders), a large discrepancy between the NDT-measured dynamic modulus and the compression static modulus was noted. Again, the literature has very little discussion on this topic, and it is an area of significant future research need.

In conclusion, the lack of a standardized process for characterizing the elastic and resilient modulus of stabilized soil and soil/RAP materials makes it difficult to establish a comparison with prior research studies. Differences in terminology used in various publications also makes it difficult to replicate some of the procedures and results. The biggest lesson learned in this study is that clear, concise documentation of every aspect of the project (i.e. experimental setup, testing

procedures, and material descriptions) is critical to ensuring that future studies can replicate the work and make valid and useful comparisons.

5.2 Conclusions

Based on the test results, the following conclusions were drawn:

1. The literature review indicated that resilient modulus was a complex phenomenon dependent upon the mechanisms and interactions of the cement and the aggregate. The nature of these mechanisms and their interaction made it difficult to predict with certainty the characteristics of various factors in determining resilient modulus. However, the literature review generally indicated the following conclusions:
    a. Resilient modulus increased with the increase of deviator stress.
    b. Resilient modulus of uniformly graded aggregate was higher than other graded aggregates.
    c. The increase of fine aggregate might cause the decrease of resilient modulus value.
2. Compressive strength of CSAB increased with increasing cement content; however, it could be a convex curve or concave curve depending upon the aggregate source.
3. Increased curing duration increased the compressive strength and resilient modulus of CSAB regardless of cement content and aggregate source.
4. Measured elastic modulus values were relatively low, specifically when compared to the resilient modulus values; however, there is currently no standardized procedure to measure elastic modulus of CSAB, CMRB, or S-C materials.
5. Dry shrinkage values of CSAB increased with increasing cement content with the data following a concave-curve trend due to the impacts of water loss and hydration behavior.
6. Stress-strain curves for CSAB, CMRB, and S-C exhibited a noticeable increase with the increase of stress regardless of cement content. This implies that the resilient modulus was generally stress-dependent.
7. OMC and MDD of clayey soil-based and sandy soil-based CMRB showed an opposite change tendency with the increase of RAP content: OMC values went down while MDD values increased.
8. Compressive strength and resilient modulus of CMRB and S-C both increased with increasing cement content; however, compressive strength exhibited different increasing trends over time. After 7 days curing, the strength curve exhibited a concave trend, while after 28 days-curing, it showed a convex trend.
9. Increased curing duration significantly increased both the compressive strength and resilient modulus of CMRB and S-C regardless of cement content, RAP content, and soil type.
10. Compressive strength and resilient modulus values of sandy soil-based CMRB and S-C were higher than clayey soil-based samples, regardless of cement content, RAP content, and curing duration. Additionally, this difference increased as cement content increased.

11. The soil test pit results indicated that the resilient modulus measured using the AASHTO T-307 method of a GAB material (MC) matched the “real-life” loading behavior of a 12” thick GAB layer. This appears to validate the AASHTO T-307 results for GAB materials.

5.3 Recommendations

Based on the test results and data analysis, the following recommendations are made:

1. Because there is currently no standardized procedure to measure the elastic modulus of CSAB, CMRB, or S-C materials, it is recommended to use resilient modulus values, as indicated in the current version of AASHTO PavementME, for analysis and design of CSAB, CMRB, and S-C.
2. It is recommended that SCDOT conduct a study to investigate the effect of coupled load and moisture content on the destructive and non-destructive physical deformation.
3. It is recommended that SCDOT consider developing a performance deterioration database to contain vital parameters such as resilient modulus at various important time points like new construction, 1 year, 5 years, 10 years, and reestablishment.
4. It is recommended that SCDOT conduct a study to investigate the effects of aggregate chemical composition on the moisture susceptibility of cement treated mixtures to address the interaction and bonding capabilities of the aggregate and cement.

5.4 Implementation Plan

In order to achieve the above-mentioned goals, the following implementation process will be followed: a) conducting sensitivity analysis; b) recommending input values for base and subbase material characteristics; c) determining the needed resources and requirements; d) identifying the various testing procedures alternatives; and e) developing a final implementation plan. All of these steps will include and will need the support of SCDOT engineers and staff. This will ensure a successful implementation plan for the Agency in order to have a successfully developed and functional system.

REFERENCES

[1] Erlingsson S, Rahman M. Evaluation of permanent deformation characteristics of unbound granular materials by means of multistage repeated-load triaxial tests. Transportation Research Record: Journal of the Transportation Research Board. 2013(2369):11-9.

[2] Gu F. Characterization and Performance Prediction of Unbound Granular Bases with and Without Geogrids in Flexible Pavements. 2015.

[3] Li XW, Dong MM. Experimental Research on Pavement Performance of Cement Stabilized Base Recycled Mixture. Applied Mechanics & Materials. 2011;94-96:31-7.

[4] Park SW, Park SW. Effect of Stress-Dependent Modulus and Poisson's Ratio on Rutting Prediction in Unbound Pavement Foundations. Journal of the Korean Geotechnical Society. 2007;23(3):15-24.

[5] Tseng K-H, Lytton RL. Prediction of permanent deformation in flexible pavement materials. Implication of aggregates in the design, construction, and performance of flexible pavements: ASTM International; 1989.

[6] Li Z, Chen Y, Xing Z. Experimental Study of Asphalt Treated Base Binder Course for Pavement Design.

[7] Xu Q, Bian J, Meng S. Study of Flexible Base and Semi-Rigid Base Asphalt Pavement Performance Under Accelerated Loading Facility (ALF). 2008.

[8] Kazemi F, Hill K. Effect of permeable pavement basecourse aggregates on stormwater quality for irrigation reuse. Ecological Engineering. 2015;77:189-95.

[9] Mcallister WT, Vinton WG. Recycled Material Insulation. US; 2008.

[10] Ellis CI. Pavement Engineering in Developing Countries. TRRL Supplementary Report (Transport and Road Research Laboratory, Great Britain). 1979(537).

[11] Lekarp F, Isacsson U, Dawson A. State of the art. I: Resilient response of unbound aggregates. Journal of transportation engineering. 2000;126(1):66-75.

[12] Monismith CL, Seed HB, Mitry F, Chan C. Predictions of Pavement Deflections from Laboratory Tests. Second International Conference on the Structural Design of Asphalt Pavements1967.

[13] Smith W, Nair K. Development of procedures for characterization of untreated granular base course and asphalt-treated base course materials. 1973.

[14] Hanifa K, Abu-Farsakh MY, Gautreau GP. Design Values of Resilient Modulus for Stabilized and Non-Stabilized Base. 2015.

[15] Morgan J. The response of granular materials to repeated loading. Australian Road Research Board Proc. 1966.

[16] HICKS R. Factors Influencing the resilient properties of granular materials‟‟‟‟. PhD thesis, University of California, Berkeley, Calif. 1970.

[17] Luong M. Mechanical aspects and thermal effects of cohesionless soils under cyclic and transient loading. Proc IUTAM Conf on Deformation and Failure of Granular materials, Delft1982. p. 239-46.

[18] Thom N, BROWN S. The Mechanical Properties of Unbound Aggregates from Various Sources. Unbound Aggregates in Roads. Proceedings of the 3rd International Symposium, University of Nottingham, April 11-13, 1989. Publication of: Butterworth and Company, Limited. 1989.

[19] Boyce J, Brown S, Pell P. The resilient behaviour of a granular material under repeated loading. Australian Road Research Board Conference Proc1976.

[20] Allen JJ. The effects of non-constant lateral pressures on the resilient response of granular materials: University Microfilms; 1977.

[21] Colorado Department of Transportation Asphalt Pavement White Paper. Implementation Report. 1992.

[22] Wen H, Wu M. Evaluation of high percentage recycled asphalt pavement as base materials. 2011.

[23] Vuong B. Influence of density and moisture content on dynamic stress-strain behaviour of a low plasticity crushed rock. Road and Transport Research. 1992;1(2).

[24] Haynes JH. Effects of repeated loading on gravel and crushed stone base course materials used in the AASHO Road Test. 1961.

[25] Nur A, Byerlee JD. An exact effective stress law for elastic deformation of rock with fluids. Journal of Geophysical Research. 1971;76(26):6414–9.

[26] Madsen OS. Wave-induced pore pressures and effective stresses in a porous bed. Géotechnique. 1978;28(4):377-93.

[27] Houghton JD, Wu J, Godwin JL, Neck CP, Manz CC. Effective Stress Management: A Model of Emotional Intelligence, Self-Leadership, and Student Stress Coping. Journal of Management Education. 2012;36(61):220-38.

[28] Bishop AW, Blight GE. Some Aspects of Effective Stress in Saturated and Partly Saturated Soils. Géotechnique. 1963;13(3):177-97.

[29] Seed H, Mitry F, Monismith C, Chan C. Prediction of flexible pavement deflections from laboratory repeated-load tests. NCHRP Report. 1967(35).

[30] Mitry FG. Determination of the modulus of resilient deformation of untreated base course materials: University of California, Berkeley; 1965.

[31] Dawson A, Thom N, Paute J. Mechanical characteristics of unbound granular materials as a function of condition. Gomes Correia, Balkema, Rotterdam. 1996:35-44.

[32] Hanifa K, Abufarsakh MY, Gautreau GP. Design Values of Resilient Modulus for Stabilized and Non-Stabilized Base. 2015.

[33] Fall M, Sawangsuriya A, Benson CH, Edil TB, Bosscher PJ. On the Investigations of Resilient Modulus of Residual Tropical Gravel Lateritic Soils from Senegal (West Africa). Geotechnical and Geological Engineering. 2008;26(1):13-35.

[34] Ba M, Fall M, Samb F, Sarr D, Ndiaye M. Resilient Modulus of Unbound Aggregate Base Courses from Senegal (West Africa). Open Journal of Civil Engineering. 2011;01(01):1-6.

[35] Bilodeau JP, Plamondon CO, Dore G. Estimation of resilient modulus of unbound granular materials used as pavement base: combined effect of grain-size distribution and aggregate source frictional properties. Materials and Structures. 2016;49(10):4363-73.

[36] Plaistow L. Non-linear behaviour of some pavement unbound aggregates: MS Thesis, Dept. of Civ. Engrg., University of Nottingham, Nottingham, England; 1994.

[37] Heydinger A, Xie Q, Randolph B, Gupta J. Analysis of resilient modulus of dense-and open-graded aggregates. Transportation Research Record: Journal of the Transportation Research Board. 1996(1547):1-6.

[38] Van Niekerk AA, Molenaar AAA, Houben L. Effect of Material Quality and Compaction on the Mechanical Behaviour of Base Course Materials and Pavement Performance. Proceedings of the 6th International Conference on the Bearing Capacity of Roads and Airfields, Lisbon, Portugal, 24-26 June 2002.

[39] Fuller WB, Thompson SE. The laws of proportioning concrete. 1907.

[40] Hornych P, Kazai A, Piau J. Study of the resilient behaviour of unbound granular materials. Proc BCRA. 1998;98:1277-87.

[41] Wu M. Evaluation of High Percentage Recycled Asphalt Pavement as Base Course Materials: Washington State University; 2011.

[42] Wen H, Wang J, Wu M. Development of rutting model for unbound aggregates containing recycled Asphalt pavement. 2013.

[43] Xiao F, Amirkhanian SN. Resilient Modulus Behavior of Rubberized Asphalt Concrete Mixtures Containing Reclaimed Asphalt Pavement. Road Materials & Pavement Design. 2008;9(9):633-49.

[44] Maher A, Bennert TA. Evaluation of Poisson's ratio for use in the mechanistic empirical pavement design guide (MEPDG). 2008..

[45] Walubita LF, Walubita LF. Computational Modeling of Perpetual Pavements Using the MEPDG Version 0.910 Software2007.

[46] Gu F, Zhang Y, Droddy CV, Luo R, Lytton RL. Development of a New Mechanistic Empirical Rutting Model for Unbound Granular Material. Journal of Materials in Civil Engineering. 2016:04016051.

[47] Gu F, Sahin H, Luo X, Luo R, Lytton RL. Estimation of resilient modulus of unbound aggregates using performance-related base course properties. Journal of Materials in Civil Engineering. 2014;27(6):04014188.

[48] Lekarp F, Isacsson U, Dawson A. Permanent strain response of unbound aggregates. J Transp Engng-ASCE. 2000;126(1):66-83.

[49] Xiao Y, Tutumluer E, Mishra D. Performance Evaluations of Unbound Aggregate Permanent Deformation Models for Various Aggregate Physical Properties. Transportation Research Record: Journal of the Transportation Research Board. 2015(2525):20-30.

[50] Tutumluer E. Practices for unbound aggregate pavement layers2013.

[51] Lytton RL, Uzan J, Fernando EG, Roque R, Hiltunen D, Stoffels SM. Development and validation of performance prediction models and specifications for asphalt binders and paving mixes: Strategic Highway Research Program Washington, DC; 1993.

[52] Brown SF, Lashine AKF, Hyde AFL. Repeated load triaxial testing of a silty clay. Géotechnique. 1975;25(1):95-114.

[53] Gabr A, Cameron D. Permanent strain modeling of recycled concrete aggregate for unbound pavement construction. Journal of Materials in Civil Engineering. 2012;25(10):1394-402.

[54] AASHTO T. 307 (2003) Determining the Resilient Modulus of Soils and Aggregate Materials. American Association of State Highway and Transportation Officials, Washington, DC. 2003.

[55] Korkiala-Tanttu L. Verification of rutting calculation for unbound road materials. Proceedings of the Institution of Civil Engineers-Transport: Thomas Telford Ltd; 2009. p. 107-14.

[56] Chow L, Mishra D, Tutumluer E. Framework for development of an improved unbound aggregate base rutting model for mechanistic-empirical pavement design. Transportation Research Record: Journal of the Transportation Research Board. 2014(2401):11-21.

[57] Ghabchi R, Singh D, Zaman M. Evaluation of moisture susceptibility of asphalt mixes containing RAP and different types of aggregates and asphalt binders using the surface free energy method. Construction & Building Materials. 2014;73(73):479-89.

[58] Fu P, Jones D, Harvey JT. The effects of asphalt binder and granular material characteristics on foamed asphalt mix strength. Construction & Building Materials. 2011;25(2):1093-101.

[59] Wirtgen G. Foamed Bitumen–The Innovative Binding Agent for Road Construction. Wirtgen GmbH. 2002.

[60] Xu S, Xiao F, Amirkhanian S, Singh D. Moisture characteristics of mixtures with warm mix asphalt technologies – A review. Construction and Building Materials. 2017;142:148-61.

[61] Hadley WO, Hudson WR, Kennedy TW. Correlation of Indirect Tensile Test Results with Stability and Cohesiometer values for Asphalt-Treated Materials. 1970;V 39.

[62] Benkelman A, Kingman R, Schmitt H. Performance of Treated and Untreated Aggregate Bases. Highway Research Board Special Report. 1962(73).

[63] Xiao F, Li R, Zhang H, Amirkhanian S. Low Temperature Performance Characteristics of Reclaimed Asphalt Pavement (RAP) Mortars with Virgin and Aged Soft Binders. Applied science, 2017.

[64] Tayebali AA, Rowe GM, Sousa JB. Fatigue response of asphalt-aggregate mixtures. Asphalt Paving Technology 1992, February 24, 1992 - February 26, 1992. Charleston, SC, USA: Publ by Assoc of Asphalt Paving Technologists; 1992. p. 333-60.

[65] Hanson DI, Brown ER. Study to improve asphalt mixes in South Carolina. Volume 1. Final report, 1 April 1994-1 July 1995. 1995.

[66] Netemeyer RL. Rutting Susceptibility of Bituminous Mixtures by the Georgia Loaded Wheel Tester. 1998.

[67] Collins R, Watson D, Campbell B. Development and use of Georgia loaded wheel tester. Transportation Research Record. 1995(1492):202-7.

[68] Kandhal PS, Mallick RB. Evaluation of asphalt pavement analyzer for HMA mix design: National Center for Asphalt Technology; 1999.

[69] Mohammad LN, Nazzal MD, King B, Austin A. Development of a Design Methodology for Asphalt Treated Mixtures. Report No FHWA/LA. 2013;9:453.

[70] Pan T, Tutumluer E, Carpenter S. Effect of Coarse Aggregate Morphology on the Resilient Modulus of Hot-Mix Asphalt. Transportation Research Record Journal of the Transportation Research Board. 2005;1929(1):1-9.

[71] Terrel RL, Awad. IS. Resilient Behavior of Asphalt Treated Base Course Material. Bituminous Aggregates. 1972.

[72] Tayebali AA, Rowe GM, Sousa JB. Fatigue response of asphalt-aggregate mixtures. Journal of the Association of Asphalt Paving Technologists. 1993;62.

[73] Li R, Xiao F, Amirkhanian S, You Z, Huang J. Developments of nano materials and technologies on asphalt materials – A review. Construction and Building Materials. 2017;143:633-48.

[74] Li WY, Xie KC. Energy Sources, Part A: Recovery, Utilization, and Environmental Effects Foreword. Energy Sources Part A-Recovery Util Environ Eff. 2009;31(18):1591-2.

[75] Kandhal PS, Chakraborty S. Effect of Asphalt Film Thickness on Short and Long-Term Aging of Asphalt Paving Mixtures. Transportation Research Record Journal of the Transportation Research Board. 1996;1535(1):83-90.

[76] Cogliano JA. Asphalt foam. US; 1986.

[77] Deacon JA, Tayebali AA, Rowe GM, Monismith CL. Validation of SHRP A-003A Flexural Beam Fatigue Test. Astm Special Technical Publication. 1994(1265):16.

[78] Collins R, Shami H, Lai J. Use of Georgia Loaded Wheel Tester to Evaluate Rutting of Asphalt Samples Prepared by Superpave Gyratory Compactor. Transportation Research Record Journal of the Transportation Research Board. 1996;1545(1):161-8.

[79] Kandhal PS, Cooley Jr LA. Accelerated Laboratory Rutting Tests Evaluation of the Asphalt Pavement Analyzer. Nchrp Report. 2003.

[80] Tsai CC, Anderson GB, Thompson R. Low temperature growth of epitaxial and amorphous silicon in a hydrogen-diluted silane plasma. Journal of Non-Crystalline Solids. 1991;s 137–138(137):673-6.

[81] Fu P, Harvey JT. Temperature sensitivity of foamed asphalt mix stiffness: Field and lab study. International Journal of Pavement Engineering. 2007;8(2):137-45.

[82] Sun ZH, Ma J, Su XM, Yang GF, Hou ZQ. Grey Relational Analysis of Fatigue Performance of Semi-Rigid Pavement Structure. Applied Mechanics & Materials. 2014;651-653:1164-7.

[83] Sha AM, Kan J, Xiao-Gang LI. Fatigue performances of semi-rigid base course materials. Journal of Traffic & Transportation Engineering. 2009;9(3):29-33.

[84] Wei LY, Liu JL, Ma SB, Wang QZ. Study on the Performance of Graded Gravel Roadbase in Freeway Asphalt Pavement. Applied Mechanics & Materials. 2012;178-181:1649-52.

[85] Zhu YS, Guo ZY, Chen CJ, Wen PW, Wu sheng QI. A Study on Experiments of Dry Shrinkage and Temperature Shrinkage Performances of Semi-Rigid Base Course Materials. Highway. 2006.

[86] Casanova FJ. An Alternative Approach to Assess the Cement Content for Soil Stabilization. 1997.

[87] Guthrie WS, Scullion T. Interlaboratory Study of the Tube Suction Test. Granular Bases. 2003.

[88] Sebesta S. Use of Microcracking to Reduce Shrinkage Cracking in Cement-Treated Bases2005.

[89] Scullion T. Precracking of Soil-Cement Bases to Reduce Reflection Cracking: Field Investigation. Transportation Research Record Journal of the Transportation Research Board. 2002;1787(1):22-30.

[90] Guthrie WS, Sebesta SD, Scullion T. Selecting Optimum Cement Contents for Stabilizing Aggregate Base Materials. Compressive Strength. 2002.

[91] Gervais F, Piriou B. Temperature dependence of transverse- and longitudinal-optic modes in Ti${mathrm{O}}_{2}$ (rutile). Physical Review B Condensed Matter. 1974;10(4):1642-54.

[92] Williams R. Cement-Treated Pavements: Materials, Design, and Construction. Road Materials. 1986;18.

[93] Shahin MY, Kohn SD. Pavement Maintenance Management for Roads and Parking Lots. Pavement Maintenance Management for Roads & Parking Lots. 1981.

[94] Adaska WS, Luhr DR. Controls of Reflective Cracking in Cement Stabilized Pavements. Qadi. 2004.

[95] Sharma S, Das A. Backcalculation of pavement layer moduli from falling weight deflectometer data using an artificial neural network. Canadian Journal of Civil Engineering. 2008;35(1):57-66.

[96] Miller HJ, Guthrie WS, Crane RA, Smith B. Evaluation of Cement-Stabilized Full-Depth-Recycled Base Materials for Frost and Early Traffic Conditions. 2006.

[97] Molenaar AAA, Pu B. Prediction of fatigue cracking in cement treated base courses. Rilem International Conference on Cracking in Pavements, 6th, 2008, Chicago, Illinois, USA2008.

[98] Mullaney J, Trueman SJ, Lucke T, Bai SH. The effect of permeable pavements with an underlying base layer on the ecophysiological status of urban trees. Urban Forestry & Urban Greening. 2015;14(3):686-93.

[99] Brattebo BO, Booth DB. Long-term stormwater quantity and quality performance of permeable pavement systems. Water Research. 2013;37(18):4369-76.

[100] Hearn G. CDOT (Colorado Department of Transportation) Flex-Post Rockfall Fence. Final Reoprt. Dynamic Tests. 1991.

[101] Harvey JT, Plessis LD, Long F, Deacon JA, Guada I, Hung D, et al. CAL/APT program: test results from accelerated pavement test on pavement structure containing asphalt treated permeable base (ATPB): section 500RF. Cracking. 1997.

[102] Officials HT. Rigid pavement design & rigid pavement joint design: AASHTO; 1998.

[103] Mallela J, Titusglover L, Sadasivam S, Bhattacharya B, Darter M, Von Quintus H. Implementation of the AASHTO Mechanistic-Empirical Pavement Design Guide for Colorado. Pavement Performance. 2013.

[104] Suthahar N, Ardani A, Morian DA. Early Evaluation of LTPP Specific Pavement Studies - 2, Colorado. Concrete Pavements. 2000.

[105] Kamara VS, Koroma AA. Simulating the Performance of Pavement Sections Containing Treated and Untreated Permeable Bases Using MEPDG Software. European Scientific Journal. 2014(14):323-36.

[106] Schmitt R, Owusuababio S, Crovetti J. Performance Evaluation of Open Graded Base Course with Doweled and Non-doweled Transverse Joints on USH 18/151, STH 29, and USH 151. Optics Express. 2010;18(23):23554-61.

[107] Chang JR, Su YS, Huang TC, Kang SC, Hsieh SH. Measurement of the International Roughness Index (IRI) Using an Autonomous Robot (P3-AT). Isarc Proceedings. 2009.

[108] Tennis PD, Leming ML, Akers DJ. Pervious Concrete Pavements. Detention Basins. 2004.

[109] Zhan G, Bu T. Factors Analysis on Influencing Reserves Grade of Low-Permeable Dense Sandstone Gas Pool. Natural Ctas Exploraiton & Development. 2004.

[110] Kipp W, Walters B, Ahearn WE. Evaluation of Asphalt Treated Permeable Base. 2013.

[111] Mathis DM. Permeable base design and construction. International Conference on Concrete Pavement Design and Rehabilitation, 4th, 1989, West Lafayette, USA1989.

[112] Masad E, Birgisson B, Al-Omari A, Cooley A. Analytical Derivation of Permeability and Numerical Simulation of Fluid Flow in Hot-Mix Asphalt. Journal of Materials in Civil Engineering. 2004;16(5):487-96.

[113] Kandhal PS. Field and laboratory investigation of stripping in asphalt pavements: State of the art report. Transportation Research Record. 1994(1454).

[114] Chen JS, Lin KY, Young SY. Effects of Crack Width and Permeability on Moisture-Induced Damage of Pavements. Journal of Materials in Civil Engineering. 2004;16(3):276-82.

[115] Gao J, Guo C, Liu Y. Measurement of pore water pressure in asphalt pavement and its effects on permeability. Measurement. 2015;62(4):81-7.

[116] Kringos N, Scarpas A. Physical and mechanical moisture susceptibility of asphaltic mixtures. International Journal of Solids & Structures. 2008;45(9):2671-85.

[117] Al-Omari A, Masad E. Three dimensional simulation of fluid flow in X-ray CT images of porous media. International Journal for Numerical and Analytical Methods in Geomechanics. 2004;28(13):1327-60.

[118] Kettil P, Engstr, M, G., Wiberg NE. Coupled hydro-mechanical wave propagation in road structures. Computers & Structures. 2005;83(21–22):1719-29.

[119] Yang B, Mo S, Wang L, Ji Y. Differential Constitutive Relation for Creep of Large-Stone Porous Asphalt Mixture. Asian Journal of Chemistry. 2014;26(17):5739-44.

[120] Wang ED, Zhang HL, Wang XC. Experimental research of MAC modified large stone porous asphalt mixture. Journal of Traffic & Transportation Engineering. 2008.

[121] Shijie MA, Jiancun FU, Wei J, Gao X. Study on Dynamic Modulus Prediction Model of Large Stone Porous Asphalt Mixture. Journal of Highway & Transportation Research & Development. 2010.

[122] Cui XZ, Cui XZ. Dynamic Numerical Analysis of Antimoisture-Damage Mechanism of Permeable Pavement Base. International Journal of Geomechanics. 2010;10(6):230-5.

[123] Copeland A, Cecil Jones PE, Bukowski J. Reclaiming Roads. Public Roads. 2010;73.

[124] Xiao F, Amirkhanian SN. Laboratory investigation of utilizing high percentage of RAP in rubberized asphalt mixture. Materials and Structures. 2010;43(1):223.

[125] Avirneni D, Peddinti PRT, Saride S. Durability and long term performance of geopolymer stabilized reclaimed asphalt pavement base courses. Construction & Building Materials. 2016;121:198-209.

[126] Xiao F, Hou X, Amirkhanian S, Kim KW. Superpave evaluation of higher RAP contents using WMA technologies. Construction & Building Materials. 2016;112:1080-7.

[127] Taha R, Alshamsi K. Characterization of road bases and subbases made of reclaimed asphalt pavement and recycled concrete aggregate. 2008.

[128] Xiao F, Amirkhanian S, Juang CH. Rutting Resistance of Rubberized Asphalt Concrete Pavements Containing Reclaimed Asphalt Pavement Mixtures. Journal of Materials in Civil Engineering. 2007;19(6):475-83.

[129] Wen H. Development of Rutting Model for Unbound Aggregates Containing Recycled Asphalt Pavement. Geotechnical Testing Journal. 2013;36(36):236-41.

[130] Edil TB. Specifications and Recommendations for Recycled Materials Used as Unbound Base Course. Concrete Aggregates. 2011.

[131] Arulrajah A, Piratheepan J, Aatheesan T, Bo MW. Geotechnical Properties of Recycled Crushed Brick in Pavement Applications. Journal of Materials in Civil Engineering. 2011;23(10):1444-52.

[132] Serres N, Braymand S, Feugeas F. Environmental evaluation of concrete made from recycled concrete aggregate implementing Life Cycle Assessment. Journal of Building Engineering. 2015;5:24-33.

[133] Arulrajah A, Disfani MM, Horpibulsuk S, Suksiripattanapong C, Prongmanee N. Physical properties and shear strength responses of recycled construction and demolition materials in unbound pavement base/subbase applications. Construction & Building Materials. 2014;58(4):245-57.

[134] Arulrajah A, Mohammadinia A, Phummiphan I, Horpibulsuk S, Samingthong W. Stabilization of Recycled Demolition Aggregates by Geopolymers comprising Calcium Carbide Residue, Fly Ash and Slag precursors. Construction & Building Materials. 2016;114:864-73.

[135] Pcs LAW. Protocol P07 Test Method for Determining the Creep Compliance , Resilient Modulus and Strength of Asphalt Materials Using the Indirect Tensile Test Device. 2001.

[136] Wen H, Warner J, Edil T, Wang G. Laboratory Comparison of Crushed Aggregate and Recycled Pavement Material With and Without High Carbon Fly Ash. Geotechnical and Geological Engineering. 2010;28(4):405-11.

[137] Kim W, Labuz JF, Dai S. Resilient Modulus of Base Course Containing Recycled Asphalt Pavement. Transportation Research Record Journal of the Transportation Research Board. 2007;2005(1):27-35.

[138] Copeland A. Reclaimed Asphalt Pavement in Asphalt Mixtures: State of the Practice. 2011.

[139] Airey GD, Choi YK, Rahman MM, Collop AC, Akisetty CK, Lee SJJ, et al. User Guidelines for Waste and Byproduct Materials in Pavement Construction. Costs. 1998.

[140] Macgregor J, Highter W, Degroot D. Structural Numbers for Reclaimed Asphalt Pavement Base and Subbase Course Mixes. Transportation Research Record Journal of the Transportation Research Board. 1999;1687(1):22-8.

[141] Ayan, Vahid. Assessment of recycled aggregates for use in unbound subbase of highway pavement. Kingston University. 2011.

[142] Richter CA. Seasonal variations in the moduli of unbound pavement layers. Mathematical Prediction. 2006.

[143] Sargious M, Mushule N. Behaviour of recycled asphalt pavements at low temperatures. Canadian Journal of Civil Engineering. 1991;18(3):428-35.

[144] Wen H, Wu M, Uhlmeyer JS. Evaluation of the Effects of Climatic Conditions on Modulus of Base Materials with Recycled Asphalt Pavement. Transportation Research Board 90th Annual Meeting2011.

[145] Jablonski B, Regehr J, Rempel G. Guide for Mechanistic-Empirical Design of New and Rehabilitated Pavement Structures. Final Report Part Design Analysis. 2004.

[146] https://en.wikipedia.org/wiki/Subbase_(pavement).

[147] Bowen MM. Performance evaluation of cement-treated roadway bases. Field Studies. 2000.

[148] Kim S, Ceylan H, Gopalakrishnan K. Effect of M-E Design Guide Inputs on Flexible Pavement Performance Predictions. Road Materials & Pavement Design. 2007;8(3):375-97.

[149] M.S. Hossain, D.S. Lane, Development of a catalog of resilient modulus values for aggregate base for use with the mechanistic-empirical pavement design guide (MEPDG), Virginia Center for Transportation Innovation and Research, 2015.

[150] M.S. Hossain, H. Nair, H.C. Ozyildirim, Determination of mechanical properties for cement-treated aggregate base, Virginia Transportation Research Council, 2017.

[151] Yau, A. and Von Quintus, H. L., Study of LTTP laboratory resilient modulus test data and response characteristics, Federal Highway Administration, 2002.

APPENDIX A

Measured vs. Predicted Resilient Modulus of VG, HJ, MB, and MC at Various Cement Contents (3%, 5%, and 7%)

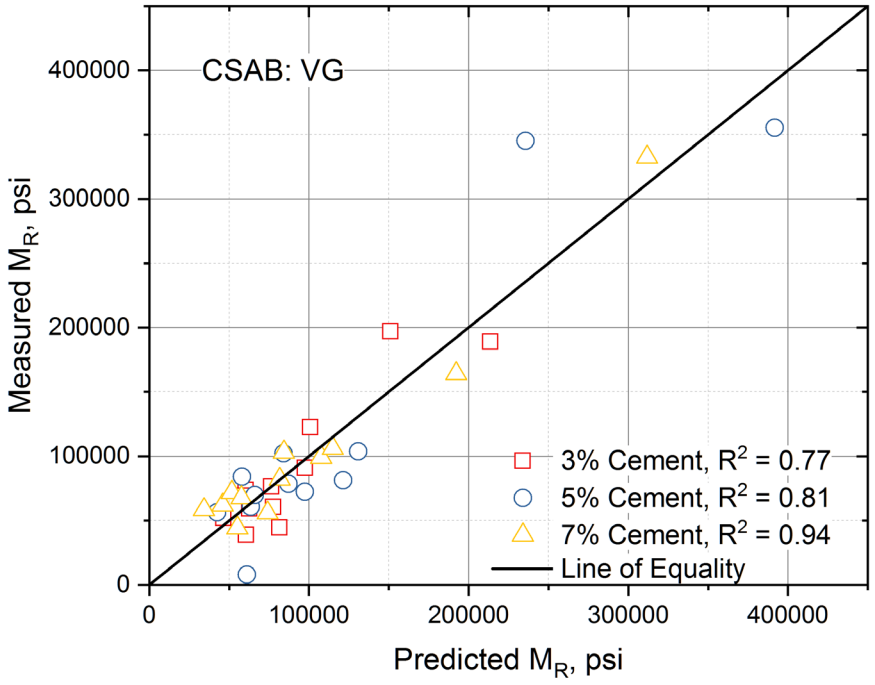

Figure A-1: Measured vs. Predicted Resilient Modulus of VG at Various Cement Contents

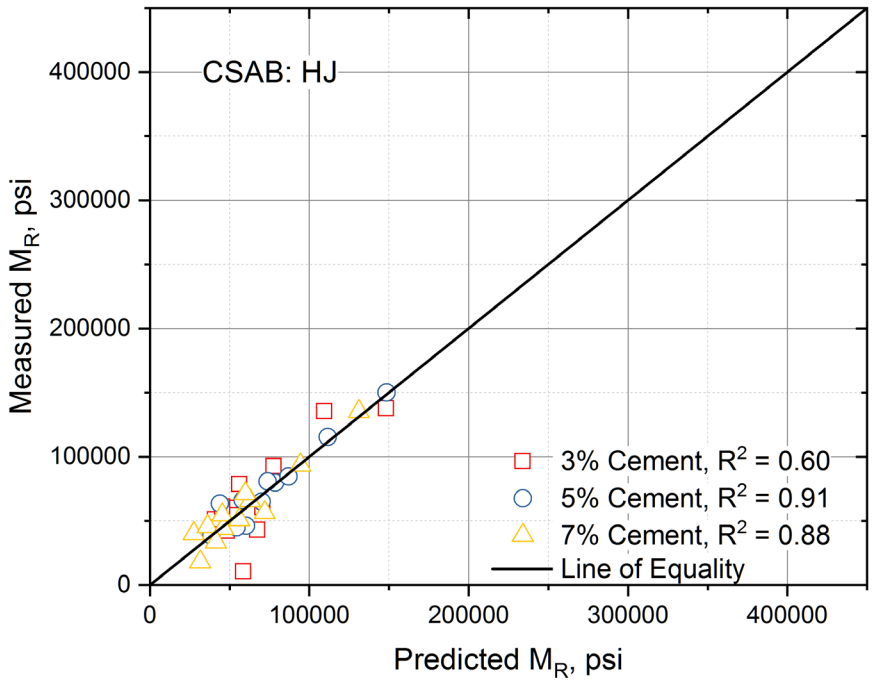

Figure A-2: Measured vs. Predicted Resilient Modulus of HJ at Various Cement Contents

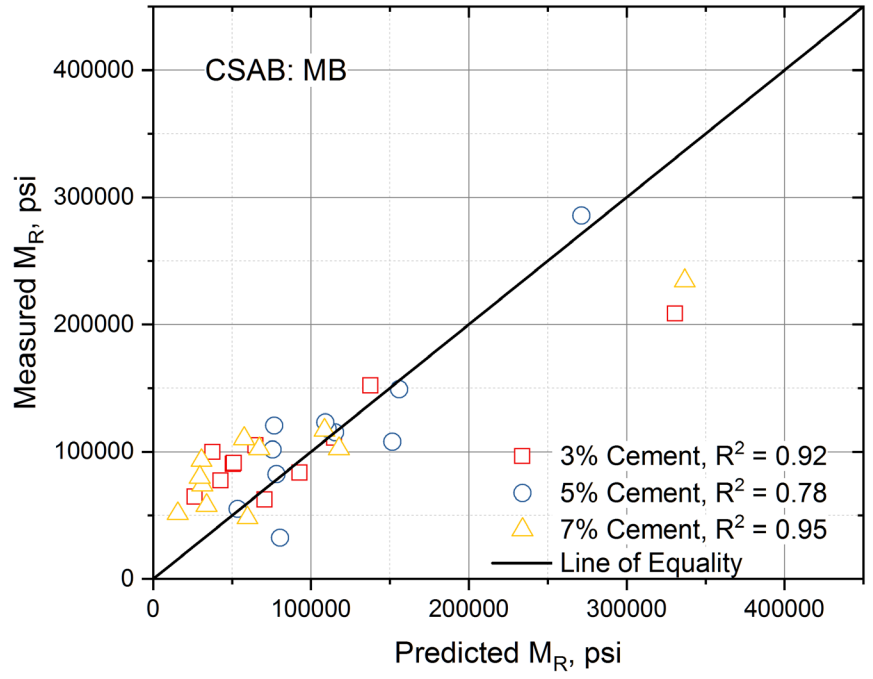

Figure A-3: Measured vs. Predicted Resilient Modulus of MB at Various Cement Contents

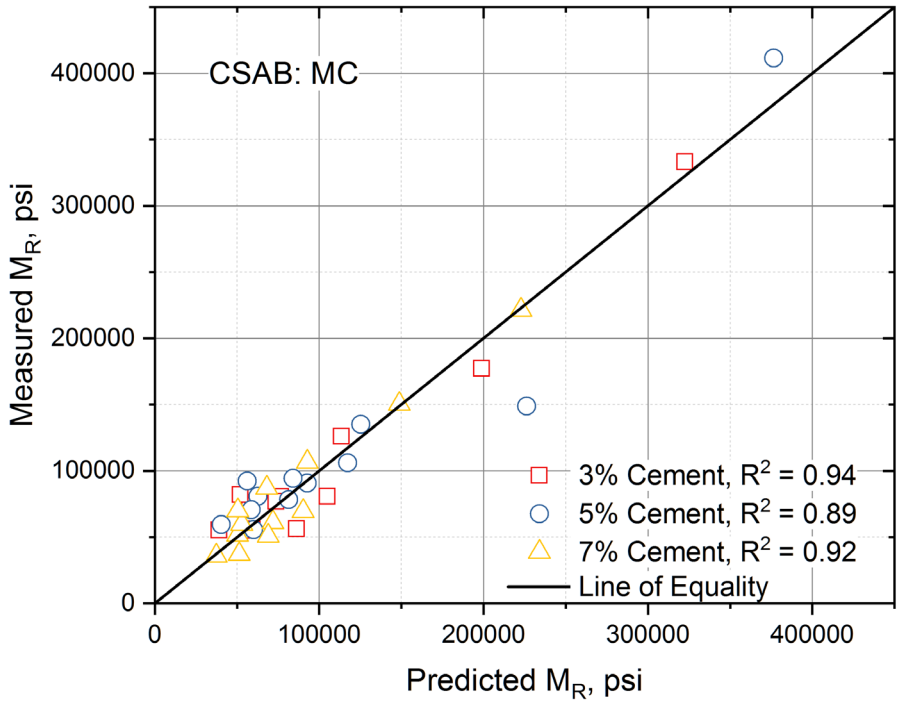

Figure A-4: Measured vs. Predicted Resilient Modulus of MC at Various Cement Contents

APPENDIX B

Stress and Strain Summation Curves of VG, HJ, MB, and MC at Various Cement Contents (3%, 5%, and 7%)

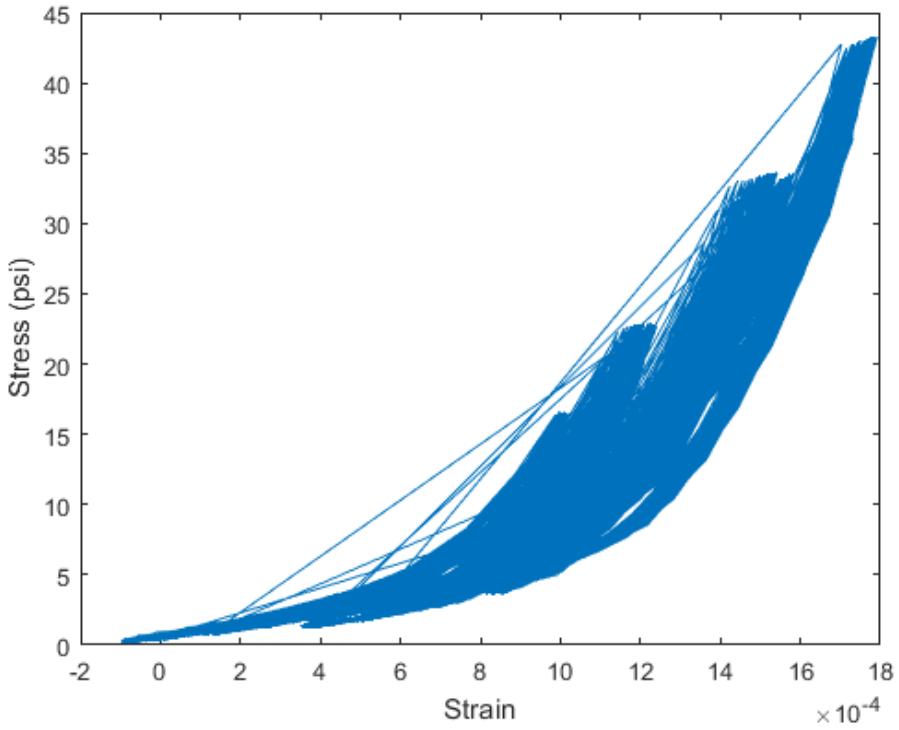

Figure B-1: Stress and Strain Summation Curve of VG at 3% Cement Content

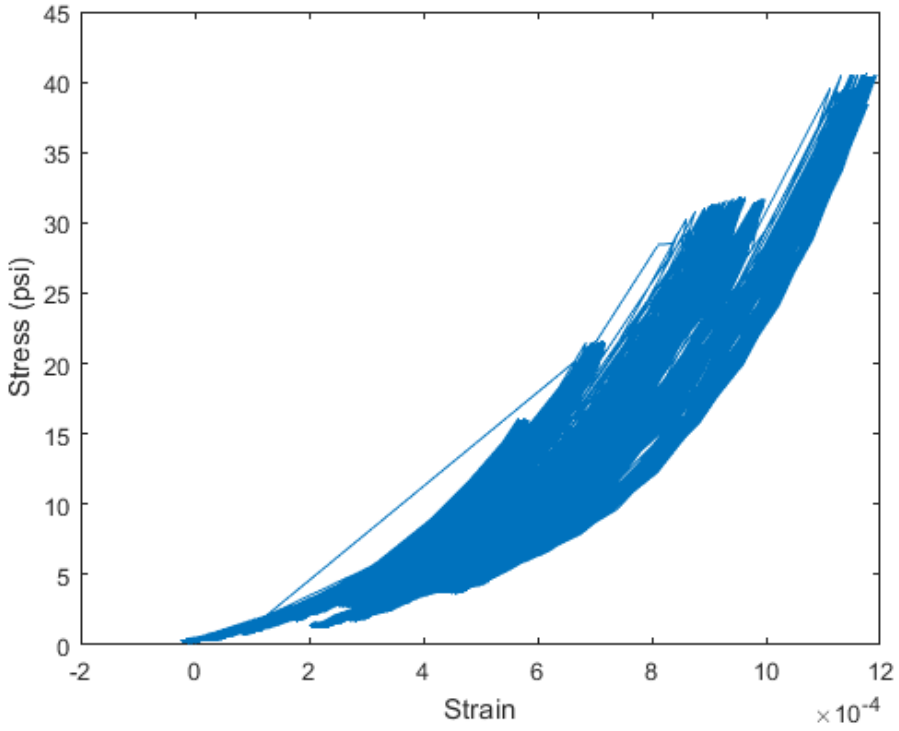

Figure B-2: Stress and Strain Summation Curve of VG at 5% Cement Content

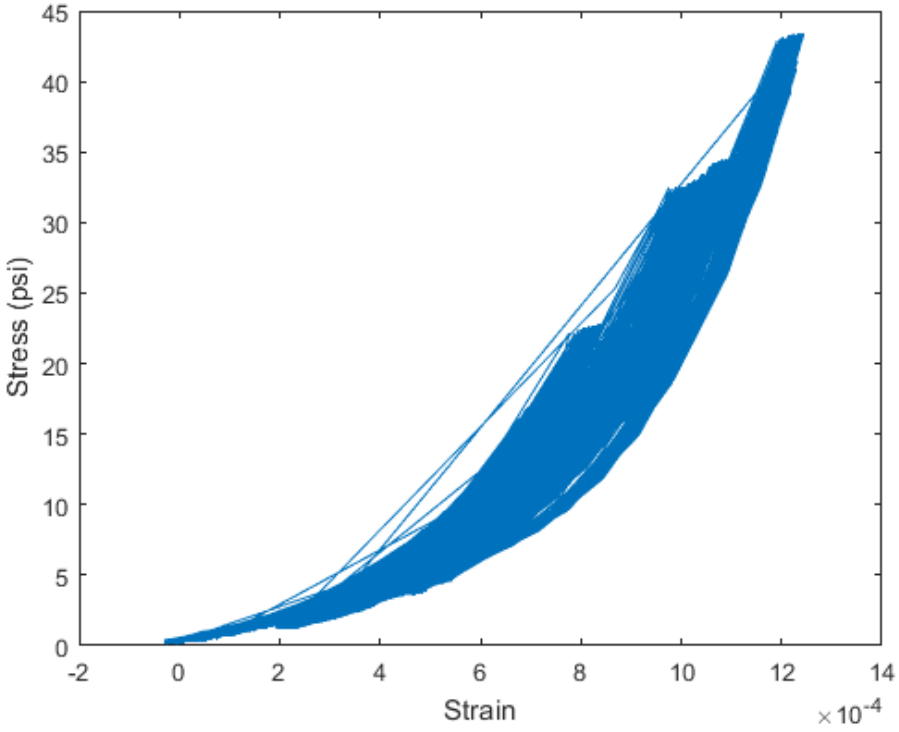

Figure B-3: Stress and Strain Summation Curve of VG at 7% Cement Content

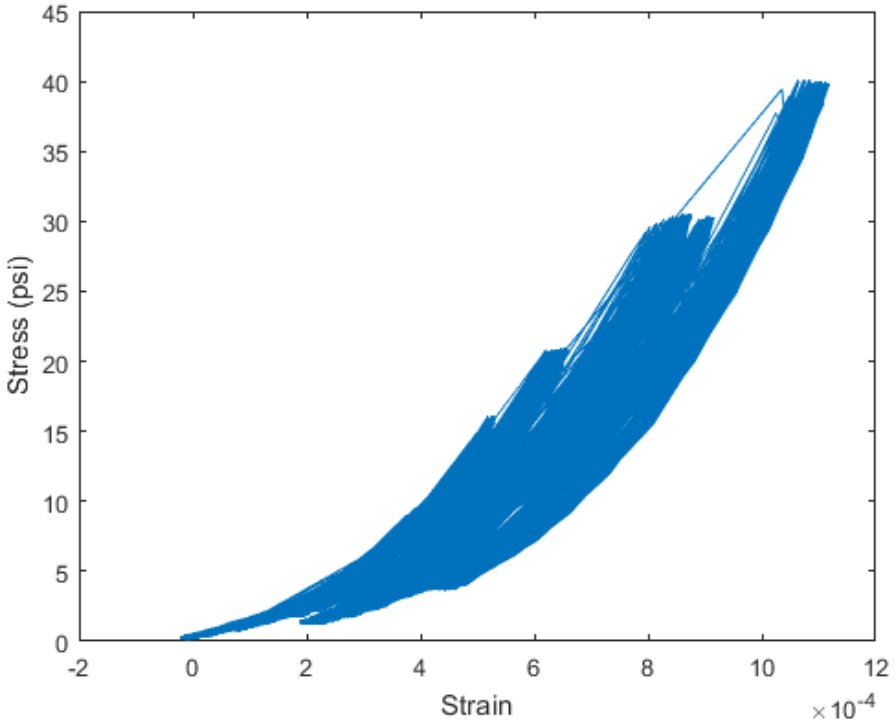

Figure B-4: Stress and Strain Summation Curve of HJ at 3% Cement Content

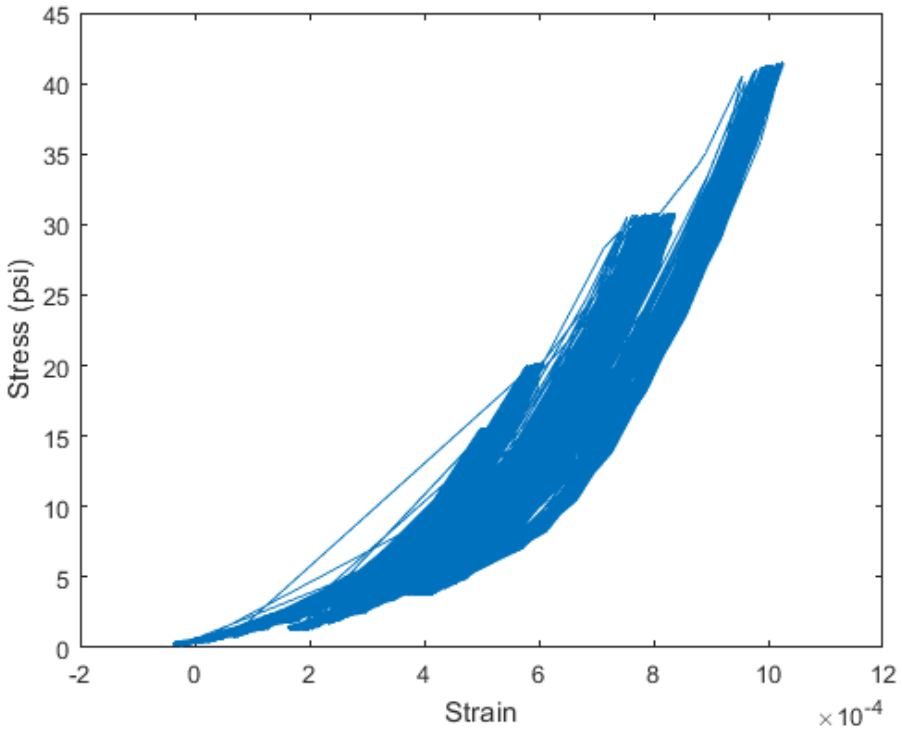

Figure B-5: Stress and Strain Summation Curve of HJ at 5% Cement Content

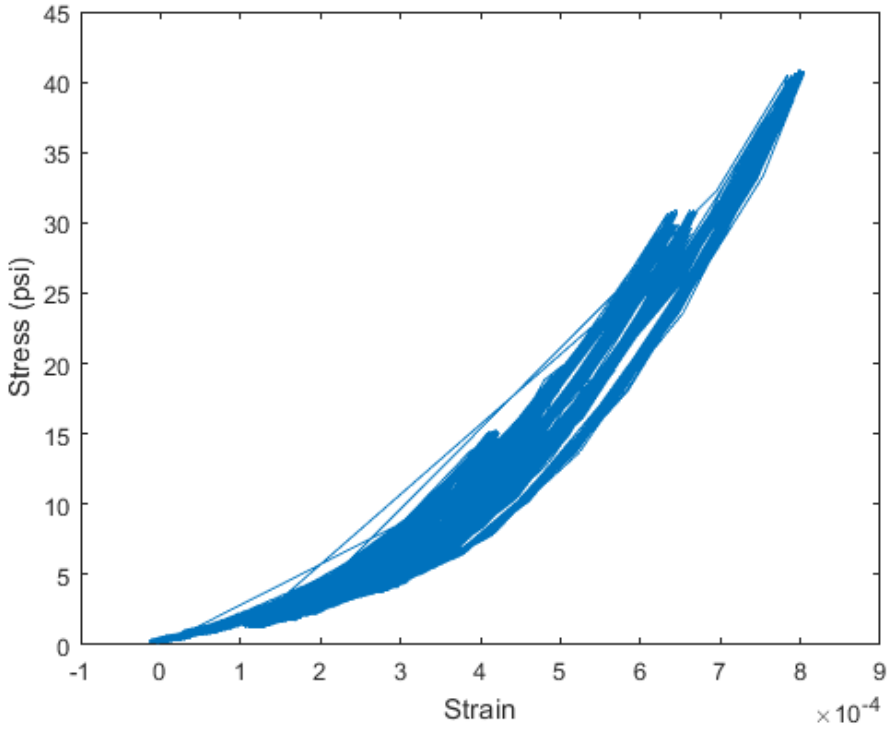

Figure B-6: Stress and Strain Summation Curve of HJ at 7% Cement Content

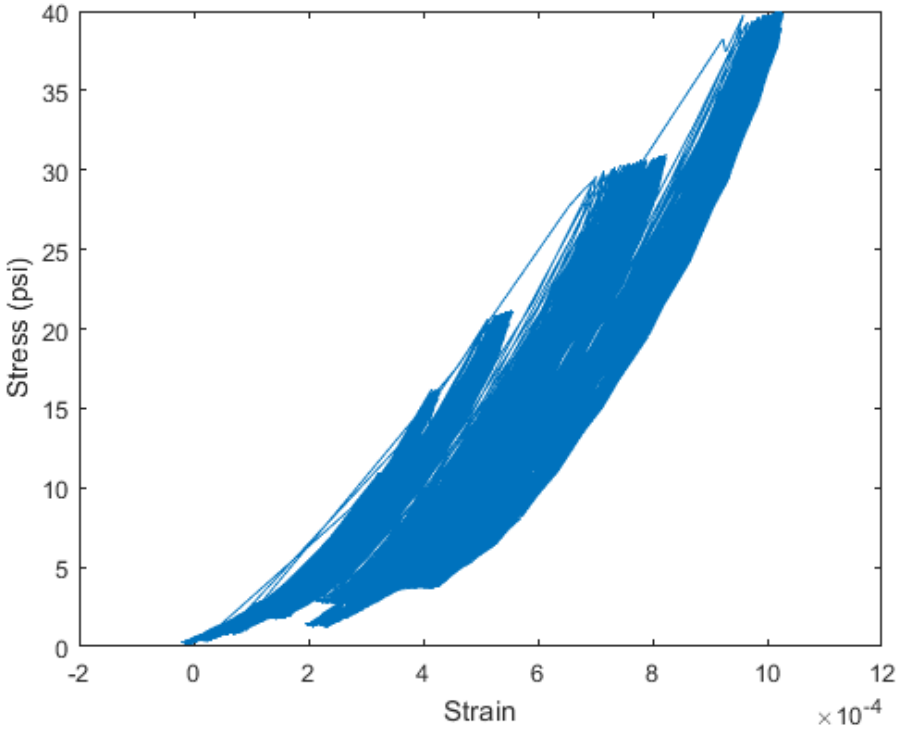

Figure B-7: Stress and Strain Summation Curve of MB at 3% Cement Content

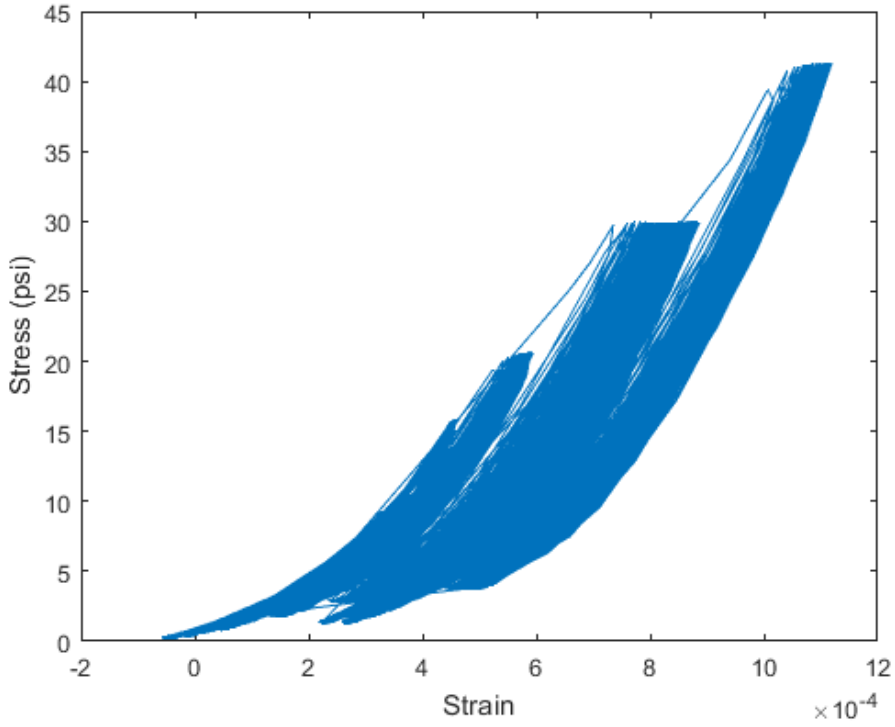

Figure B-8: Stress and Strain Summation Curve of MB at 5% Cement Content

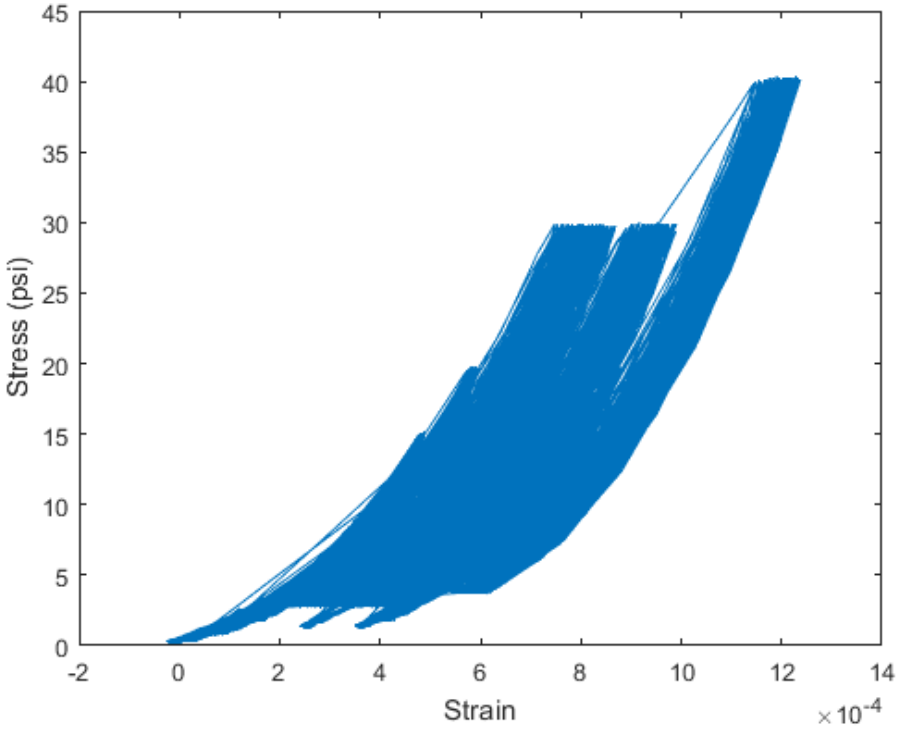

Figure B-9: Stress and Strain Summation Curve of MB at 7% Cement Content

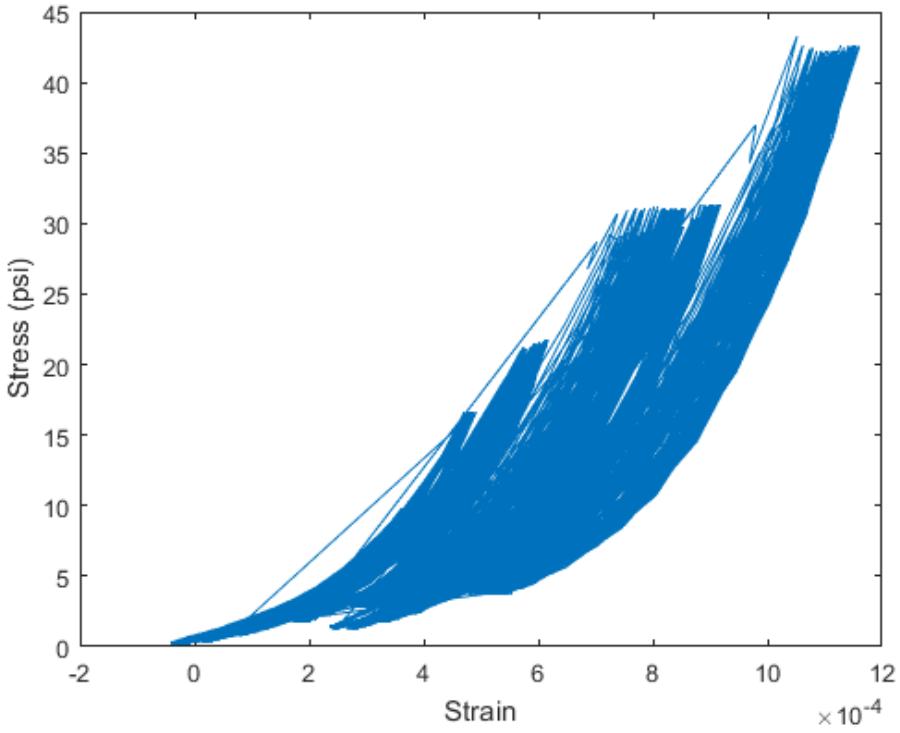

Figure B-10: Stress and Strain Summation Curve of MC at 3% Cement Content

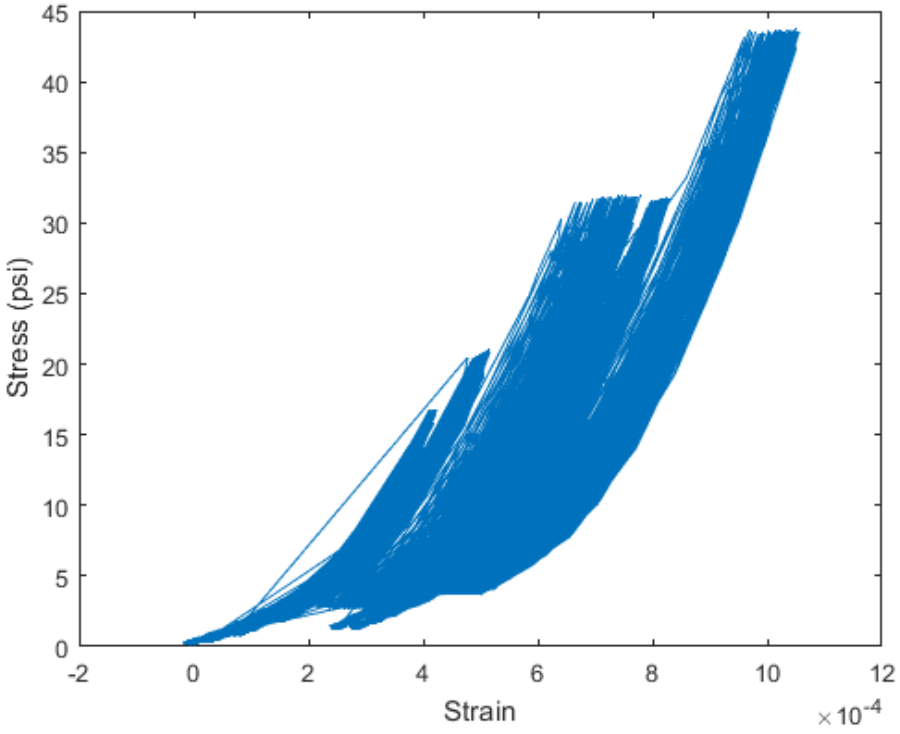

Figure B-11: Stress and Strain Summation Curve of MC at 5% Cement Content

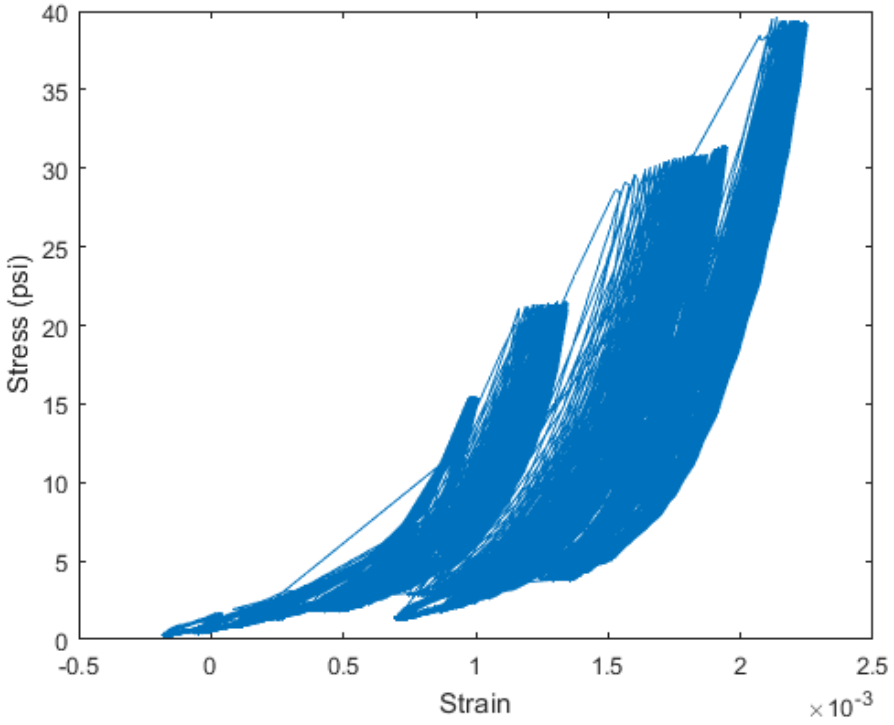

Figure B-12: Stress and Strain Summation Curve of MC at 7% Cement Content

APPENDIX C

Compressive Strength Fitting Results of Sandy Soil-Based CMRB and S-C at Various RAP Contents (0%, 25%, 50%, and 75%)

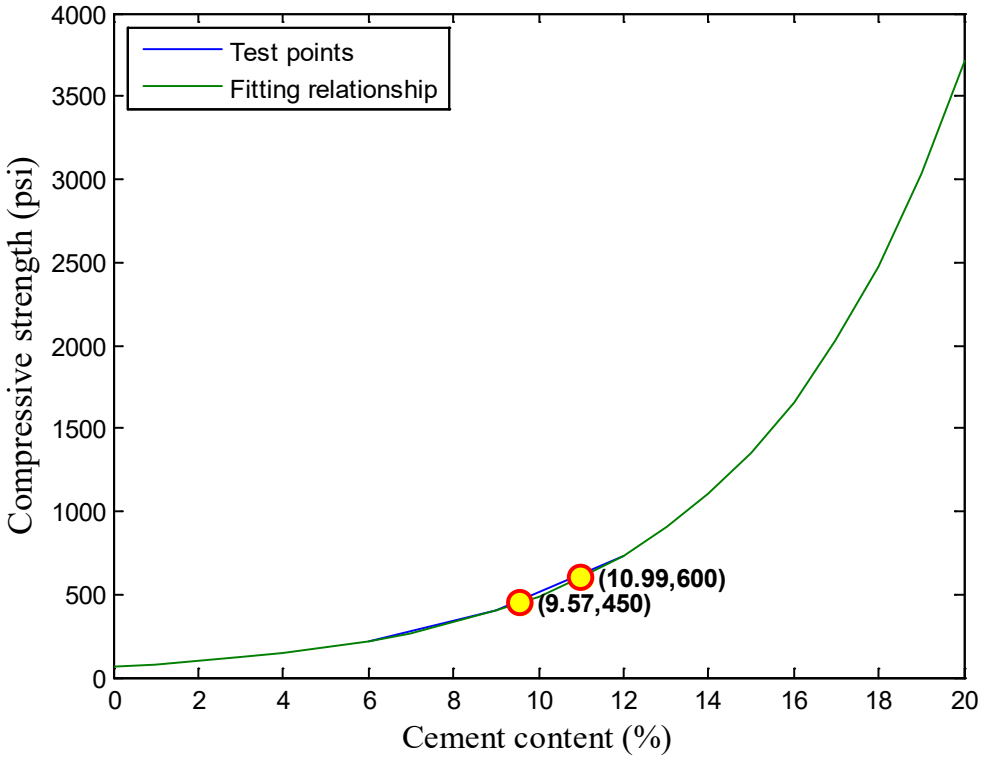

Figure C-1: Fitting Results of SS-0% Compressive Strength at 7 Days

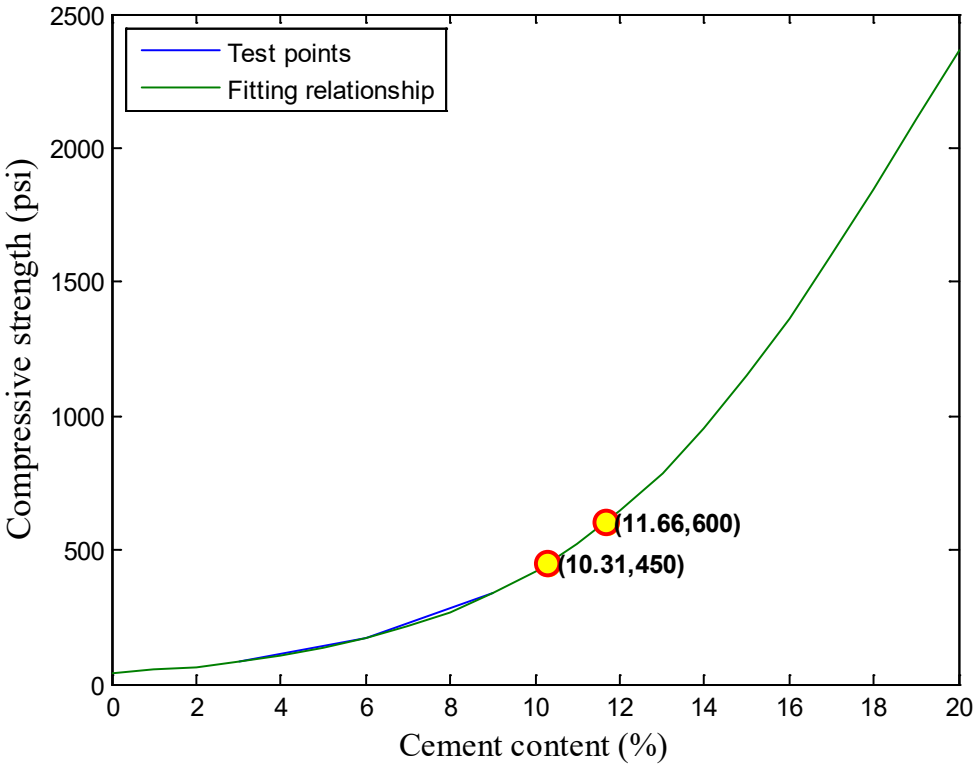

Figure C-2: Fitting Results of SS-25% Compressive Strength at 7 Days

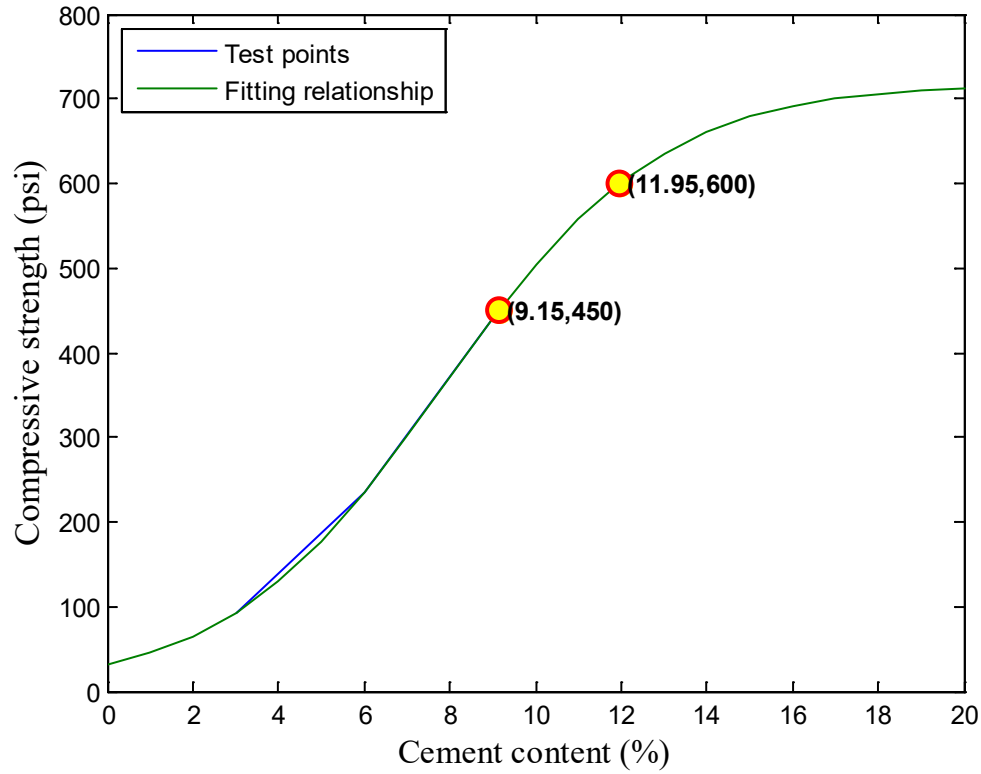

Figure C-3: Fitting Results of SS-50% Compressive Strength at 7 Days

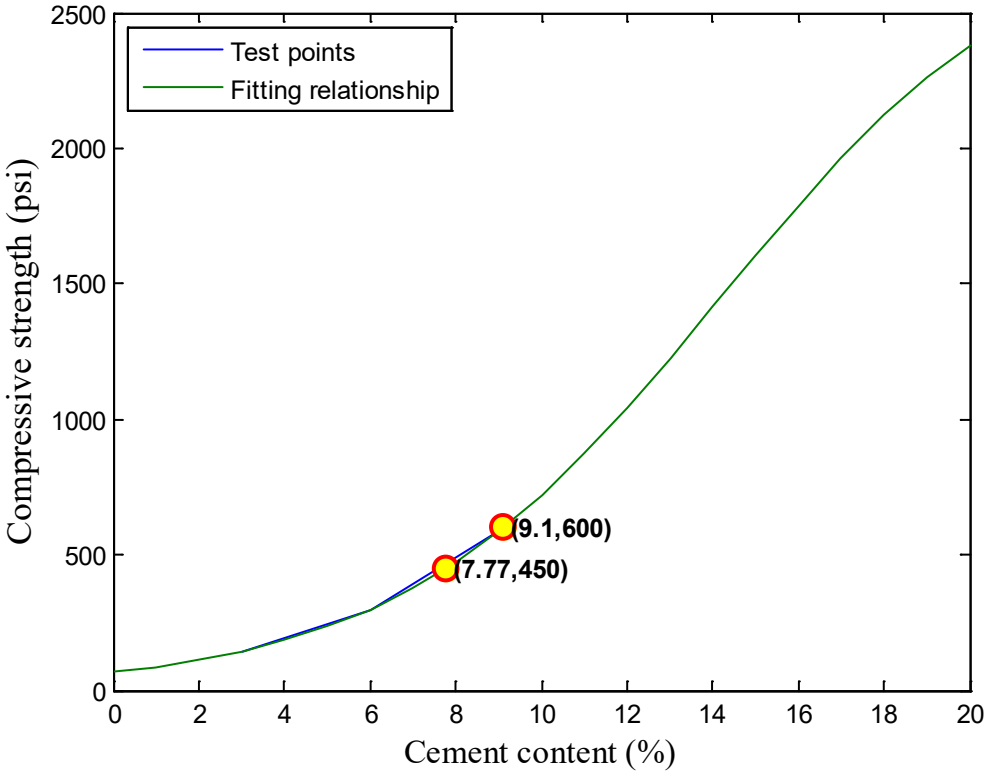

Figure C-4: Fitting Results of SS-75% Compressive Strength at 7 Days

APPENDIX D

Measured vs. Predicted Resilient Modulus of CMRB and S-C with Various Soil Types at Various Cement Contents

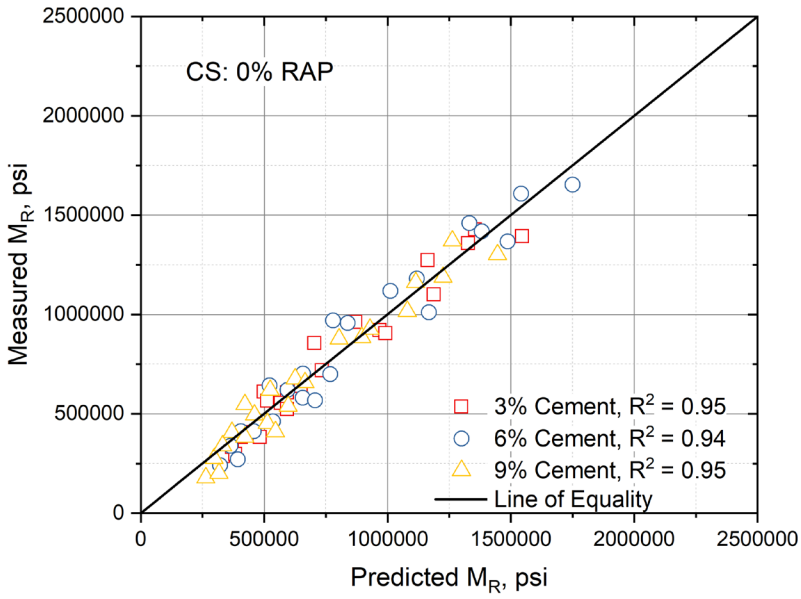

Figure D-1: Measured vs. Predicted Resilient Modulus of S-C with Clayey Soil at Various Cement Contents

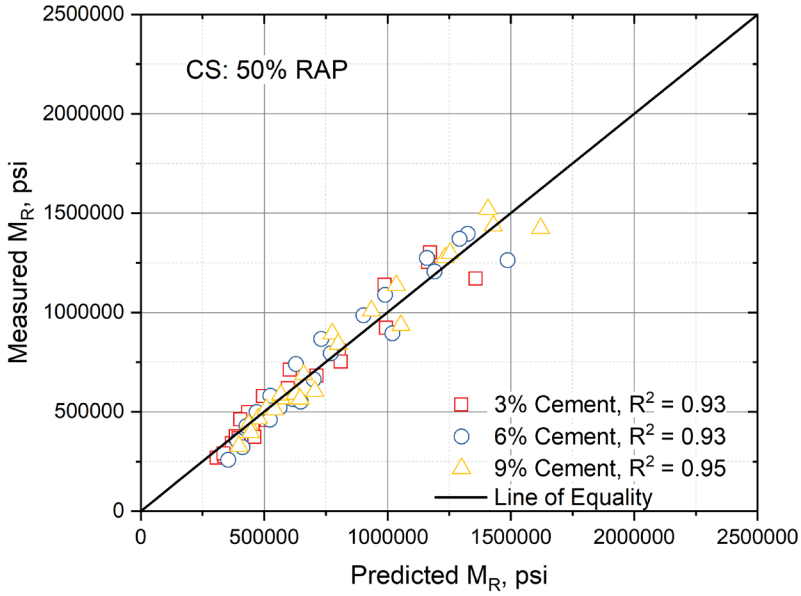

Figure D-2: Measured vs. Predicted Resilient Modulus of CMRB with Clayey Soil and 50% RAP at Various Cement Contents

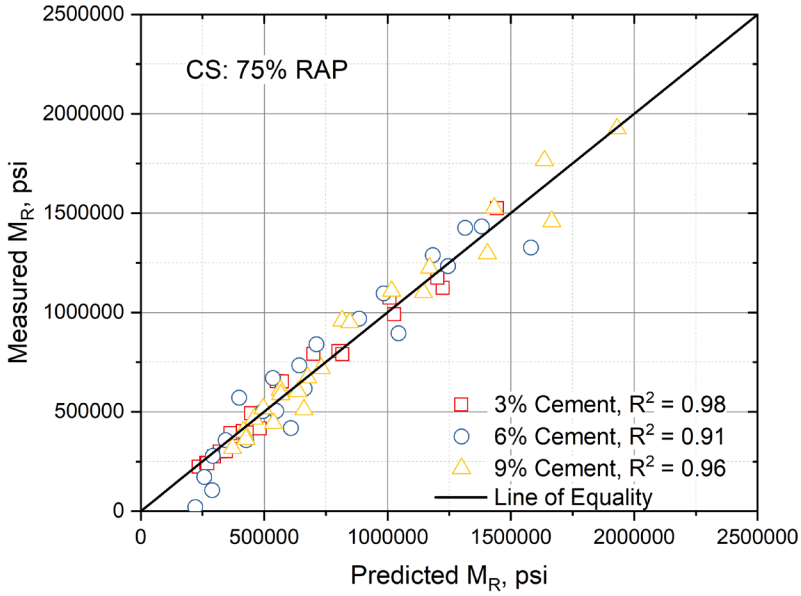

Figure D-3: Measured vs. Predicted Resilient Modulus of CMRB with Clayey Soil and 75% RAP at Various Cement Contents

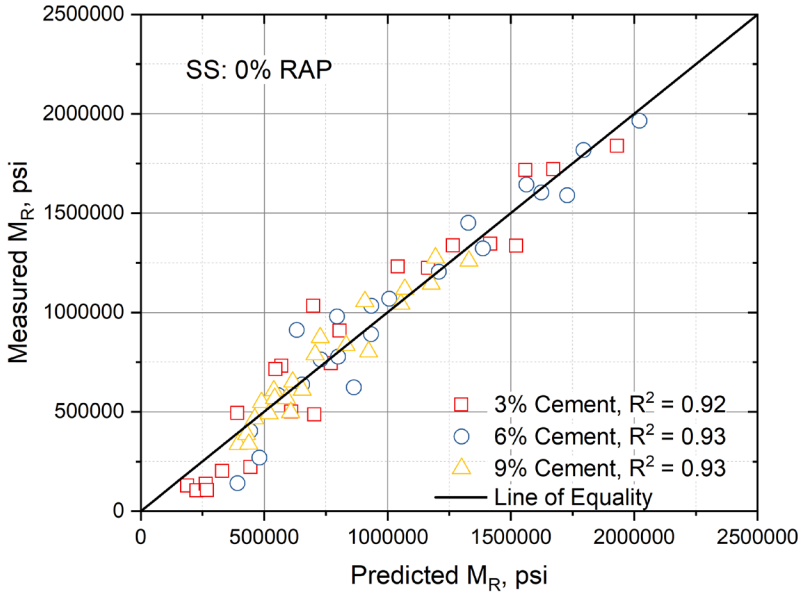

Figure D-4: Measured vs. Predicted Resilient Modulus of S-C with Sandy Soil at Various Cement Contents

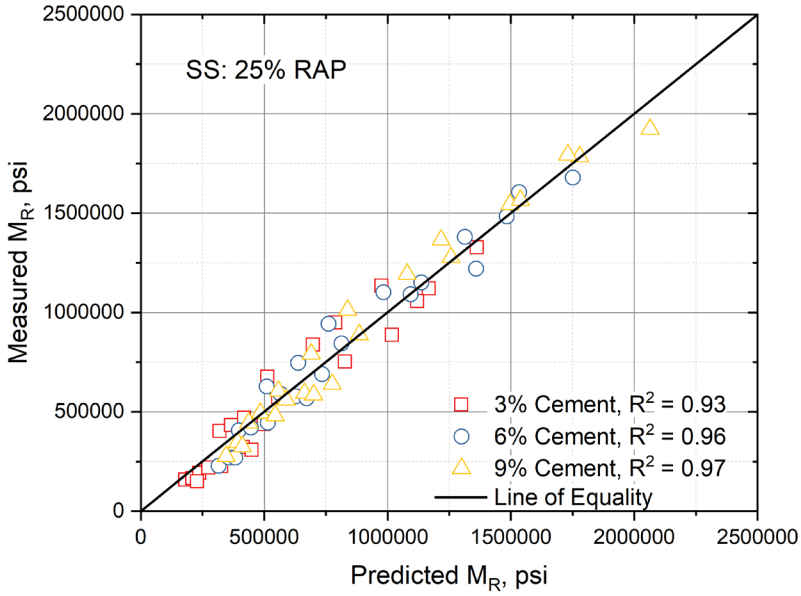

Figure D-5: Measured vs. Predicted Resilient Modulus of CMRB with Sandy Soil and 25% RAP at Various Cement Contents

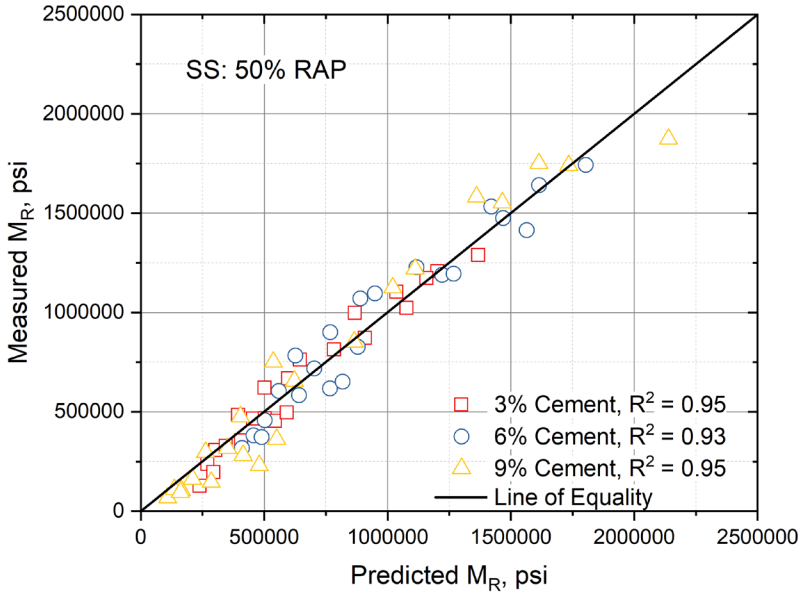

Figure D-6: Measured vs. Predicted Resilient Modulus of CMRB with Sandy Soil and 50% RAP at Various Cement Contents

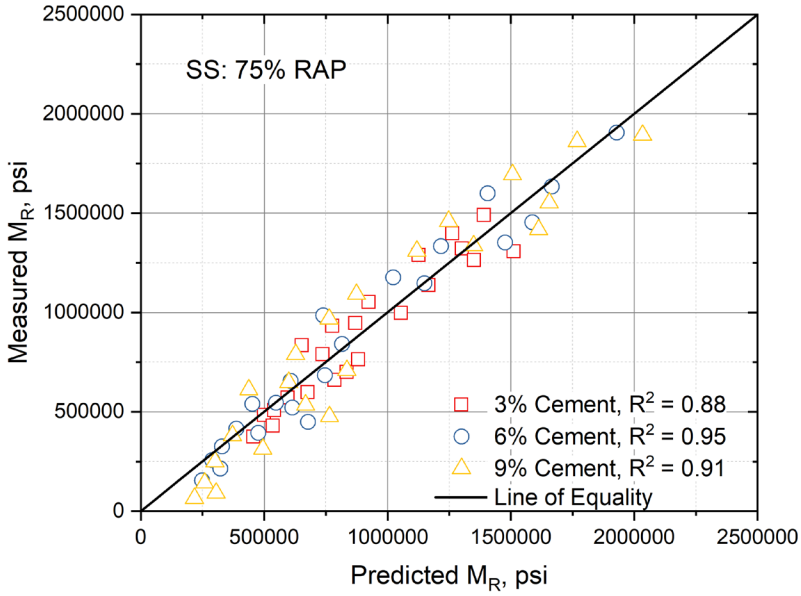

Figure D-7: Measured vs. Predicted Resilient Modulus of CMRB with Sandy Soil and 75% RAP at Various Cement Contents

APPENDIX E

Stress and Strain Summation Curves of Clayey Soil-Based and Sandy Soil-Based CMRB and S-C at Various Cement Contents (3%, 6%, 9% and 12%)

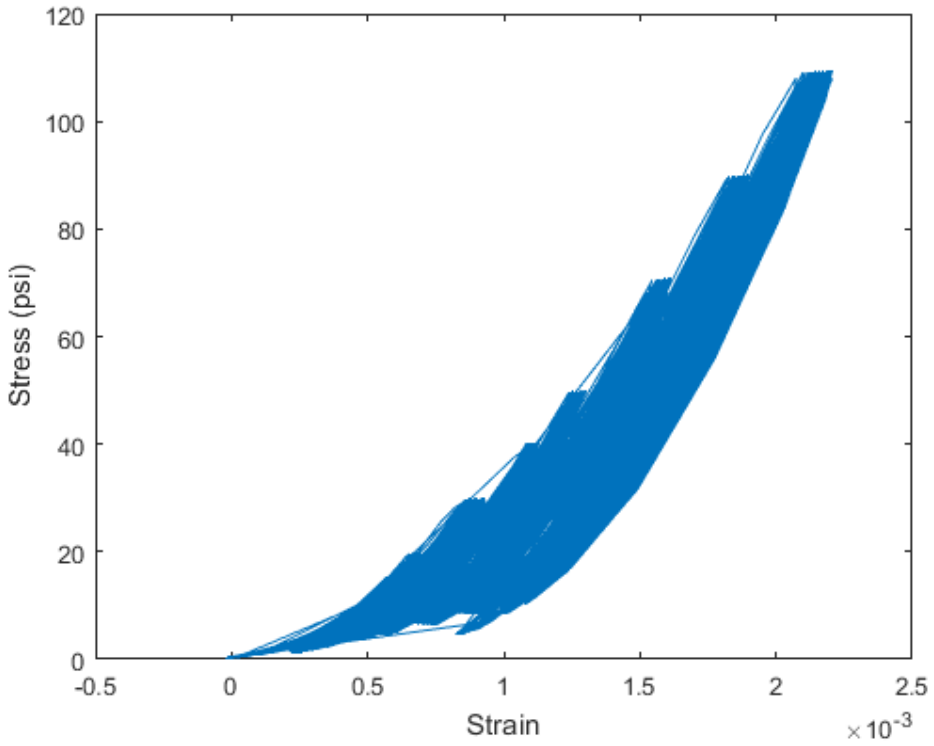

Figure E-1: Stress and Strain Summation Curve of CS-0% at 9% Cement Content

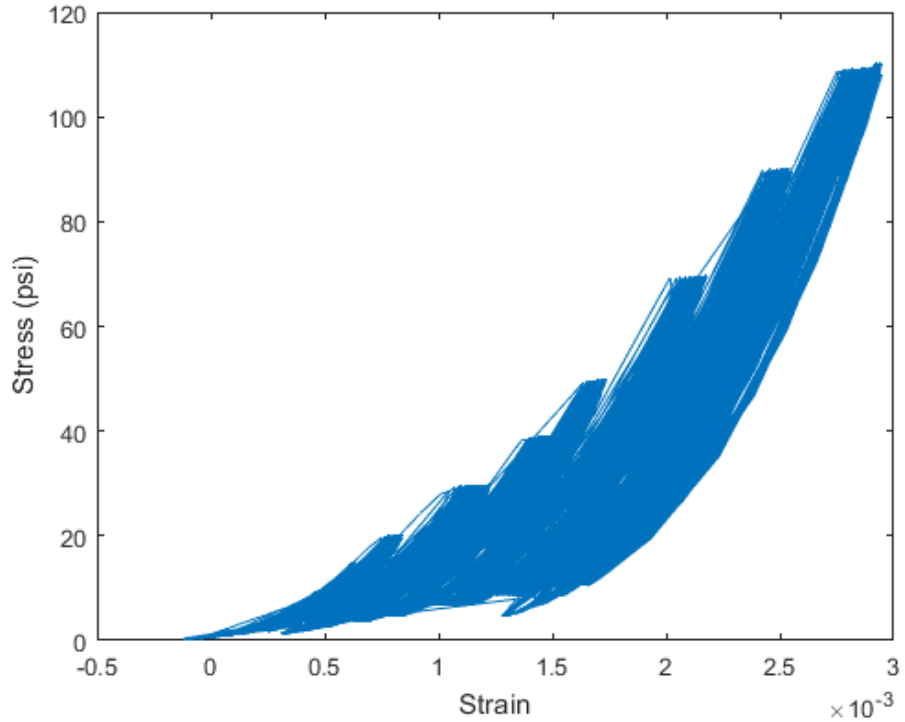

Figure E-2: Stress and Strain Summation Curve of CS-0% at 12% Cement Content

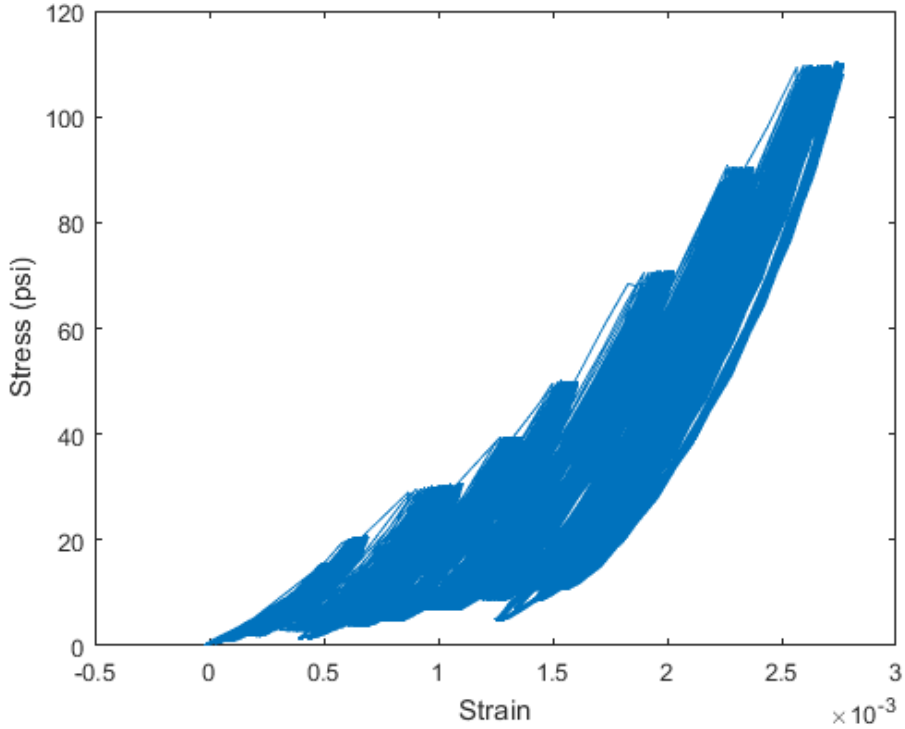

Figure E-3: Stress and Strain Summation Curve of CS-25% at 3% Cement Content

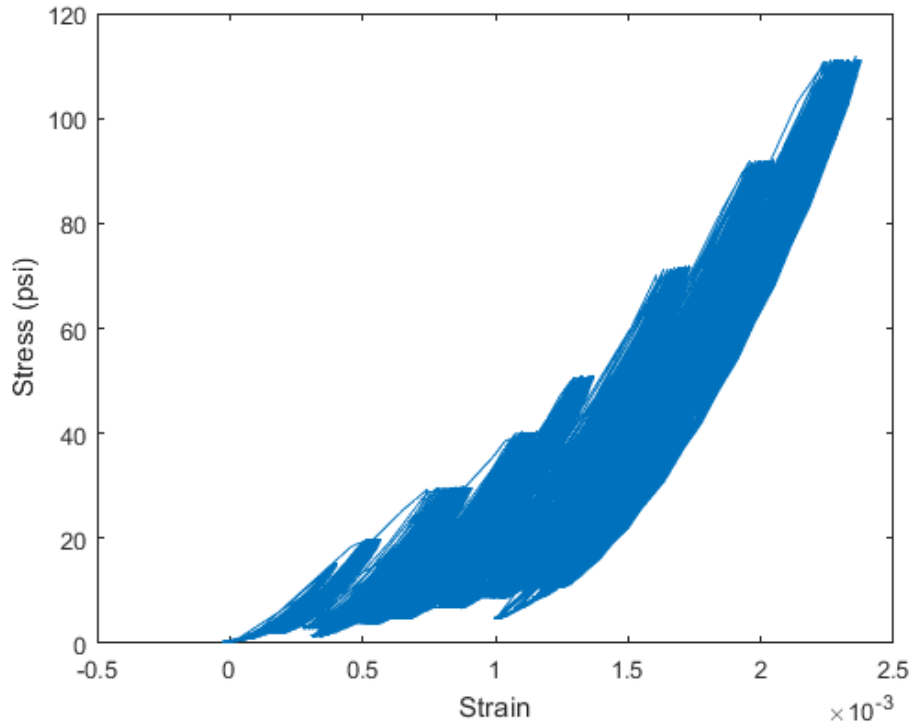

Figure E-4: Stress and Strain Summation Curve of CS-25% at 6% Cement Content

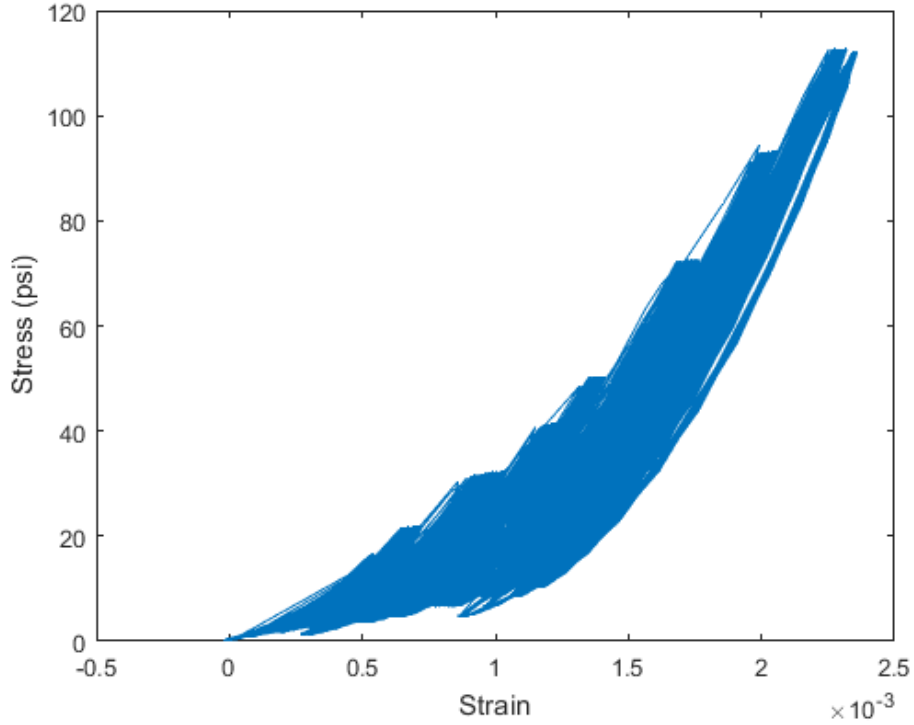

Figure E-5: Stress and Strain Summation Curve of CS-25% at 9% Cement Content

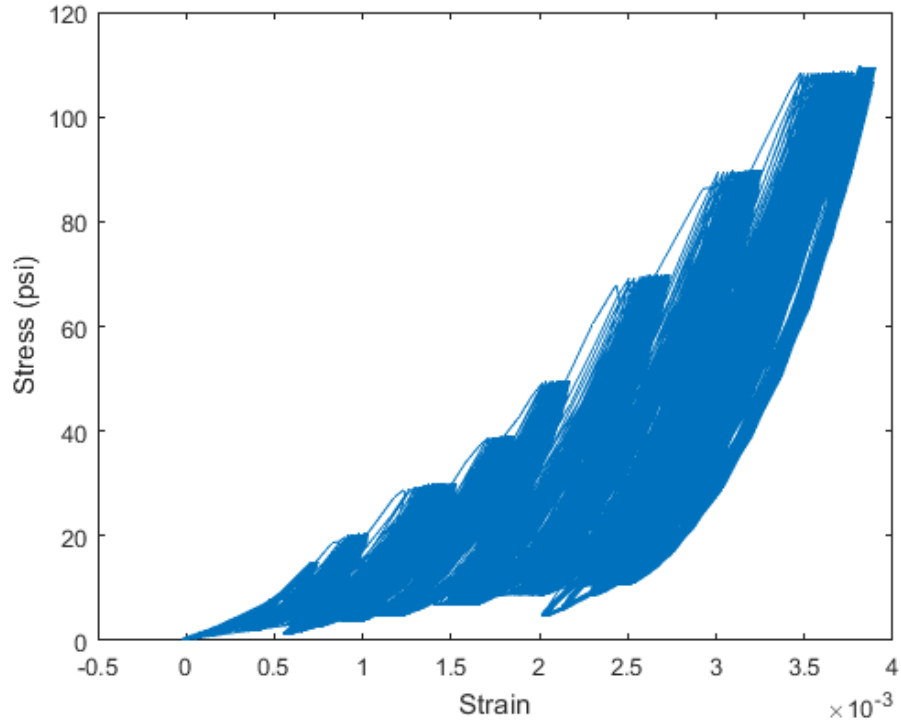

Figure E-6: Stress and Strain Summation Curve of CS-50% at 3% Cement Content

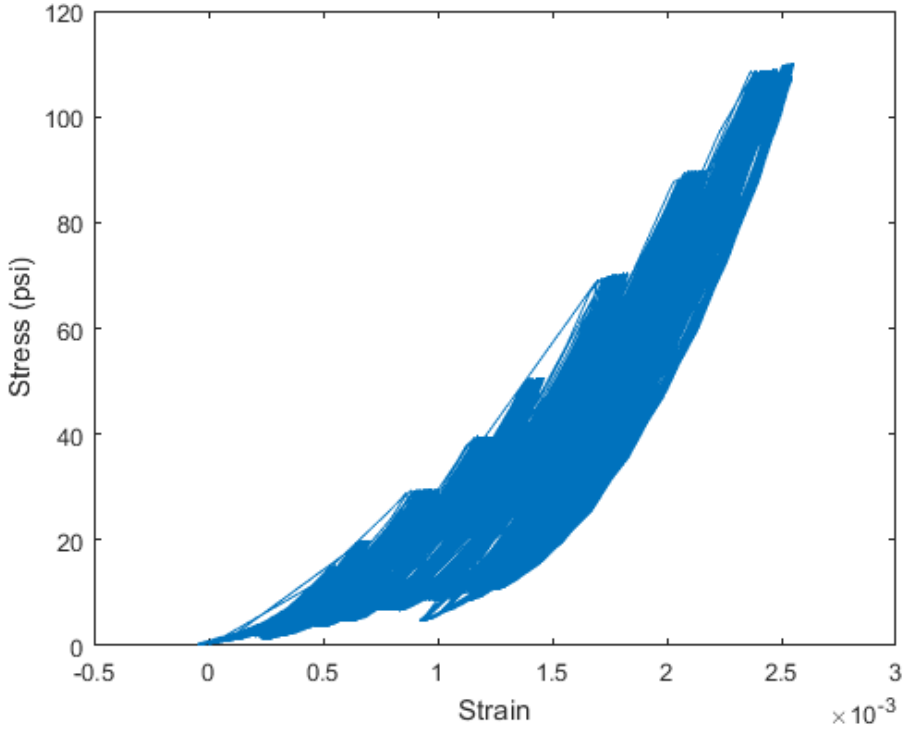

Figure E-7: Stress and Strain Summation Curve of CS-50% at 6% Cement Content

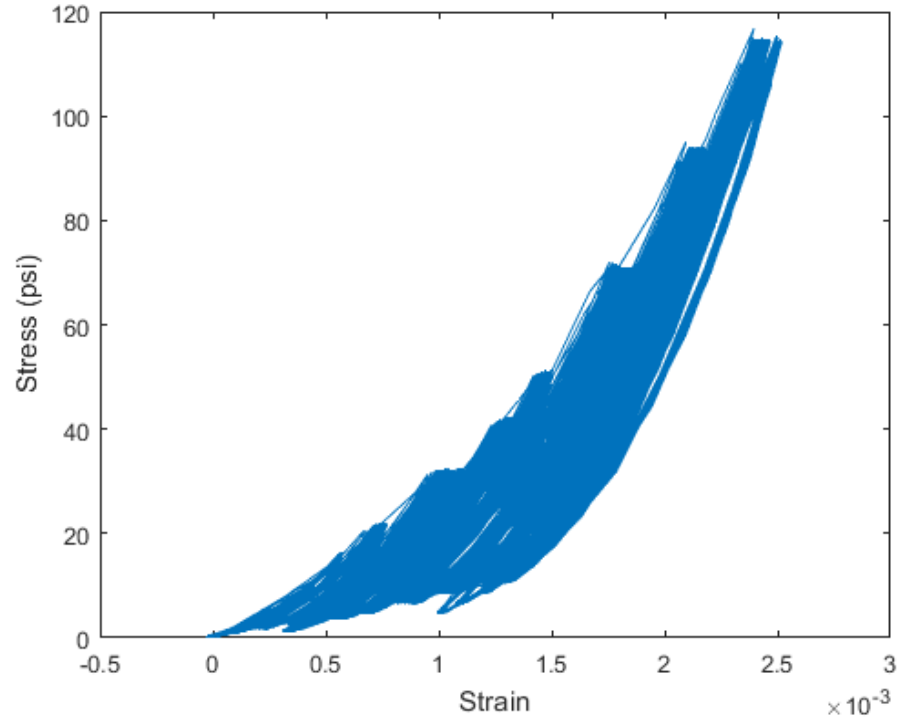

Figure E-8: Stress and Strain Summation Curve of CS-50% at 9% Cement Content

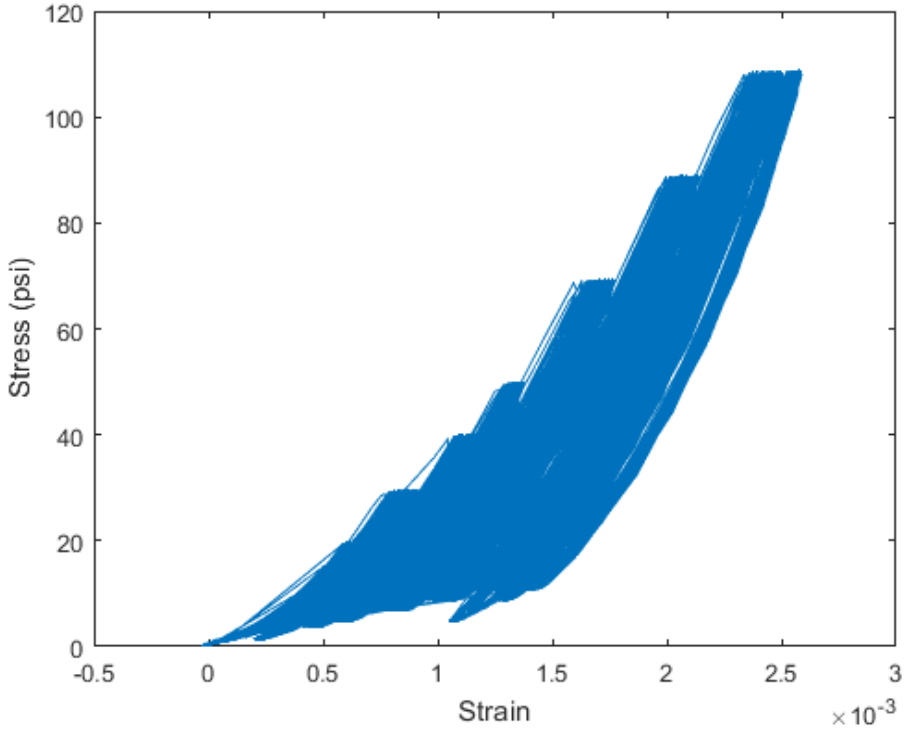

Figure E-9: Stress and Strain Summation Curve of CS-75% at 3% Cement Content

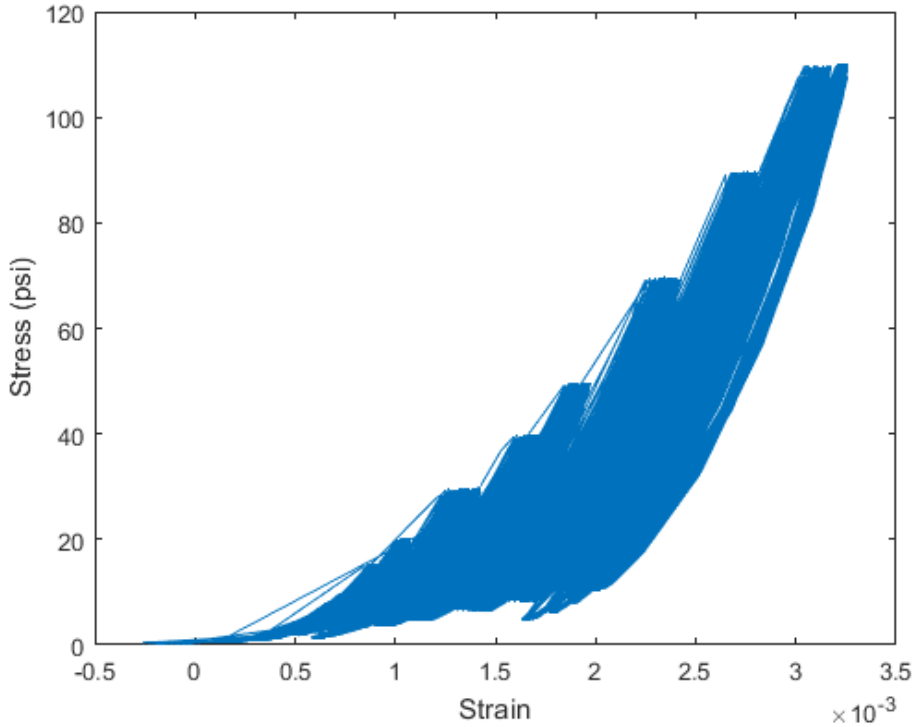

Figure E-10: Stress and Strain Summation Curve of CS-75% at 6% Cement Content

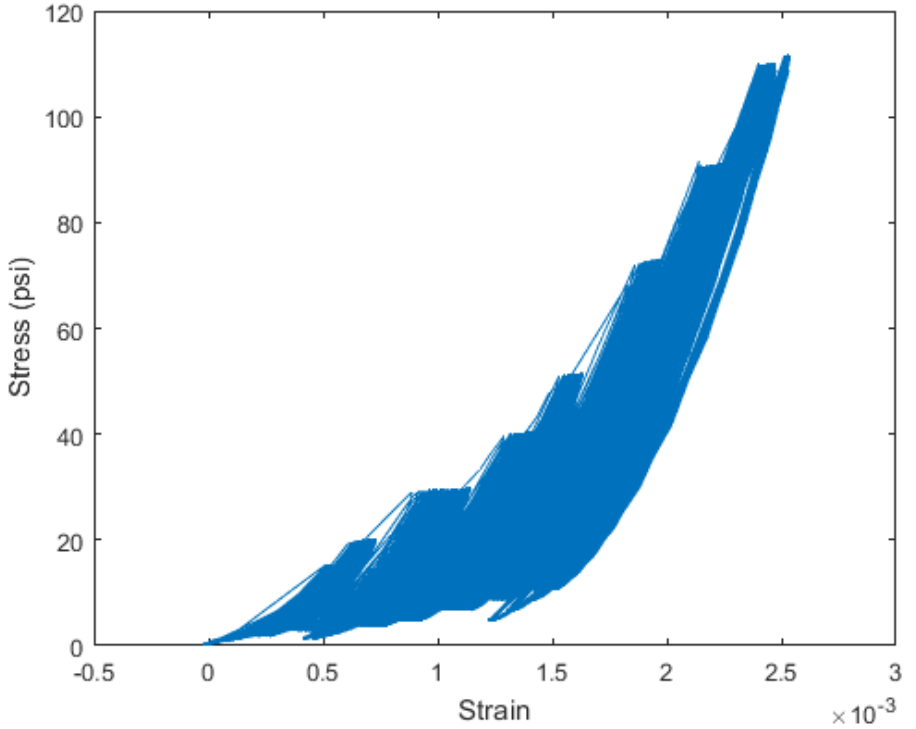

Figure E-11: Stress and Strain Summation Curve of CS-75% at 9% Cement Content

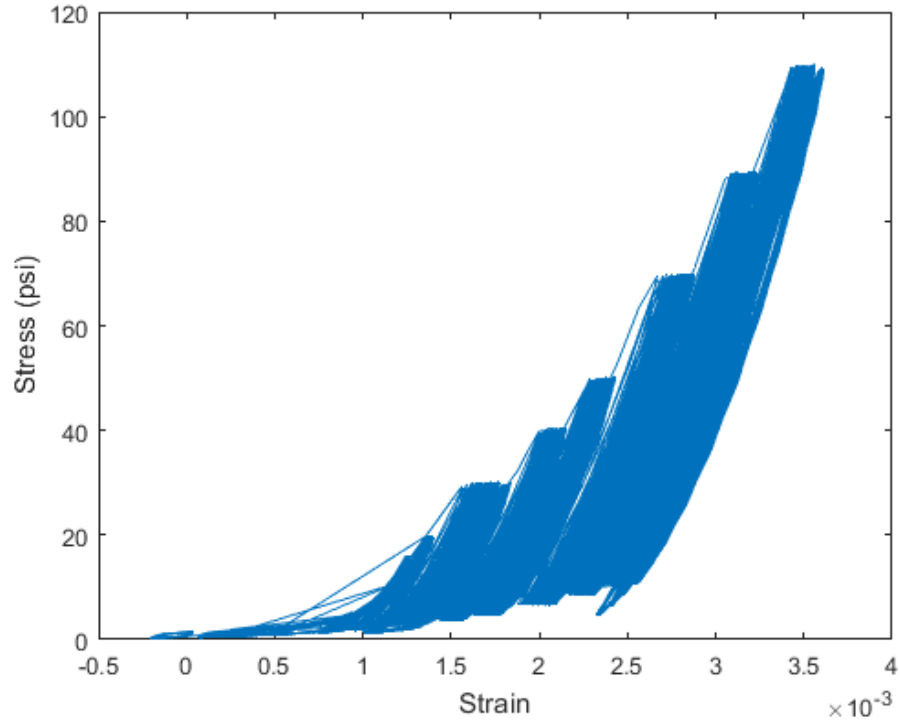

Figure E-12: Stress and Strain Summation Curve of SS-0% at 6% Cement Content

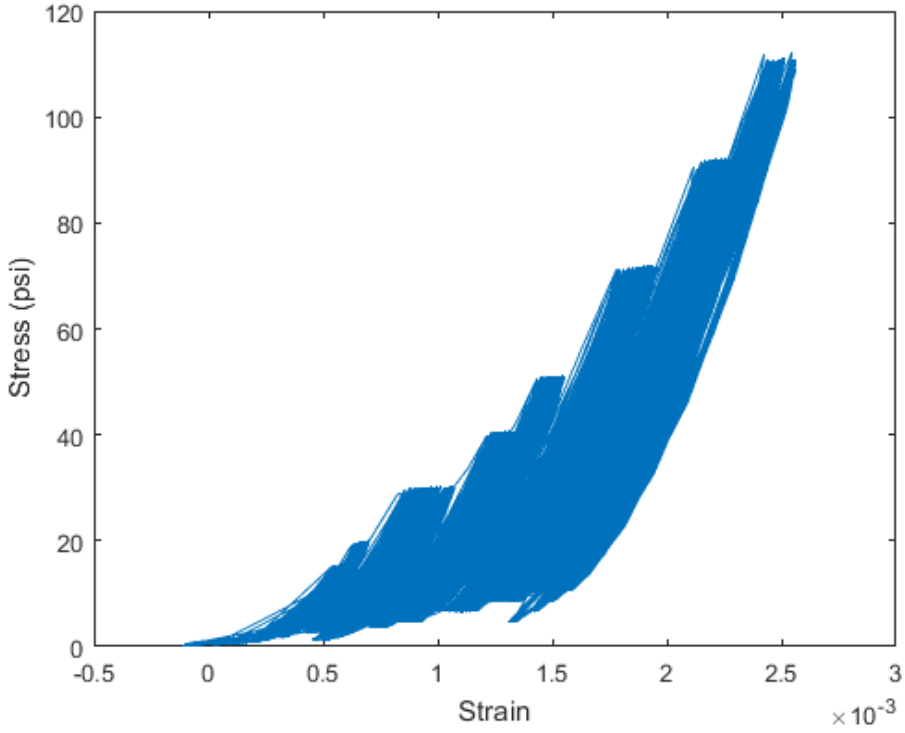

Figure E-13: Stress and Strain Summation Curve of SS-0% at 9% Cement Content

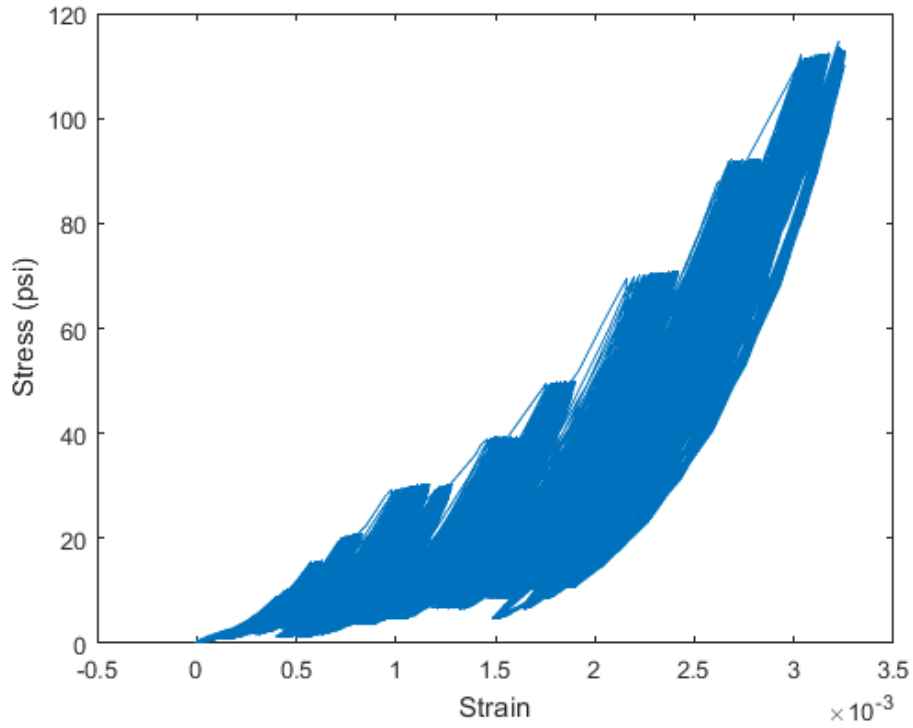

Figure E-14: Stress and Strain Summation Curve of SS-0% at 12% Cement Content

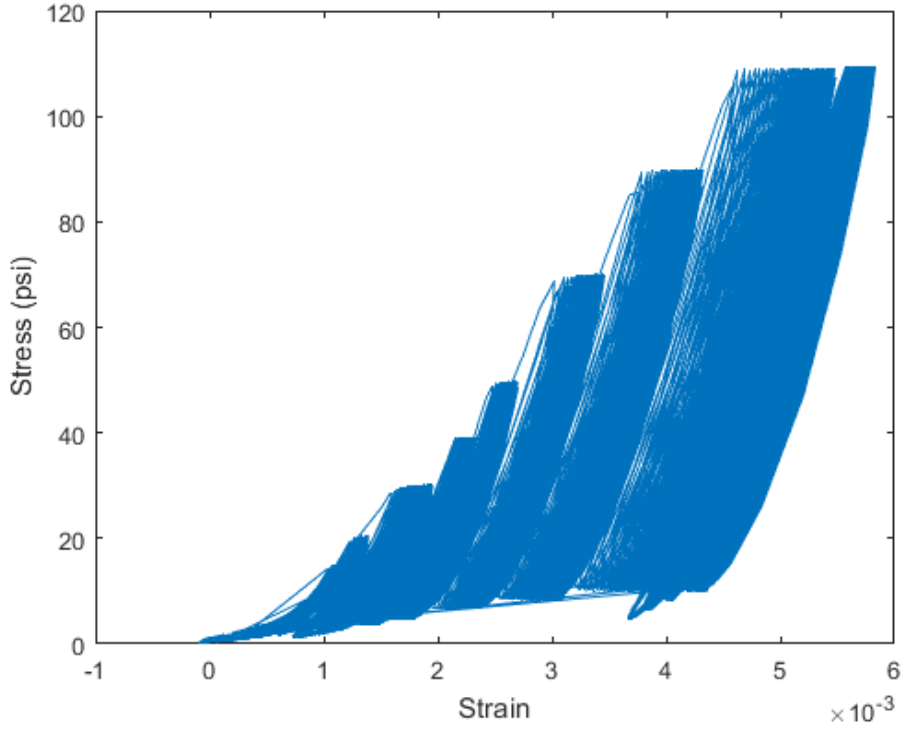

Figure E-15: Stress and Strain Summation Curve of SS-25% at 3% Cement Content

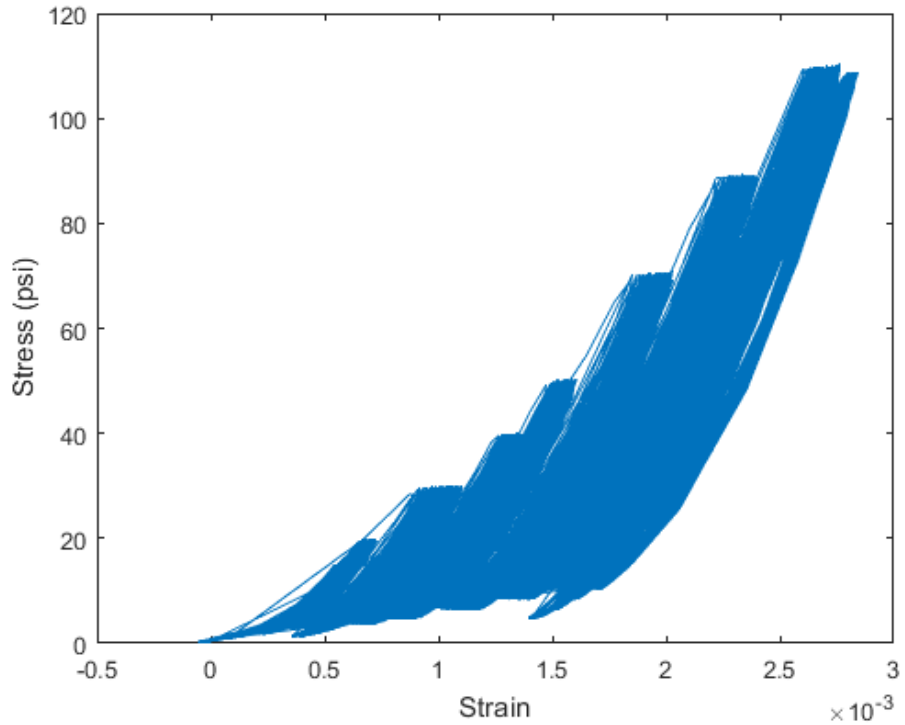

Figure E-16: Stress and Strain Summation Curve of SS-25% at 6% Cement Content

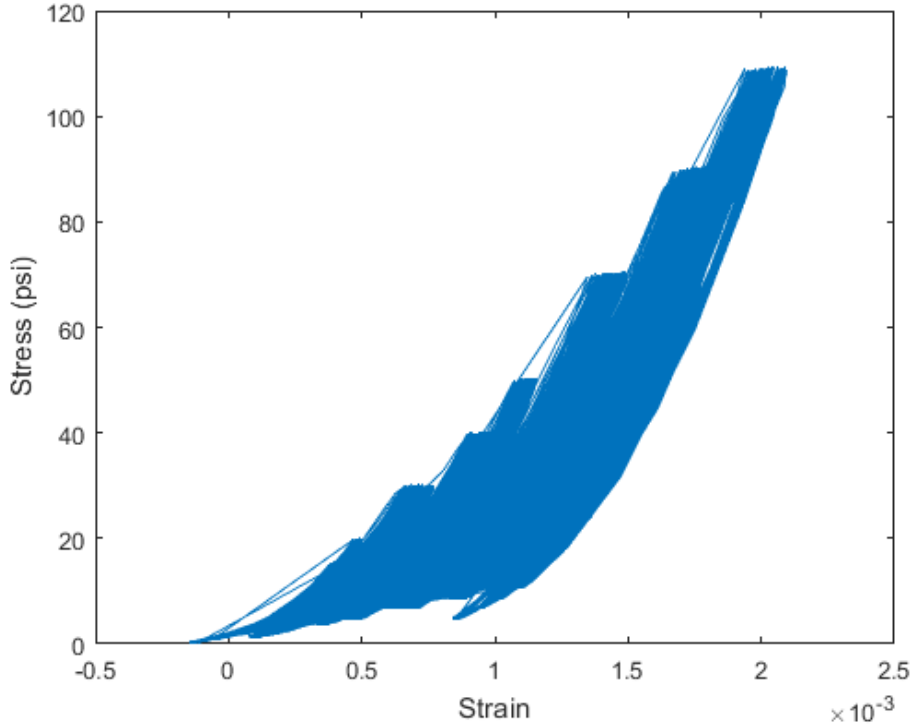

Figure E-17: Stress and Strain Summation Curve of SS-25% at 9% Cement Content

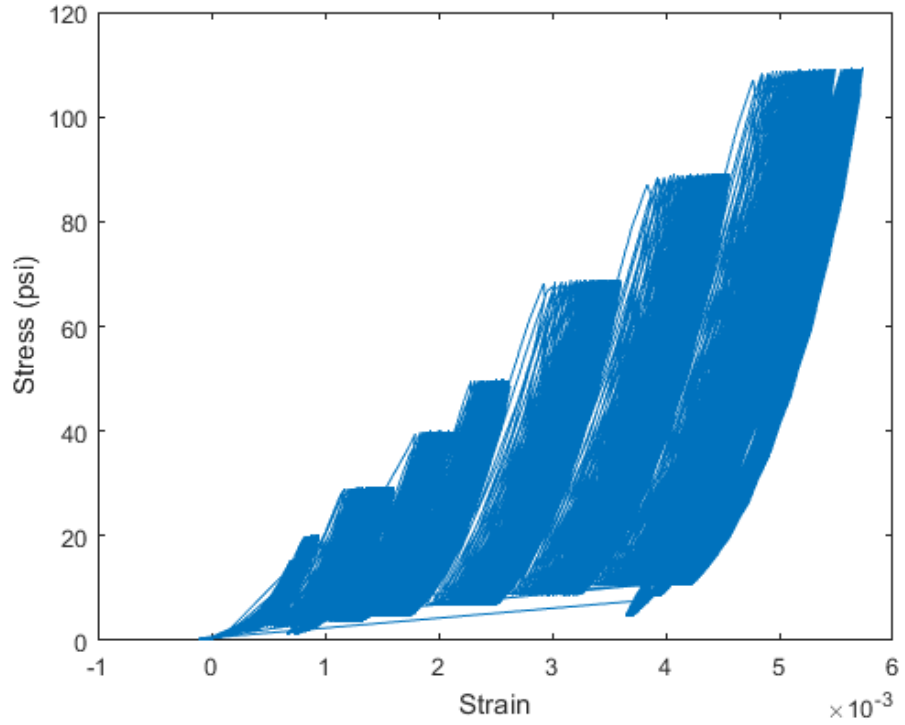

Figure E-18: Stress and Strain Summation Curve of SS-50% at 3% Cement Content

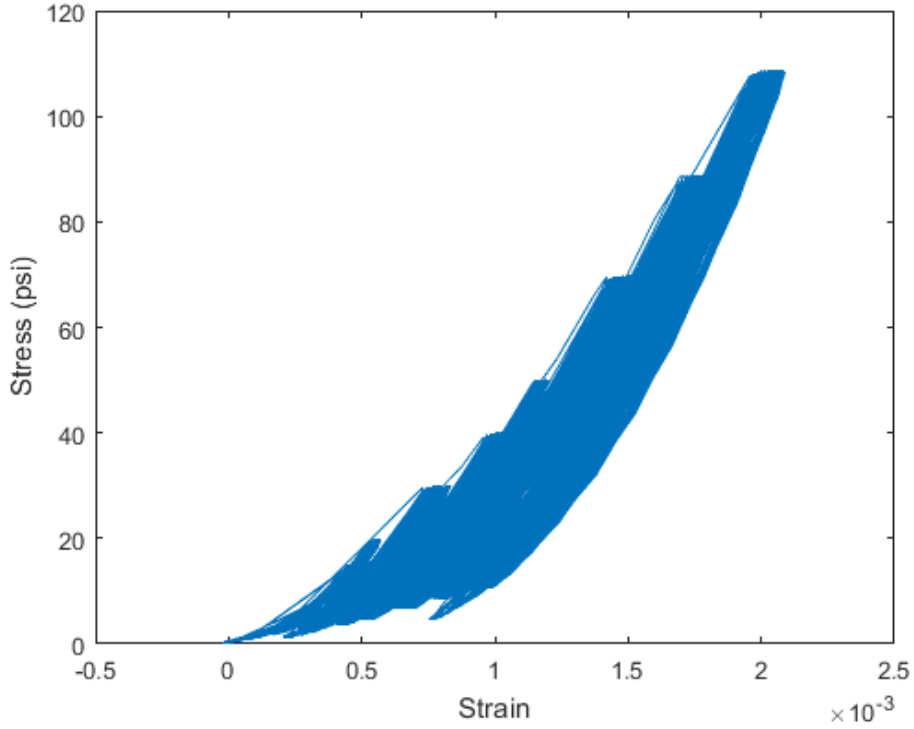

Figure E-19: Stress and Strain Summation Curve of SS-50% at 6% Cement Content

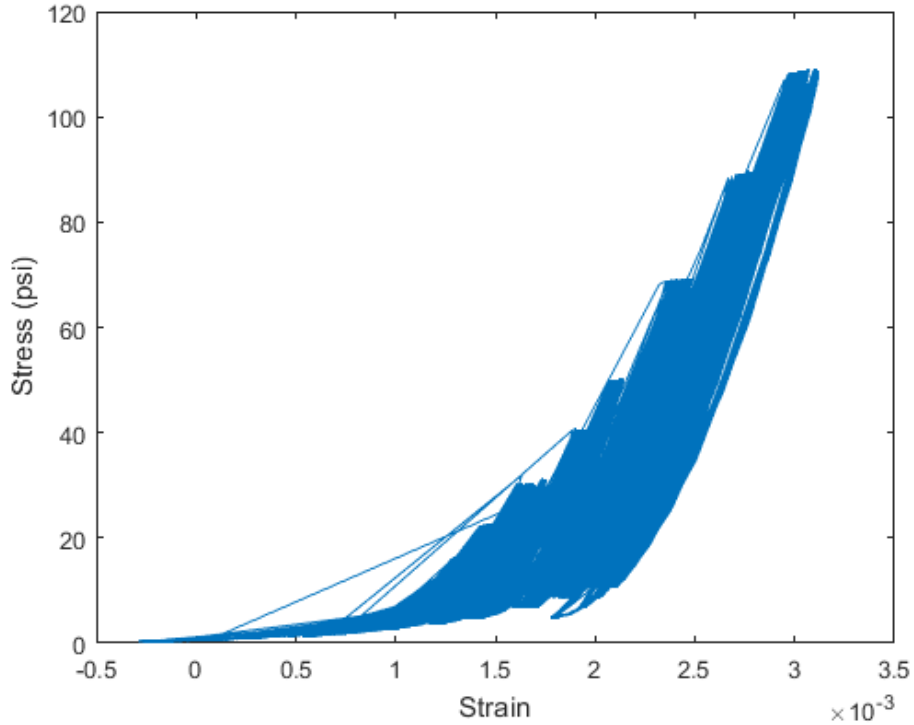

Figure E-20: Stress and Strain Summation Curve of SS-50% at 9% Cement Content

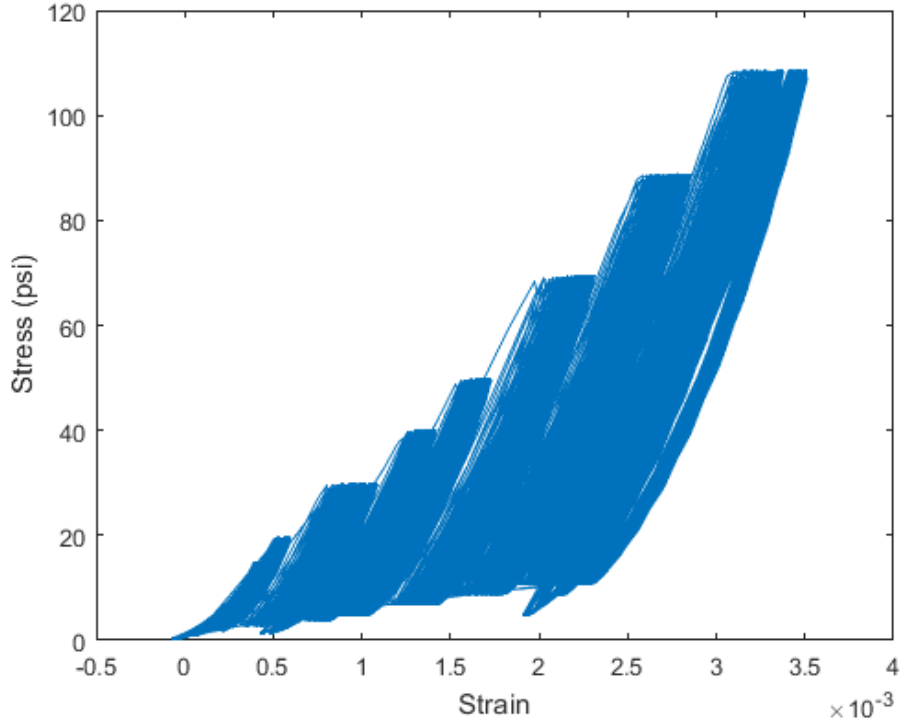

Figure E-21: Stress and Strain Summation Curve of SS-75% at 3% Cement Content

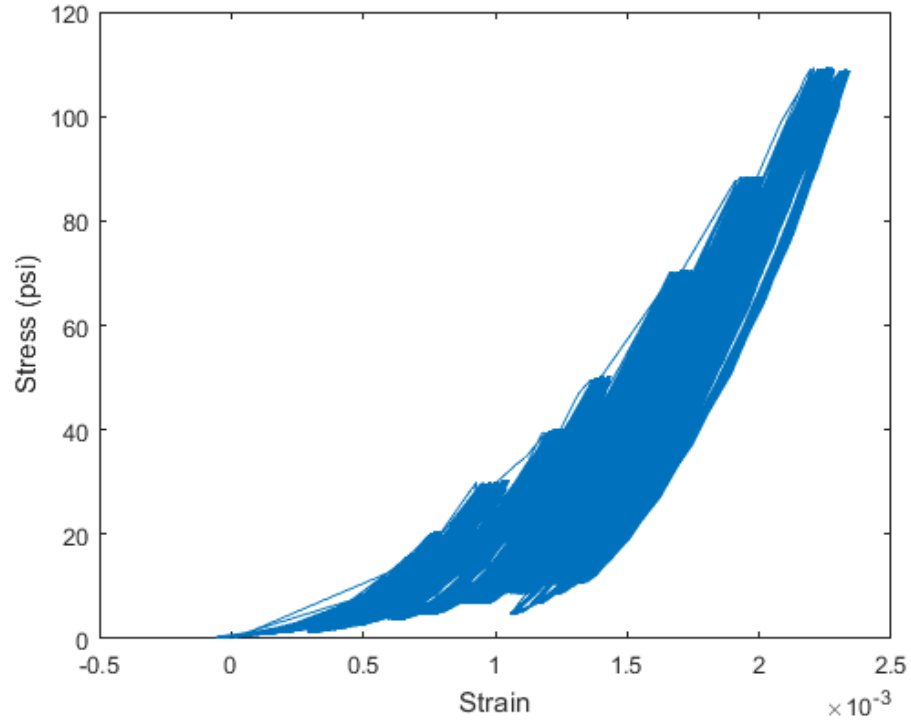

Figure E-22: Stress and Strain Summation Curve of SS-75% at 6% Cement Content

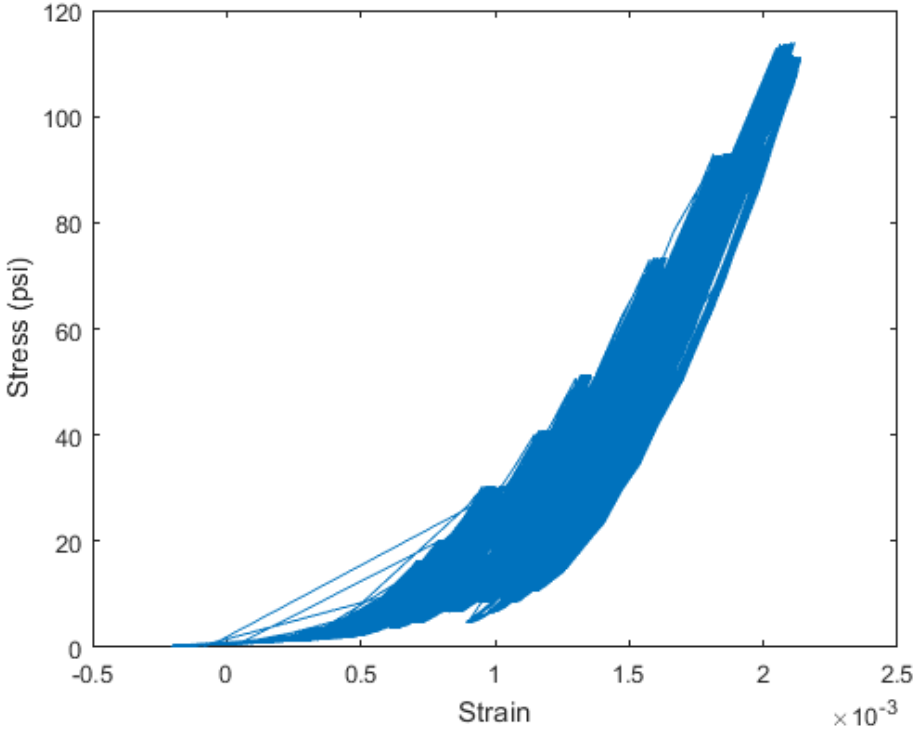

Figure E-23: Stress and Strain Summation Curve of SS-75% at 9% Cement Content

APPENDIX F

Elastic Modulus of CSAB, CMRB, and S-C

Table F-1: Elastic Modulus of CSAB

Aggregate Source	Elastic Modulus (psi)					
	3% Cement		5% Cement		7% Cement	
	7 days	28 days	7 days	28 days	7 days	28 days
WN	106,453.5	134,870.8	176,611.3	301,925.6	364,294.8	395,895.7
VG	42,889.2	67,558.7	127,985.9	222,401.3	222,550.7	307,451.6
HJ	62,891.4	98,422.8	225,947.4	358,795.0	261,845.8	406,527.0
MB	38,652.6	60,814.4	47,337.5	99,902.2	100,295.2	108,459.4
MC	52,928.7	81,308.3	83,364.9	138,873.9	175,149.3	236,208.9

Notes: VG ~ Vulcan Gray Court; MC ~ Martin Marietta Cayce; MB ~ Martin Marietta Berkeley; WN ~ Wake Stone North Myrtle Beach; HJ ~ Hanson Jefferson

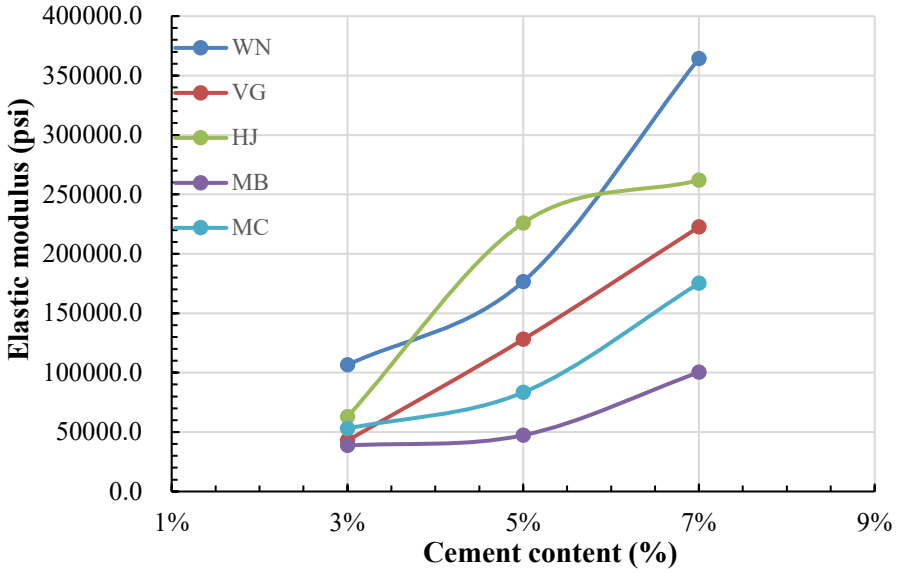

Figure F-1: Influence of Cement Content on Elastic Modulus of CSAB at 7 Days

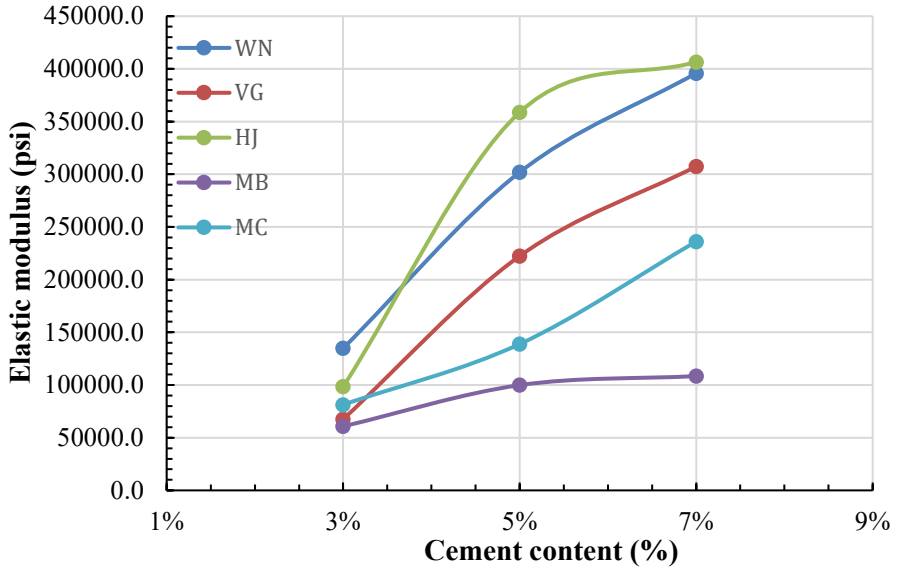

Figure F-2: Influence of Cement Content on Elastic Modulus of CSAB at 28 Days

Table F-2: Elastic Modulus of CMRB and S-C

Soil Type and RAP Content (%)	Elastic Modulus (psi)							
	3% Cement		6% Cement		9% Cement		12% Cement	
	7 days	28 days	7 days	28 days	7 days	28 days	7 days	28 days
CS-0%			9,686.1	11,022.9	14,246.5	17,242.6	21,583.7	27,670.7
CS-25%	19,451.9	24812.3	37,677.0	58,189.0	79,902.2	94,789.7		
CS-50%	29,607.2	37311.5	48,942.7	72,062.4	91,018.3	107,915.1		
CS-75%	41,335.9	48878.6	69,147.5	93,131.3	123,780.0	134,828.4		
SS-0%			14,464.5	16,800.3	30,001.6	37,854.9	78,941.1	99,810.4
SS-25%	34,222.5	29230.5	60,758.3	77,816.5	125,610.4	144,671.6		
SS-50%	27,595.1	35046.5	79,051.8	107,579.6	168,059.5	185,567.7		
SS-75%	45,235.3	56773.7	106,046.1	135,380.3	214,289.3	231,128.0		

Notes: CS ~ clayey soil; SS~ sandy soil

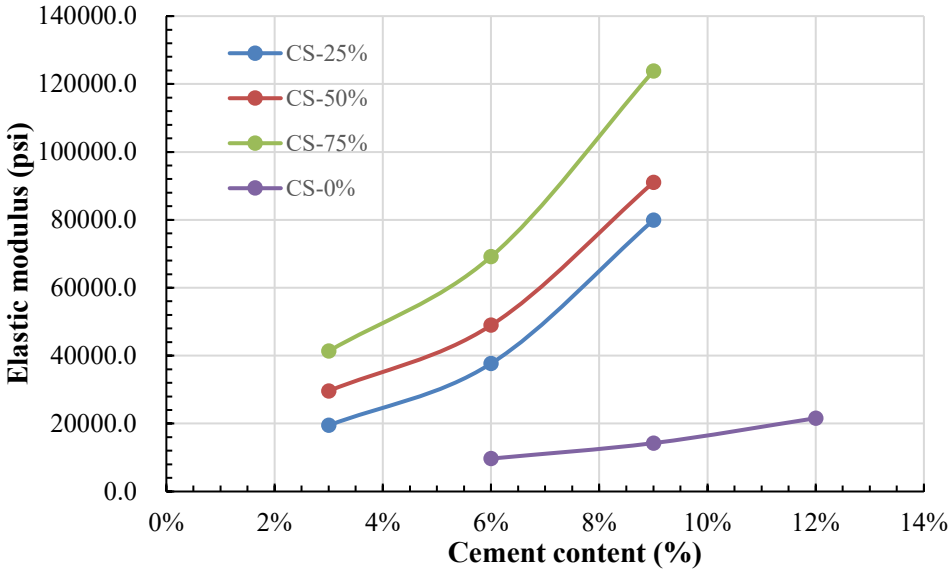

Figure F-3: Influence of Cement Content on Elastic Modulus of CMRB and S-C with Clayey Soil at 7 Days

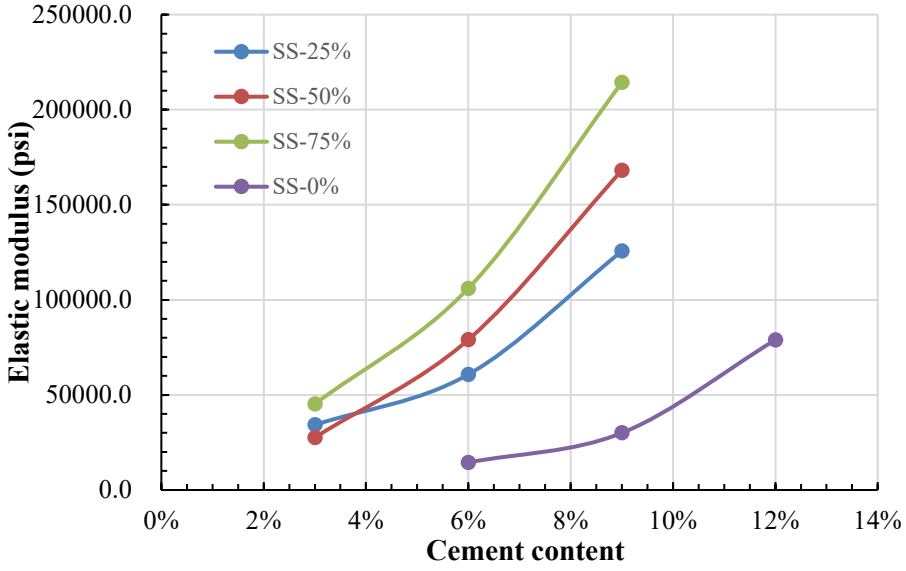

Figure F-4: Influence of Cement Content on Elastic Modulus of CMRB and S-C with Sandy Soil at 7 Days

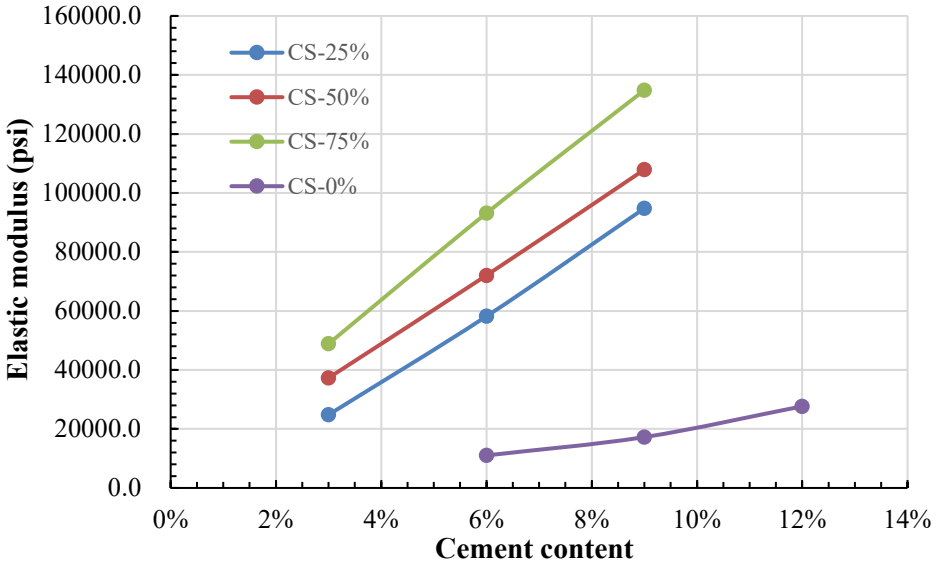

Figure F-5: Influence of Cement Content on Elastic Modulus of CMRB and S-C with Clayey Soil at 28 Days

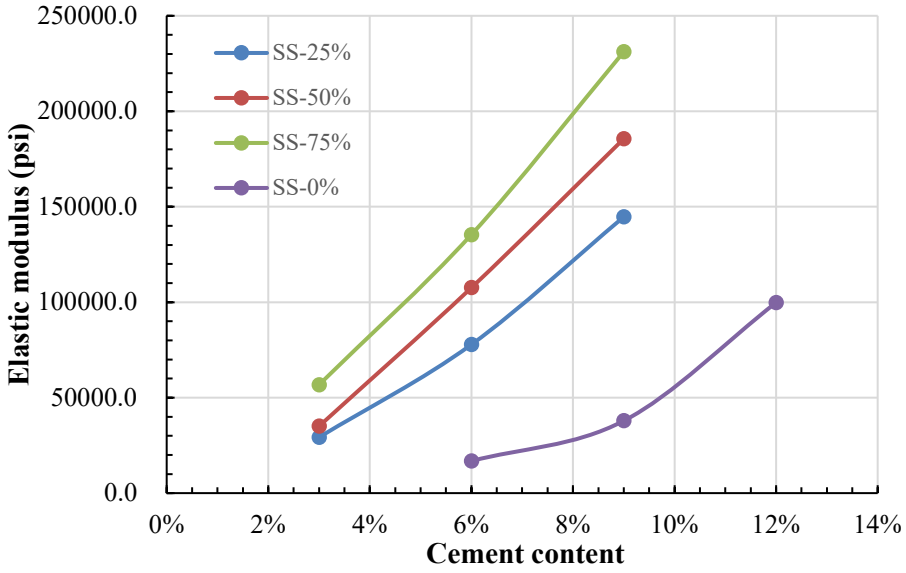

Figure F-6: Influence of Cement Content on Elastic Modulus of CMRB and S-C with Sandy Soil at 28 Days